

THE UNIVERSITY OF CALGARY

**Exploring the Activation of Olefin Polymerisation Catalysts
with Density Functional Theory**

by

Kumar Vanka

**A THESIS SUBMITTED TO THE FACULTY OF GRADUATE STUDIES IN PARTIAL
FULFILLMENT OF THE REQUIREMENTS FOR THE DEGREE OF MASTER OF
SCIENCE**

DEPARTMENT OF CHEMISTRY

CALGARY, ALBERTA

AUGUST, 2000



National Library
of Canada

Acquisitions and
Bibliographic Services

395 Wellington Street
Ottawa ON K1A 0N4
Canada

Bibliothèque nationale
du Canada

Acquisitions et
services bibliographiques

395, rue Wellington
Ottawa ON K1A 0N4
Canada

Your file Votre référence

Our file Notre référence

The author has granted a non-exclusive licence allowing the National Library of Canada to reproduce, loan, distribute or sell copies of this thesis in microform, paper or electronic formats.

The author retains ownership of the copyright in this thesis. Neither the thesis nor substantial extracts from it may be printed or otherwise reproduced without the author's permission.

L'auteur a accordé une licence non exclusive permettant à la Bibliothèque nationale du Canada de reproduire, prêter, distribuer ou vendre des copies de cette thèse sous la forme de microfiche/film, de reproduction sur papier ou sur format électronique.

L'auteur conserve la propriété du droit d'auteur qui protège cette thèse. Ni la thèse ni des extraits substantiels de celle-ci ne doivent être imprimés ou autrement reproduits sans son autorisation.

0-612-55250-0

Canada

Abstract

Theoretical studies based on density functional theory have been conducted to investigate the activation of single site olefin polymerisation catalyst precursors by different co-catalysts and activators, leading to the formation of ion-pairs. Pre-catalysts that have been investigated include mono-cyclopentadienyl, constrained geometry and the bis-cyclopentadienyl systems, the activator considered in these cases being the co-catalyst $B(C_6F_5)_3$. Solvent effects have been incorporated, with toluene being used as the solvent and the formation of sandwiched, solvent separated ion-pair species has been considered. The analogous olefin separated ion-pair species have also been investigated for these systems and the relative ease of formation of such species for each of the ion-pair systems has been evaluated. Based on the results, it has been concluded that the bis-cyclopentadienyl systems would be the most effective catalysts. The relative abilities of different boron and aluminium based co-catalysts, and systems of the type $[CPh_3^+][A^-]$, in activating the pre-catalyst $[(1,2Me_2Cp)_2ZrMe_2]$ have been investigated. After the formation of the ion-pair, partial dissociation leading to the formation of solvent (toluene) separated ion-pairs, has been considered the most favourable in each case, in contrast to the total dissociation of the ions. From the results, the $[CPh_3^+][A^-]$ type systems have been found to be the best activators. The ease of activation has been found to improve with the increase in the polarity of the solvent. The possibility of the co-catalyst, pre-catalyst, solvent and trimethyl-aluminium (TMA), competing with the counterion for the vacant site in the cationic catalyst, has been considered for the $[(1,2Me_2Cp)_2ZrMe^+][B(C_6F_5)_3CH_3]$ system. The pre-catalyst and TMA have been found to form stable, dormant complexes with the cation. The stability of these complexes is seen to decrease with the increase in the alkyl chain length associated with the catalyst. The formation of dormant sandwiched, TMA (or pre-catalyst) separated ion-pairs, analogous to the solvent separated species, is also found to be a distinct possibility. A comparison between olefin separated and solvent separated ion-pair species for four different ion-pair systems of the type $[(1,2Me_2Cp)_2ZrMe^+][A^-]$ shows that the formation of olefin separated ion-pair species is thermodynamically the more favoured in all the cases. A study of the approach of the ethylene monomer towards the $[(1,2Me_2Cp)_2ZrMe^+][B(C_6F_5)_4^-]$ ion-pair suggests that the most favourable approach of the monomer could be from the side opposite to the counterion, leading to an S_N2 type displacement of the counterion from the catalyst.

Table of Contents

Approval Page	ii
Abstract	iii
Table of Contents	iv
Acknowledgements	vii
Dedication	viii
List of Tables	ix
List of Figures	xi
Chapter 1. Introduction	
1.1 Motivations and Objectives	1
1.2 Computational Details	5
Chapter 2. Activation and Ion-Pair Formation in Group IV Metalocene and Related Olefin Polymerization Catalysts : A DFT study	
2.1 Introduction	7
2.2 Results and Discussion	8
2.2.1 Catalyst Activation	8
2.2.2 Formation of Separated Ion-Pairs - Influence of the Anion on Olefin Complexation	15
2.2.3 Influence of the Solvent on Ion-Pair Formation	22
2.2.4 Implications for the initial stages of ethylene polymerization	31
2.3 Concluding remarks	33
Chapter 3. Activation of the Metallocene Precursor (1,2Me₂Cp)₂ZrMe₂ by different cocatalysts : A DFT study	
3.1 Introduction	35

3.2	Results and Discussion	38
3.2.1	Catalyst Activation using Boranes	38
3.2.2	Aluminium based Co-catalysts	44
3.2.3	Ion-pair Dissociation - Contact Ion-pairs with a Methide Bridge	48
3.2.4	Ion-pair Dissociation - Contact Ion-pairs without a Methide Bridge	50
3.2.5	Influence of Solvent on ion-pair Dissociation - Implicit Effect	52
3.2.6	Influence of Solvent on ion-pair Dissociation - Explicit Effect	53
3.2.7	Coordination of Solvent in Arene Separated Ion-Pairs	56
3.3	Concluding remarks	59

**Chapter 4. A DFT Study of the Competing Processes Taking Place
in Solution during Polymerisation**

4.1	Introduction	61
4.2	Results and Discussion	63
4.2.1	Formation of Dormant Products before Monomer Insertion	63
4.2.2	Complexes formed after Ethylene Monomer Insertion	68
4.2.3	Formation of Sandwiched Compounds	72
4.2.4	Ethylene Separated Ion-Pairs	73
4.2.5	Comparison of Complexes of Ethylene Coordinated from Different Directions to the Counterion	76
4.2.6	Solvent Effects on Loss of Counterion From the Π -Complex	80

4.3	Concluding remarks	81
	Chapter 5. Summary and Future Prospects	84
	Bibliography	86

Acknowledgements

I would like to take this opportunity to thank my supervisor, Professor Tom Ziegler, for taking the time and trouble to support and guide me over the past few years, and for sharing his knowledge and expertise with me.

I wish to thank my supervisory committee, Professors R. Paul and W. Piers and Dr. L. Fan for their support and advice. I would also like to thank Professors T.W. Swaddle, H. Wieser and D. Hearn for their stimulating lectures, from which I've benefited a great deal.

I am indebted to all past and present members of the Ziegler-group, especially Dr. Mary Chan for her collaboration on this project. Her work contributed substantially to the second chapter of this thesis. I would also like to thank Drs. Artur Michalak, Laurent Petitjean, Sergei Patchkovskii, Tim Firman, Rocchus Schmid, Liqun Deng and Jochen Autschbach for sharing their experience with me. A special word of thanks is due for Jana Khandogin for her advice and help during my early days in Canada. I would like to extend my thanks to all other members of the group.

I acknowledge the support from The Department of Chemistry and The Faculty of Graduate Studies as well as Academic Computer Services of The University of Calgary. In particular, I wish to thank Ms. Greta Prihodko for her kind help.

I also thank all my friends - Arnab, Chari, Rajesh, Sharmaji, Smriti, Panditji and Umaji - for their friendship and support, and especially for all the fun-time we've shared together.

Finally, I thank my parents, my sister and brother-in-law for their unfailing love and support for me over all these years. They remain a constant source of encouragement and inspiration for me.

To My Family

List of Tables

Table 2.1	Selected bond distances and bond angles for the crystal structure and optimized structure of $[(\text{Me}_5\text{C}_5)_2\text{ZrMe}]^+[\text{MeB}(\text{C}_6\text{F}_5)_3]$10
Table 2.2	Enthalpy change (ΔH_{ipf}) for methide abstraction from the pre-catalysts by $\text{B}(\text{C}_6\text{F}_5)_3$ 11
Table 2.3	Enthalpy Change for Methide Abstraction and Total Charges for the Constrained Geometry Catalyst Precursor as a Function of Substitution on the Nitrogen Atom14
Table 2.4	Enthalpy for methide abstraction as a function of substitution on the cyclopentadienyl ligand15
Table 3.1	Selected experimental and calculated bond distances (\AA) and bond angles for contact ion-pair [3]Ia40
Table 3.2	Formation energies (ΔH_{ipf}) for methide bridge ion-pairs containing borates42
Table 3.3	Total charge on C_6F_5 -Group in neutral co-catalyst (A) and corresponding ion-pair $(1,2\text{-Me}_2\text{Cp})_2\text{ZrMe}-(\mu\text{-Me})\text{-A}$44
Table 3.4	Formation energies (ΔH_{ipf}) for methide bridge ion-pairs without borates48
Table 3.5	Enthalpy of ion-pair dissociation (ΔH_{ips}) for contact ion-pairs with a methide bridge49
Table 3.6	Enthalpy of ion-pair dissociation (ΔH_{ips}) for contact ion-pairs without a methide bridge50
Table 3.7	Influence of solvent on the calculated ion-pair dissociation energy (ΔH_{ips})53
Table 3.8	Enthalpy of formation of solvent separated ion-pair (ΔH_{SS}) formed from contact ion-pairs with a methide bridge55

Table 3.9	Enthalpy of formation of solvent separated ion-pair (ΔH_{SS}) formed from contact ion-pairs without a methide bridge56
Table 3.10	Enthalpy of formation of solvent separated ion-pair (ΔH_{SS}) for ion-pair [3]Ia in three different solvents57
Table 4.1	Selected experimental and calculated bond distances (\AA) and bond angles for contact ion-pair [4]Ia65
Table 4.2	Enthalpy of formation of dormant products (ΔH_{dp}) from the coordinated complex for anions [4]1a and [4]1d66
Table 4.3	Enthalpy of formation of dormant products (ΔH_{dp}) from the coordinated complex for anions [4]1a and [4]1d , after the insertion of the ethylene monomer69
Table 4.4	Enthalpy of formation of ethylene separated ion-pair (ΔH_{ES}) and the solvent separated ion-pair (ΔH_{SS}) for anions 1a-4a with the cation P'75
Table 4.5	Enthalpy of total separation of the ethylene complexed compounds (ΔH_{TS}) in three different solvents for the complexes [4]IIIA'(i) and [4]IIIA'(ii)81

List of Figures

Figure 1.1	Polymerisation scheme for the insertion of ethylene	1
Figure 1.2	Possible reactions of the contact ion-pair under typical polymerization conditions	3
Figure 2.1	General structures for the mono-cyclopentadienyl, constrained geometry and bis-cyclopentadienyl catalyst precursors	8
Figure 2.2	LDA optimized structure of the $[(\text{Me}_5\text{C}_5)_2\text{ZrMe}]^+[\text{MeB}(\text{C}_6\text{F}_5)_3]^-$ contact ion-pair	9
Figure 2.3	Charge analysis of ligands and functional groups in the neutral precursors and ion-pair	12
Figure 2.4	Olefin Complexed Ions and Ion-Pairs from the CpTiMe_3 Precursor	17
Figure 2.5	Olefin Complexed Ions and Ion-Pairs from the $\text{H}_2\text{SiCp}(\text{NH})\text{TiMe}_2$ Precursor	20
Figure 2.6	Olefin Complexed Ions and Ion-Pairs from the Cp_2TiMe_2 Precursor	21
Figure 2.7	Toluene Complexed Ions and Ion-Pairs from the CpTiMe_3 Precursor	24
Figure 2.8	Toluene Complexed Ions and Ion-Pairs from the CpZrMe_3 Precursor	25
Figure 2.9	Toluene Complexed Ions and Ion-Pairs from the $\text{H}_2\text{SiCp}(\text{NH})\text{TiMe}_2$ Precursor	27
Figure 2.10	Toluene Complexed Ions and Ion-Pairs from the $\text{H}_2\text{SiCp}(\text{NH})\text{ZrMe}_2$ Precursor	28
Figure 2.11	Toluene Complexed Ions and Ion-Pairs from the Cp_2TiMe_2 Precursor	30
Figure 2.12	Proposed mechanism of activation for the mono-cyclopentadienyl and constrained geometry precursors	32
Figure 3.1	Examples of the three different types of activators studied	37
Figure 3.2	LDA optimised structures of the $[(1,2\text{Me}_2\text{Cp})_2\text{ZrMe}]^+[\text{B}(\text{C}_6\text{F}_5)_3\text{Me}]^-$ contact ion-pair	39

Figure 3.3	Charge analysis of ligands and functional groups in the neutral precursors and ion-pair for the $[(1,2\text{Me}_2\text{Cp})_2\text{ZrMe}]^+[\text{B}(\text{C}_6\text{F}_5)_3\text{Me}]^-$ system	41
Figure 3.4	Plot of the enthalpy of ion-pair formation against the number of fluorine atoms for a series of ion-pairs with borates as the co-catalyst	43
Figure 3.5	Structure of the contact ion-pair formed with MAO as the co-catalyst	45
Figure 3.6	Charge analysis of ligands and functional groups in the neutral precursors and ion-pair for the $[(1,2\text{Me}_2\text{Cp})_2\text{ZrMe}]^+[\text{MAOMe}]^-$ system	46
Figure 3.7	LDA optimized structure of the solvent separated ion-pair formed by the $[(1,2\text{Me}_2\text{Cp})_2\text{ZrMe}]^+[\text{B}(\text{C}_6\text{F}_5)_3\text{Me}]^-$ system in toluene	54
Figure 3.8	LDA optimized structure of the solvent separated ion-pair formed by the $[(1,2\text{Me}_2\text{Cp})_2\text{ZrMe}]^+[\text{B}(\text{C}_6\text{F}_5)_3\text{Me}]^-$ system in chlorobenzene, with the solvent coordinating through the chlorine	58
Figure 3.9	LDA optimized structure of the solvent separated ion-pair formed by the $[(1,2\text{Me}_2\text{Cp})_2\text{ZrMe}]^+[\text{B}(\text{C}_6\text{F}_5)_3\text{Me}]^-$ system in chlorobenzene, with the solvent coordinating through two carbons of the benzene ring	59
Figure 4.1	Possible competitors for the vacant coordinate site in the cationic catalyst $[(1,2\text{Me}_2\text{Cp})_2\text{ZrMe}]^+$	62
Figure 4.2	LDA optimized structure of the $[(1,2\text{Me}_2\text{Cp})_2\text{ZrMe}]^+[(1,2\text{Me}_2\text{Cp})_2\text{ZrMe}]_2$ dormant complex	64
Figure 4.3	LDA optimized structure of the $[(1,2\text{Me}_2\text{Cp})_2\text{ZrMe}]^+-\text{AlMe}_3$ dormant complex	67
Figure 4.4	Possible modes of coordination of AlMe_3 to the cation $[(1,2\text{Me}_2\text{Cp})_2\text{ZrMPr}]^+$	70
Figure 4.5	Possible modes of coordination of the precatalyst, $[(1,2\text{Me}_2\text{Cp})_2\text{ZrMe}]_2$, to the cation $[(1,2\text{Me}_2\text{Cp})_2\text{ZrMPr}]^+$	71
Figure 4.6	LDA optimized structure of the ethylene separated ion-pair complex $[(1,2\text{Me}_2\text{Cp})_2\text{ZrMe}^+]-\text{C}_2\text{H}_4-[\text{B}(\text{C}_6\text{F}_5)_4]^-$	74

Figure 4.7	Different ways in which the monomer (ethylene) can approach the ion-pair $[(1,2\text{Me}_2\text{Cp})_2\text{ZrMe}]^+[\text{B}(\text{C}_6\text{F}_5)_4]^-$ system prior to uptake by the catalyst	78
Figure 4.8	LDA optimized structures of the ethylene complexed ion-pairs formed by different approaches of the monomer (ethylene) to the $[(1,2\text{Me}_2\text{Cp})_2\text{ZrMe}]^+[\text{B}(\text{C}_6\text{F}_5)_4]^-$ ion-pair system	79

Chapter 1

Introduction

1.1 Motivations and Objectives

Single-site homogeneous catalysts have been receiving increasing attention over traditional Ziegler-Natta type heterogeneous catalysts. This is primarily due to their superior performance in achieving higher stereoselectivity, narrower molecular weight distribution, and higher activity. Another advantage is that these systems produce structurally well defined mononuclear active species. Systematic modification of these structures allows for enhanced control over polymer properties. Among the more highly active homogenous catalysts are metallocenes and related organometallic compounds containing a group 4 transition metal.

The metallocenes by themselves are not very effective as polymerization catalysts, but require activation by a co-catalyst. The general structure of these pre-catalysts contain a transition metal center (M) co-ordinated to two ligands (L) and two alkyl groups (R_1 , R_2) : $\{L\}_2 MR_1R_2$. The co-catalysts are generally Lewis acids whose function is to abstract one of the alkyl groups to produce the activated metal catalyst, which is generally accepted¹⁻¹¹ to be an electrophilic species with cationic character : $\{L\}_2 MR^+$. The generally accepted polymerisation scheme for such systems is shown in Figure 1.1, for the polymerisation of ethylene.

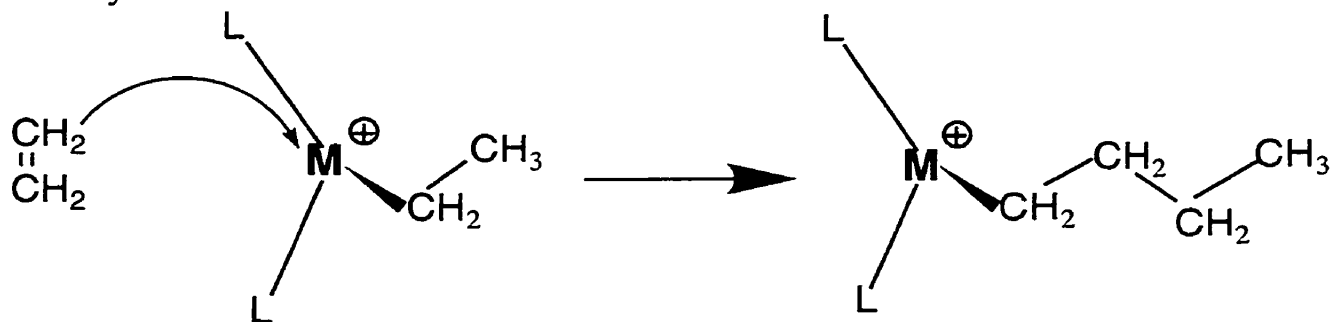


Figure 1.1 Polymerisation scheme for the insertion of ethylene

The activation of the dialkyl precatalysts using a variety of co-catalysts such as boranes⁷⁻¹¹ and aluminum based¹²⁻¹⁴ systems have been investigated experimentally. Methylalumoxane (MAO) has been the oldest and the most commonly used co-catalyst in industry. There have been experimental investigations conducted to determine the structure of MAO²⁻⁴ and to test the polymerisation activity of model compounds for MAO.^{5,6} More recently¹⁵⁻²¹ salts of carbenium ions have been used successfully as activators.

In an ideal situation, the cationic catalyst would be readily formed and would then proceed to insert the alkene monomer, leading to the formation of the polymer chain. However the path to polymerisation may be impeded in several ways. The isolated products as well as in situ NMR^{7,8} studies indicate the formation of a variety of species associated with the catalyst, the co-catalyst, the solvent, and the olefin. There is strong experimental evidence²¹⁻²⁴ to suggest that the co-catalyst and solvent have strong effects on catalyst activity. A complex equilibrium is established between these species when the polymerization is carried out in solution. A possible scheme for this equilibration is depicted in Figure 1.2. The activation of the dimethyl pre-catalyst by a Lewis acid can lead to the formation of a contact ion-pair in which the co-catalyst is co-ordinated to the metal center as shown in pathway *A* of Figure 1.2. Once produced in the reaction mixture, the contact ion-pair can dissociate into completely solvated cation and anion such as in path *B*. Alternatively, a molecule of the solvent can interact with the cationic moiety, pushing away the anion to form the solvent separated ion-pair as shown in pathway *C* of Figure 1.2. Pathway *E* indicates that further solvation of such an ion-pair can lead to the formation of a solvent complexed cation with the counterion sufficiently far away that no electrostatic interaction is possible. In the presence of the olefin, a molecule of the olefin can insert itself between the contact ion-pair in a similar fashion to produce the olefin separated ion-pair (pathway *D*). Further dissociation of this ion-pair results in the formation of the olefin complexed cation as shown in Pathay *F* of Figure 1.2.

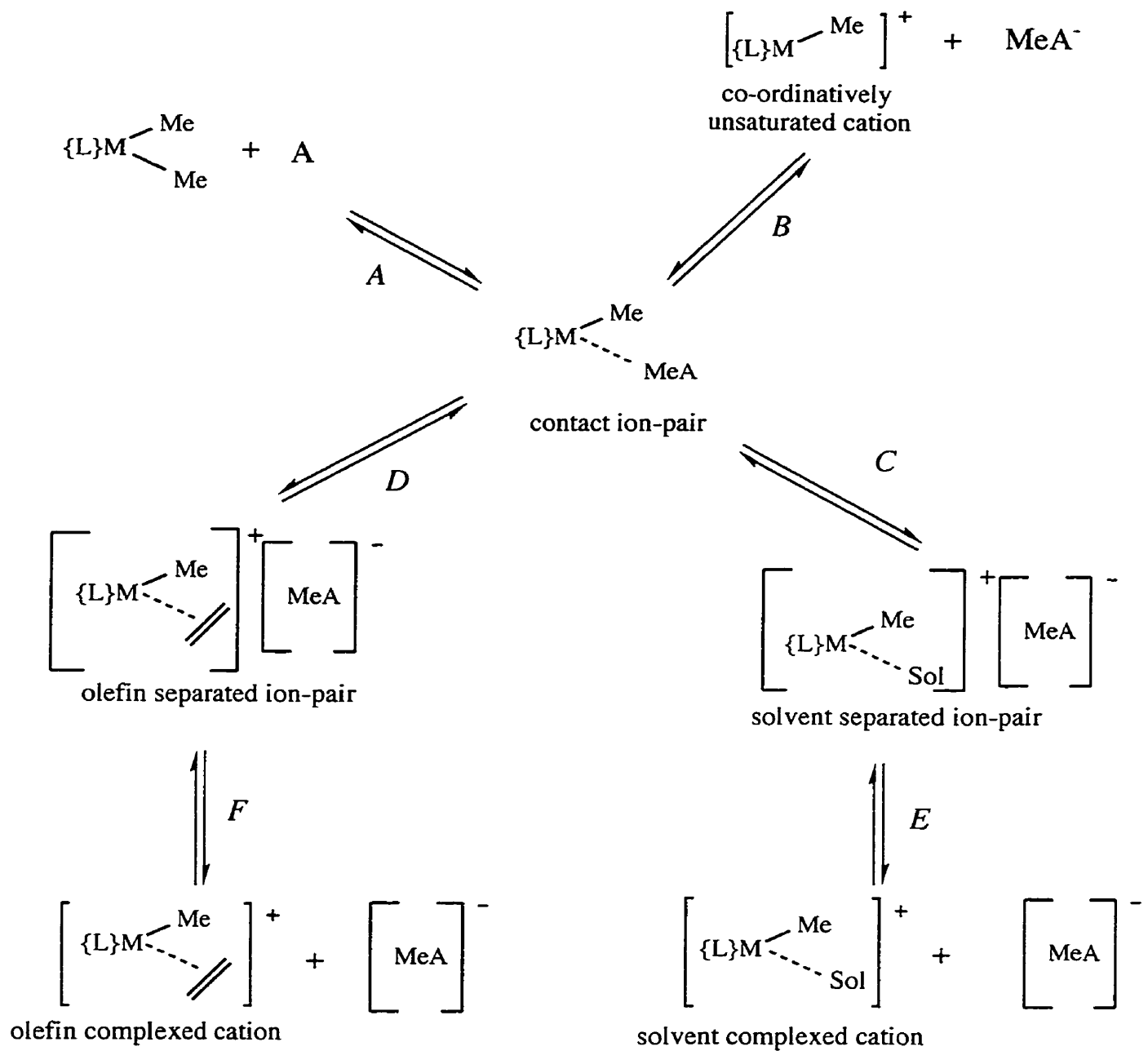


Figure 1.2 Possible reactions of the contact ion-pair under typical polymerization conditions

Experimental studies^{10,25-27} have also revealed the possibility of the pre-catalyst, co-catalyst and other species present in solution (like trimethyl aluminium) competing for the vacant cationic site of the catalyst to form dormant complexes. Such dormant complexes would have to be dissociated before catalysis can proceed.

The well defined molecular structure of these metallocene catalysts and their analogues allows for more thorough mechanistic studies by theoretical methods. Many theoretical studies²⁸⁻³⁵ have been conducted on the olefin uptake, insertion, and termination steps of the polymerization process, but comparatively little have been reported on the first step, the activation, and on the insertion process in the presence of the counterion. Lanza *et al.*^{36,37} studied the activation of the titanium constrained geometry precatalyst by tris(pentafluorophenyl)borane, $B(C_6F_5)_3$, using ab initio methods. Klesing *et al.*³⁸ used density functional theory (DFT) to study dimerization and ion-pair formation enthalpies for silicon bridged bis-indenyl zirconocenes with a hexameric 3-D model for MAO used as co-catalyst. Their results demonstrated that the degree of steric bulk on the pre-catalyst can influence the way in which MAO acts as an activator. Models of MAO have also been considered by Fusco *et al.*^{39,40} Other investigations include olefin insertion into the $Cl_2TiMe(\mu-Cl)_2AlH_2$ ion-pair by Bernardi.⁴¹

The objective of this thesis is to do a theoretical study using density functional theory, of the different processes that occur in solution during the activation process. The next chapter deals with the activation of different pre-catalysts of the type $\{L\}_2MR_2$ by the co-catalyst $B(C_6F_5)_3$ in toluene and the subsequent effect of the counterion and the solvent on the polymerisation process. Chapter 3 details the activation of the catalyst precursor $(1,2Me_2Cp)_2ZrMe_2$ by different types of cocatalysts, while the competition among the various species present in solution for the vacant site in the $(1,2Me_2Cp)_2ZrMe^+$ catalyst is discussed in Chapter 4. A discussion of the computational method used for this study is given below.

1.2 Computational Details

The density functional theory calculations were carried out using the Amsterdam Density Functional (ADF) program version 2.3.3 developed by Baerends *et al.*⁴²⁻⁴⁵ and vectorized by Ravenek⁴⁶ The numerical integration scheme applied was developed by te Velde *et al.*^{47,48} and the geometry optimization procedure was based on the method of Versluis and Ziegler.⁴⁹ Geometry optimizations were carried out using the local exchange-correlation potential of Vosko *et al.*⁵⁰ without any symmetry constraints. The electronic configurations of the molecular systems were described by a triple- ζ basis set on zirconium for 4s, 4p, 4d and 5s, augmented with a single 5p polarisation function. A triple- ζ basis set was also used for titanium for 3s, 3p, 3d and 4s, augmented with a 4p polarisation function. Double- ζ STO basis were used for carbon (2s,2p), hydrogen (1s) and nitrogen (2s,2p), augmented with a single 3d polarisation function except for hydrogen where a 2p polarisation function was used. A set of auxiliary s,p,d,f and g STO functions centred on all nuclei was used to fit the molecular density and represent Coulomb and exchange potentials accurately in each SCF cycle.⁵¹ The gas phase energy difference was calculated by augmenting the local density approximation energy with Perdew and Wang's non-local correlation and exchange corrections (PWB91).⁵² The energy difference in solution were corrected from the gas phase energy by accounting for the solvation energy calculated by the Conductor-like Screening Model (COSMO) that has recently been implemented into the ADF program.^{53,54} The solvation calculations were performed with the dielectric constant 2.38 for toluene, 5.71 for chlorobenzene and 9.93 for dichlorobenzene. The radii used for the atoms in Å were as follows : for hydrogen - 1.16, boron 1.15, carbon 2.0, oxygen 1.5, fluorine 1.2, silicon 2.2, titanium 2.3 and zirconium 2.4. These values were obtained by optimization using least-squares fitting to experimental solvation energies. The enthalpies (ΔH) reported in the following sections are potential energy differences without zero point corrections or vibrational finite temperature corrections. Such corrections are still too expensive to calculate for the size of molecules considered here. We expect these

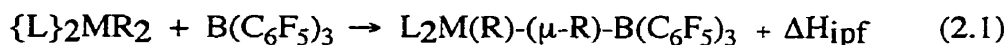
corrections to be of the order of ± 2 -3 kcal/mol. The charge distribution study for the ion-pair systems in Chapter 2 was carried out by the Hirshfield analysis^{55,56} and in Chapter 3 was carried out by the Mulliken Analysis.^{57,58}

Chapter 2

Activation and Ion-Pair Formation in Group IV Metallocene and Related Olefin Polymerization Catalysts : A DFT study

2.1 Introduction

This chapter investigates the activation of different metallocene based precatalysts of the type $\{L\}_2MR_2$ by the the activator, or cocatalyst $B(C_6F_5)_3$. The first step in the catalyst activation involves the extraction of the R^- group from the precatalyst by $B(C_6F_5)_3$. It has been experimentally established^{1,7-11} that this leads to the formation of an alkyl bridged ion-pair compound, as shown in equation 2.1 below :



ΔH_{ipf} = Enthalpy of ion-pair formation

The ion-pair thus formed can undergo different reactions in solution with the solvent or with the monomer present to give different products, as discussed earlier in Scheme 1.2. These reactions will be investigated for each of the catalyst systems. Based on the stabilities of the different complexes formed in solution for each catalyst system, conclusions will be drawn on the relative abilities of each of the compounds, $\{L\}_2MR_2$, to act as a polymerisation catalyst.

The general structures of precatalysts are shown in Figure 2.1: the mono-cyclopentadienyl system ([2]1), the constrained geometry system ([2]2) and the bis-cyclopentadienyl system ([2]3)

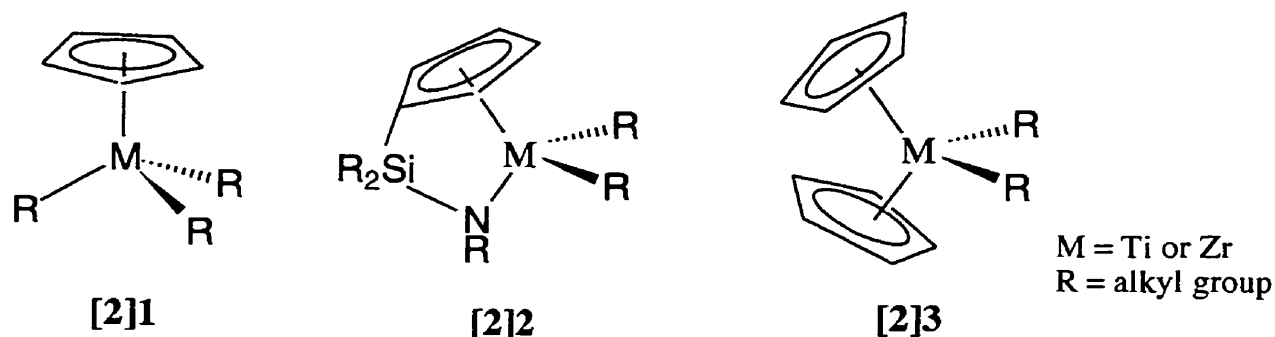


Figure 2.1 General structures for the mono-cyclopentadienyl, constrained geometry and bis-cyclopentadienyl catalyst precursors

2.2 Results and Discussion

2.2.1 Catalyst Activation

The activation of the dimethyl precursors $\{L\}MMe_2$ by $B(C_6F_5)_3$ for the three classes of catalysts of interest in this study has been examined experimentally.^{8,9,59-61} These studies suggest the formation of a contact ion-pair $[\{L\}MMe]^+[MeB(C_6F_5)_3]^-$ as opposed to completely separated ions $[\{L\}MMe]^+$ and $[MeB(C_6F_5)_3]^-$. The ion-pairs generated from the (1,2- $Me_2C_5H_3$) $ZrMe_2$ and $(Me_5C_5)_2ZrMe_2$ precursors have been characterized by X-ray diffraction studies while those generated from $(Me_5C_5)TiMe_3$ and $Me_2Si(Me_4C_5)NHTiMe_2$ have only been characterized by solution NMR data. The crystal structures of the substituted zirconocenes show that the cationic metal center is bound to the anion via an unsymmetrical $Zr-Me-B$ bridge, the $Zr-Me$ (bridging) bond being on average 0.3\AA longer than the terminal $Zr-Me$ bond while the $B-Me$ (bridging) bond is just slightly longer than in the free anion $MeB(C_6F_5)_3^-$. The geometry of these crystal structures were used as models for the starting structure in the optimization procedure for the ion-pairs in this study. The calculated structures obtained are similar to those of the crystal structures. The optimized structure of the pentamethyl zirconocene ion-pair is shown in Figure 2.2 and selected bond distances and angles are collected in Table 2.1 for comparison with the crystal structure data.

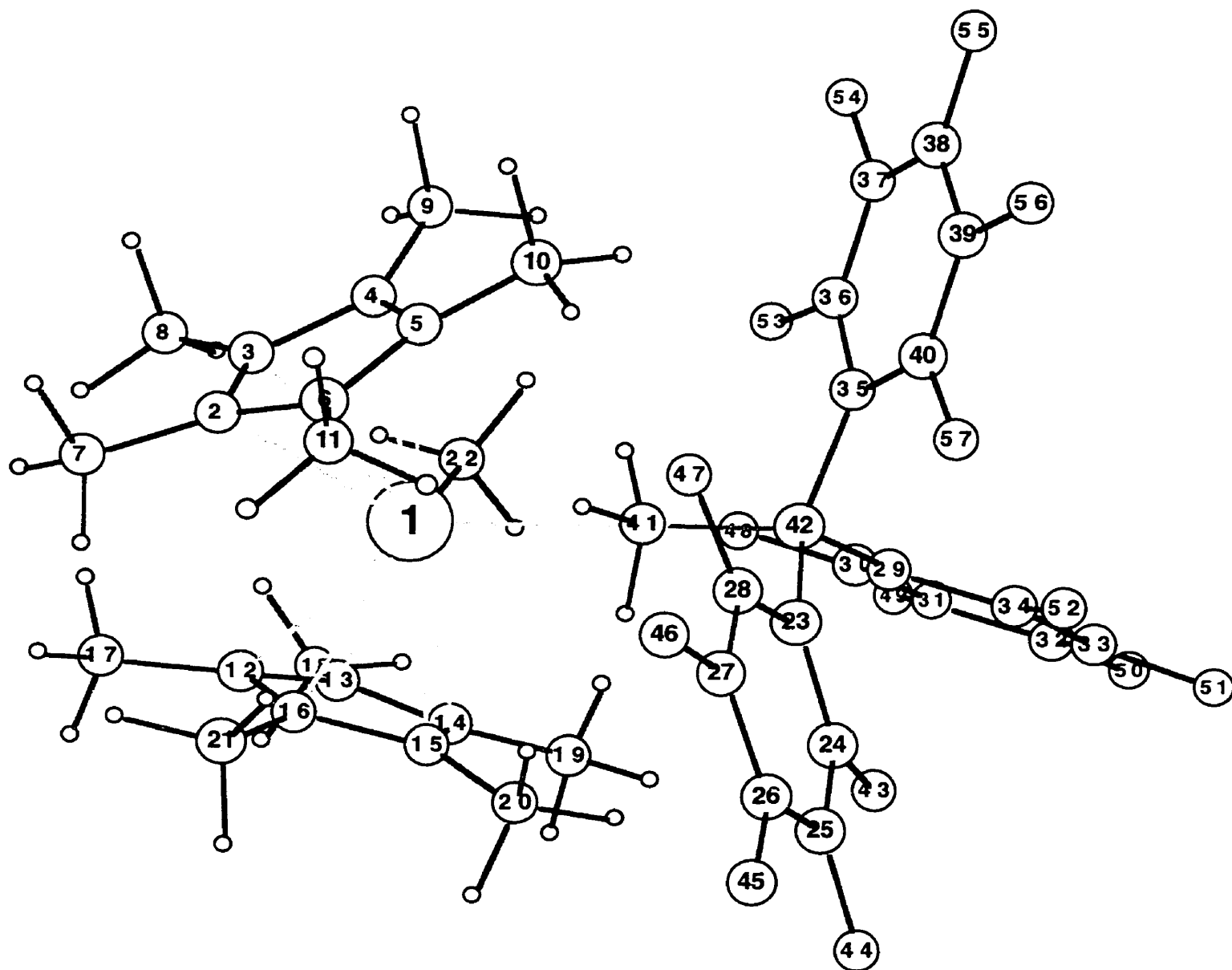


Figure 2.2 LDA optimized structure of the $[(\text{Me}_5\text{C}_5)_2\text{ZrMe}]^+[\text{MeB}(\text{C}_6\text{F}_5)_3]^-$ contact ion-pair

Table 2.1 Selected bond distances and bond angles for the crystal structure and optimized structure of $[(\text{Me}_5\text{C}_5)_2\text{ZrMe}]^+[\text{MeB}(\text{C}_6\text{F}_5)_3]^-$

	Bond Distance (Å)		Angles (deg)		
	Crystal Structure ^a	Optimized Structure	Crystal Structure ^a	Optimized Structure	
Zr-C ₂	2.558(7)	2.5193	C ₂₃ -B-C ₂₉	111.5(5)	111.32
Zr-C ₃	2.540(7)	2.5136	C ₂₃ -B-C ₃₅	114.6(5)	114.42
Zr-C ₄	2.551(7)	2.5393	C ₂₃ -B-C ₄₁	101.7(5)	101.42
Zr-C ₅	2.534(6)	2.5231	C ₂₉ -B-C ₃₅	104.2(5)	105.15
Zr-C ₆	2.509(6)	2.4814	C ₂₉ -B-C ₄₁	114.3(5)	111.43
Zr-C ₁₂	2.511(7)	2.5138	C ₃₅ -B-C ₄₁	110.9(5)	111.30
Zr-C ₁₃	2.526(7)	2.5209	Zr-C ₄₁ -B	176.6(4)	177.66
Zr-C ₁₄	2.557(7)	2.5312			
Zr-C ₁₅	2.549(7)	2.5164			
Zr-C ₁₆	2.530(7)	2.5029			
Zr-C ₂₂	2.223(6)	2.2546			
B-C ₄₁	1.66(1)	1.6470			
B-C ₂₃	1.666(9)	1.6169			
B-C ₂₉	1.64(1)	1.6144			
B-C ₃₅	1.655(9)	1.6144			

^aobtained from reference 7

The calculated enthalpy for the methide abstraction reaction is reported in Table 2.2. These values were obtained by evaluating the energy differences between the neutral precursors and the contact ion-pair. Out of the systems examined in Table 2.2, the only experimental value reported is for the Cp_2ZrMe_2 precatalyst where a ΔH_{ipf} of -23.1 kcal/mol was measured by titration calorimetry.¹¹ The calculated value of -19.1 kcal/mol is in reasonable agreement with this number. Another observation that can be made from Table 2.2 is that changing the metal center also does not cause significant changes in the abstraction energies. Abstraction from titanium precatalysts is 2 to 3 kcal/mol less favorable than from the zirconium pre-catalysts within the same

ligand system. This is in reasonably good agreement with the difference of 1.3 kcal/mol obtained from experimental values for $\text{Me}_2\text{Si}(\text{Me}_4\text{Cp})(t\text{-BuN})\text{TiMe}_2$ at -22.6 kcal/mol and $\text{Me}_2\text{Si}(\text{Me}_4\text{Cp})(t\text{-BuN})\text{ZrMe}_2$ at -23.9 kcal/mol.

Table 2.2 Enthalpy change (ΔH_{ipf}) for methide abstraction from the pre-catalysts by $\text{B}(\text{C}_6\text{F}_5)_3$

Catalyst Precursor	ΔH_{ipf} gas phase ^{a,b}	ΔH_{ipf} solution ^{a,b}
CpTiMe_3	-12.9	-12.2
CpZrMe_3	-15.7	-14.9
$\text{H}_2\text{SiCp}(\text{NH})\text{TiMe}_2$	-13.9	-14.4
$\text{H}_2\text{SiCp}(\text{NH})\text{ZrMe}_2$	-16.6	-17.5
Cp_2TiMe_2	-15.5	-16.3
Cp_2ZrMe_2	-19.1	-19.1

^a Corresponding to the process $\{\text{L}\}_2\text{MR}_2 + \text{B}(\text{C}_6\text{F}_5)_3 \rightarrow \text{L}_2\text{M}(\text{R})-(\mu\text{-R})\text{-B}(\text{C}_6\text{F}_5)_3 + \Delta H_{\text{ipf}}$

^b kcal/mol

Varying the ligands around the metal has a more pronounced effect on the abstraction enthalpy. The mono-cyclopentadienyl systems have the least negative abstraction energy, followed by the constrained geometry catalysts, and finally the bis-cyclopentadienyl systems. Ancillary ligands can influence stability of the contact ion-pair relative to the neutral starting materials in two ways: (a) steric repulsion between the ancillary ligands and the anion aryl groups and (b) electronic stabilization of the metal center. The observed trend in ΔH_{ipf} is contrary to expectations when considering steric effect, as large ancillary ligands should hinder the approach of the bulky Lewis acid $\text{B}(\text{C}_6\text{F}_5)_3$ and thus rendering the abstraction less favorable. On the other hand, electronic factors are expected to have a strong influence as the optimized structure of the contact ion-pair suggests the formation of a cationic metal fragment and an anionic boron fragment. The charge density for the neutral precursors and the contact ion-pair is shown in Figure 2.3 for the mono-cyclopentadienyl titanium system. The charge density of the individual atoms are summed in such a way as to give the total charge of ligands or the functional groups attached to the metal or the

boron. In the neutral catalyst precursor, a positive charge of 0.41 is concentrated on the titanium metal center, with the compensating negative charges provided by the organic ligands. The cyclopentadienyl ring is almost neutral while the methyl groups contribute about -0.15 each. In the neutral boron Lewis acid, the boron atom carries a positive charge of 0.11 while the compensating negative charge is distributed evenly over the aryl groups. In the ion-pair, the positive charge on the titanium remains relatively the same while the ligands on the titanium now carries significantly less electron density. The boron and the aryl groups all became significantly more negative than in the neutral precursor. The net result is a flow of electron density from the cyclopentadienyl ring and two of the methyl groups into the boron and pentafluorophenyl groups of the ion-pair with the metal fragment gaining a 0.40 positive charge that is compensated by a negative charge of the same magnitude on the boron side.

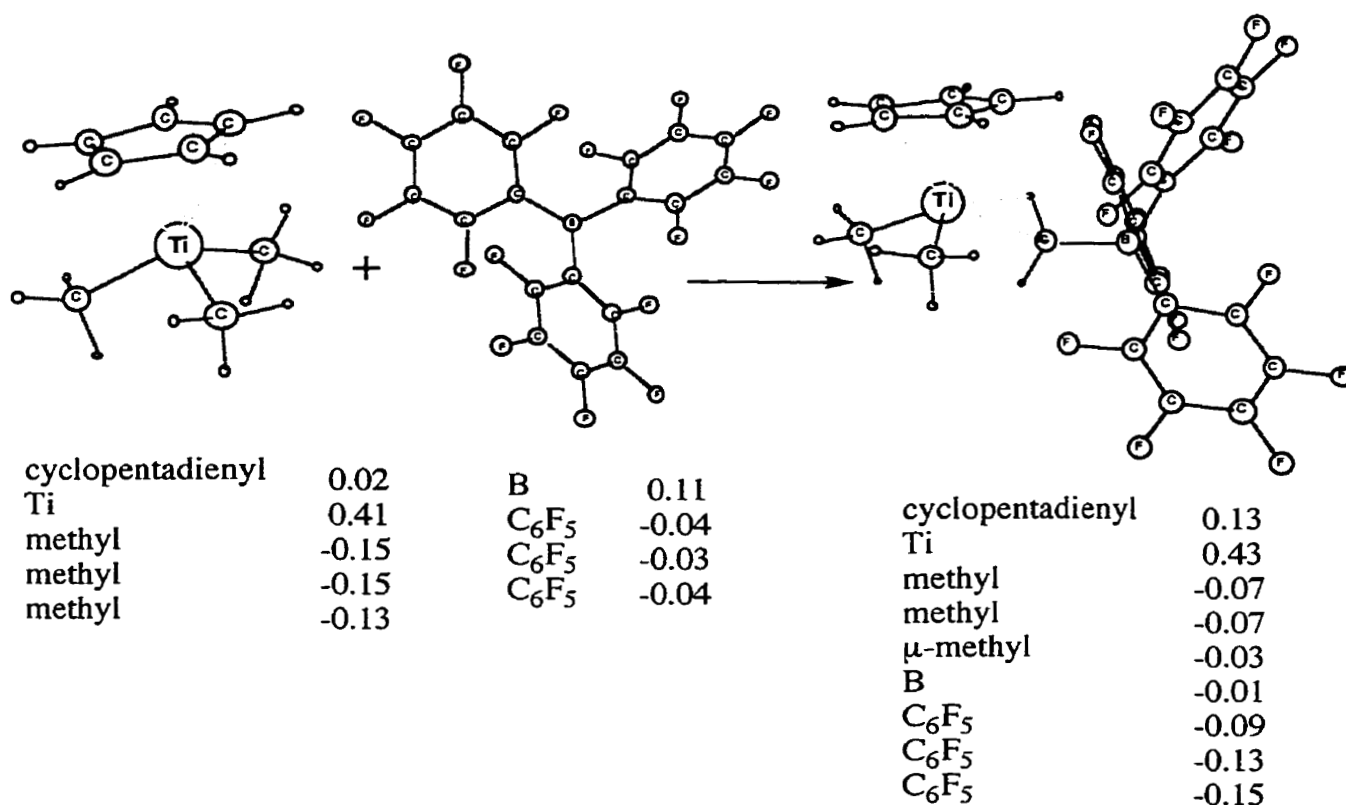


Figure 2.3 Charge analysis of ligands and functional groups in the neutral precursors and ion-pair

Replacing one methyl group with a nitrogen and a silicon bridge in the mono-cyclopentadienyl system produces the constrained geometry catalyst. This results in the ΔH_{ipf} for methide abstraction being more negative by about 2 kcal/mol. The increase in exothermicity of the abstraction process for the constrained geometry systems as compared to the mono-cyclopentadienyl system is due to the fact that the nitrogen atom can serve as a better electron donor than a methyl group. Replacing a methyl group with a cyclopentadienyl ligand on the mono-cyclopentadienyl system to form the bis-cyclopentadienyl system provides an extra stabilization of 4 kcal/mol. This again can be attributed to the better electron releasing ability of the cyclopentadienyl ligand.

A more detailed study of the electronic effects of substituents on the ancillary ligands was conducted on the constrained geometry catalyst and the bis-cyclopentadienyl catalysts. Table 2.3 shows the effect of substituting the nitrogen atom in the constrained geometry catalyst with increasingly large alkyl groups. The enthalpy of methide abstraction slowly, but steadily becomes more negative beginning from the hydrogen substituted amine to the *tert*-butyl substituted amine as indicated by the ΔH_{ipf} values in columns two and three. Experimental values for this series of catalyst precursors have not been reported. However, a ΔH_{ipf} values of -22.6 kcal/mol was measured for the $\text{Me}_2\text{Si}(\text{Me}_4\text{Cp})(t\text{-BuN})\text{TiMe}_2$ precursor whose structure is very similar to the calculated $\text{H}_2\text{SiCp}(t\text{-BuN})\text{TiMe}_2$ system. Our calculated value of -18.0 kcal/mol is in better agreement with this experimental value than the -13.0 kcal/mol obtained previously from ab initio calculations.³⁶ A rough estimate of the electron donating ability of these substituents can be obtained by looking at the change in charge density that occurs in the transformation from the neutral precursor to the ion-pair. Column four in Table 2.3 represents the total charge on the amido ligand in the neutral precursor while the total charge of the same group in the ion-pair appears in column five. In column six is the difference between the previous two columns and the positive number indicates a loss of electron density from the substituent. The observed trend corresponds to the electron donating ability of the substituents.

Table 2.3 Enthalpy Change for Methide Abstraction and Total Charges for the Constrained Geometry Catalyst Precursor as a Function of Substitution on the Nitrogen Atom

R' ^c	$\Delta H_{\text{ipf}}^{\text{a,b}}$ gas phase	$\Delta H_{\text{ipf}}^{\text{a,b}}$ COSMO	Total Charge on neutral	Total Charge in Ion-Pair	Change in Charge Density
H	-13.9	-14.4	-0.21	-0.17	0.04
Methyl	-16.1	-16.4	-0.19	-0.13	0.06
Isopropyl	-16.9	-17.0	-0.18	-0.12	0.06
<i>tert</i> -Butyl	-18.4	-18.0	-0.19	-0.10	0.09

^a Corresponding to the process $\{L\}_2MR_2 + B(C_6F_5)_3 \rightarrow L_2M(R)-(\mu-R)-B(C_6F_5)_3 + \Delta H_{\text{ipf}}$

^b kcal/mol

^c The precatalyst : $\{L\}_2MR_2$; "L" : $H_2SiCp(NR')$, where R' = H, methyl etc.

The effect of methyl substitution on the cyclopentadienyl ligand was also investigated for the bis-cyclopentadienyl system and the results are summarized in Table 2.4. Experimental ΔH_{ipf} values for the methide abstraction for this series of precursors are available the numbers are reproduced in Table 2.4 for comparison. Although there are differences in the calculated and the experimental values, the observed trends are in agreement as both find that the abstraction enthalpy becomes more negative with increasing methyl substitution on the Cp rings. This again emphasizes the influence of electronic factors on the exothermicity of methide abstraction. The more substituted pentamethyl Cp ligand is a better electron donor, and therefore it is more effective at stabilizing the developing cationic center on the metal. The higher electron donating ability of methyl substituted cyclopentadienyl ligands have been demonstrated for a variety of different metal centers.^{8,9,59-61} The calculated value of -24.0 kcal/mol for the 1,2-dimethyl zirconocene is in excellent agreement with the experimentally measured value of -24.3 kcal/mol, while the agreement for the unsubstituted zirconocene is poorer, but it is still reasonable. The major discrepancy between the calculations and the experiments appears in the ΔH value for the pentamethyl analog. The experimental values show a relatively small change of 1.2 kcal/mol between the unsubstituted and

the 1,2-dimethyl zirconocene with a large gap between the 1,2-dimethyl and the pentamethyl analog. On the other hand, the calculated values show a more even distribution with respect to methyl substitution. This is in line with previous measurements of ionization and oxidation potential where a more linear electronic influence was observed with increasing methyl substitution.⁶²⁻⁶⁵

Table 2.4 Enthalpy for methide abstraction as a function of substitution on the cyclopentadienyl ligand.

Substitution on Cp	$\Delta H_{\text{ipf}}^{\text{a,b}}$ gas phase	$\Delta H_{\text{ipf}}^{\text{a,b}}$ COSMO	Experimental ^c
H	-19.1	-19.1	-23.1
1,2-Dimethyl	-23.8	-24.0	-24.3
Pentamethyl	-27.5	-27.8	-36.7

^a Corresponding to the process $\{L\}_2MR_2 + B(C_6F_5)_3 \rightarrow L_2M(R)-(\mu-R)-B(C_6F_5)_3 + \Delta H_{\text{ipf}}$
^b kcal/mol

^c Obtained from reference 11.

2.2.2 Formation of Separated Ion-Pairs - Influence of the Anion on Olefin Complexation

The potential energy surface for the formation of ion-pairs for the CpTiMe₃ catalyst precursor is shown in Figure 2.4. The energies reported include the treatment of solvent effects within the COSMO formalism. The formation of the contact ion-pair can occur via a methyl bridge ([2]1a-Ti) as implied by the crystal structures, but in some cases, metal fluorine interactions have been detected to suggest a fluorine bridged ion-pair.^{1,25} The structure and energy of the μ -F ion-pair ([2]1e-Ti) was investigated. In this co-ordination mode, two of the fluorine atoms on one aryl group is attached to the metal center in a non-symmetric bridge, similar to those observed for the crystal structure of (Me₅Cp)₂ZrH—HB(C₆F₅)₃.⁶⁵ The Ti—F interatomic distances of 2.253 Å and 2.186 Å, are significantly larger than the average terminal Ti—F bond distance of 1.823 Å

found in the crystal structure of tetrafluoro-bis(η^5 -methyl-cyclopentadienyl)-bis(μ -fluoro)-(μ -tetrahydrofuran)-di-titanium.⁶⁶ There is also a slight elongation of the $\mu\text{F}-\text{C}$ distances to 1.371Å and 1.377Å from the average aryl $\text{C}-\text{F}$ distance of 1.329Å. The $\mu\text{-F}$ ion-pair (**[2]1e-Ti**) is much higher in energy (15.4 kcal/mol) than the $\mu\text{-Me}$ ion-pair (**[2]1a-Ti**) for this particular system. This ion-pair (**e**) is of the same order of magnitude above the $\mu\text{-Me}$ contact ion-pair (**a**) for all the other catalyst precursors investigated. Therefore, only the $\mu\text{-Me}$ ion-pair (**a**) is considered in subsequent discussions.

The complexation of the olefin to the metal center must take place in order for the ion-pair to initiate polymerization. One possible pathway for the formation of such a species is for the olefin to insert between the cation and the anion of the contact ion-pair, binding itself to the vacant co-ordination site on the metal. The optimized structure for this olefin separated ion-pair (**[2]1b-Ti**) is shown in Figure 2.4. The π bond of the ethylene is oriented parallel to the Cp ring with the two carbon atoms almost of equal distance from the titanium at 2.510Å and 2.497Å. The anion, $\text{MeB}(\text{C}_6\text{F}_5)_3^-$, however, has been pushed away from the metal center. The $\text{Ti}-\mu\text{-Me}$ distance is now 4.236Å instead of 2.194Å in the contact ion-pair (**[2]1a-Ti**). For this particular system, the olefin separated ion-pair (**[2]1b-Ti**) is 13.5 kcal/mol higher in energy than the sum of **[2]1a-Ti** and ethylene. Although the structure suggests that the anion is only weakly associated with the π -complex, further dissociation to an olefin complexed cation (**[2]1c-Ti**) and the anion requires another 16.4 kcal/mol. Complete dissociation of the contact ion-pair (**[2]1a-Ti**) into the ‘bare’ cation CpTiMe_2^+ (**[2]1d-Ti**) and the anion $\text{MeB}(\text{C}_6\text{F}_5)_3^-$ is on the order of 50 kcal/mol. It is worth mentioning that the present study looks at the olefin uptake process from a difference perspective than previous theoretical studies that did not consider the anion. In the latter cases, the olefin complexation energy was calculated to be exothermic because the reference energy is the ‘bare’ cationic catalyst and ethylene.^{28,31,33} In the present study it is endothermic by 13.5 kcal/mol because the reference was ethylene and the contact ion-pair where the electrophilic metal center is stabilized by the counterion.

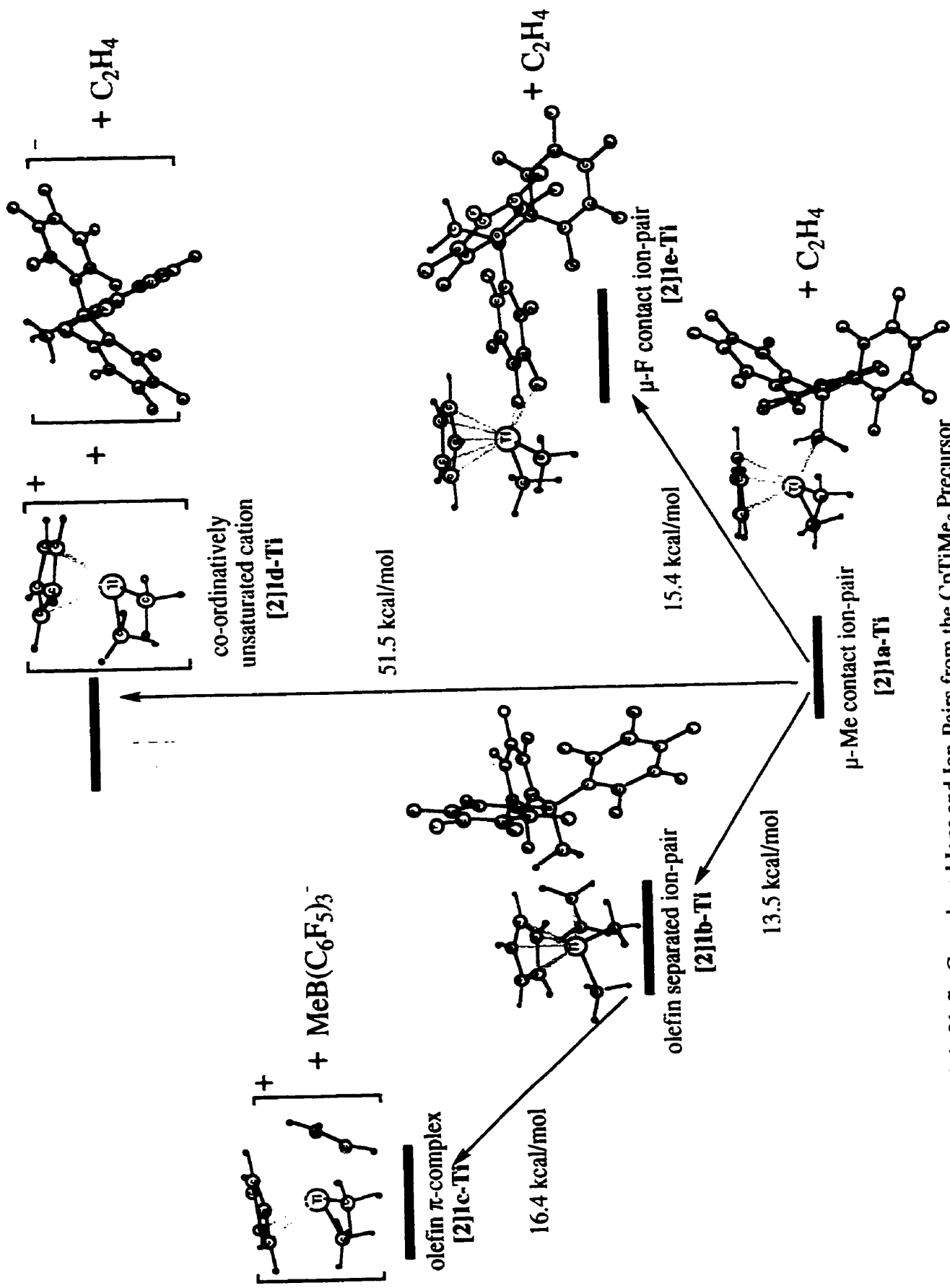


Figure 2.4 Olefin Complexed Ions and Ion-Pairs from the CpTiMe₃ Precursor

The optimized structures for the CpZrMe_3 system are very similar to those obtained for the titanium analog. The relative energies are also similar, with the exception that, relative to the contact ion-pair (**[2]1a-Zr**), the other species on the potential energy surface are located about 2 kcal/mol lower in energy than their corresponding titanium analogs. Another difference is that the olefin separated ion-pair (**[2]1b-Zr**) only 12.6 kcal/mol higher in energy than the contact ion-pair, and that dissociation into the completely separated cationic olefin π -complex (**[2]1c-Zr**) and the anion requires a further 18.3 kcal/mol. Whereas in the titanium system it was 13.5 kcal/mol for the first process and 16.4 kcal/mol for the dissociation, suggesting that the anion is bound more tightly to the zirconium olefin complex than the titanium one.

The relative energies of the olefin complexes and ion-pairs for the constrained geometry titanium precatalyst $\text{H}_2\text{SiCp}(\text{NH})\text{TiMe}_2$ is shown in Figure 2.5. The potential energy surface for the zirconium analog, $\text{H}_2\text{SiCp}(\text{NH})\text{ZrMe}_2$ has similar features and is therefore not reproduced. The behavior of these two systems with regard to olefin complexation is similar to that of the mono-cyclopentadienyl systems. The optimized structures are also similar to their mono-cyclopentadienyl counterparts. The contact ion-pairs (**[2]2a-Ti** and **[2]2a-Zr**) are connected by an unsymmetric methyl bridge. The M—Me distance is 2.162 Å for titanium and 2.340 Å for zirconium, while the Me—B bond distance is 1.634 Å for both metals. In both structures, two of the hydrogen atoms on the bridging methyl group are sufficiently close to the metal that they provide agostic stabilization. The energy required to form the olefin separated ion-pairs (**[2]2b-Ti** and **[2]2b-Zr**) were similar to the mono-cyclopentadienyl systems at 14.3 kcal/mol for titanium and 10.0 kcal/mol for the zirconium catalyst. The complete separation into the olefin complexed cation and the borate anion from this ion-pair requires another 16.7 kcal/mol for the titanium and 20.0 kcal/mol for the zirconium. In contrast to the mono-cyclopentadienyl systems, the coordination mode where the ethylene lies in a plane parallel to the Cp ring was found to be the more stable conformer in both the olefin separated ion-pairs (**[2]2b-Ti** and **[2]2b-Zr**) and the cationic π -complexes (**[2]2c-Ti** and **[2]2c-Zr**). The complete dissociation into the co-ordinately

unsaturated cations (**[2]2d-Ti** and **[2]2d-Zr**) with anion at infinite distance is again the most endothermic of all processes at roughly 50 kcal/mol in solution.

The relative energies of the ion-pairs and separated ions for the Cp_2ZrMe_2 system resembles those of the Cp_2TiMe_2 system, therefore, only the potential energy surface for the titanium precatalyst is shown in Figure 2.6. The energy required for the formation of the olefin separated ion-pairs (**[2]3b-Ti** and **[2]3b-Zr**) is the smallest found of the three systems investigated: 6.1 kcal/mol for titanium and 8.2 kcal/mol for zirconium. Their structures are slightly different from those obtained for the previous two systems. The geometry of the cationic and anionic portions are similar, but the anion has turned in such a way that one of the aryl groups (instead of the methyl group) points toward the metal center. Further dissociation into the separated cationic olefin complexes (**[2]3c-Ti** and **[2]3c-Zr**) is endothermic by 18.1 kcal/mol for the titanium and 20.4 kcal/mol for the zirconium. The infinitely separated the cation (**[2]3d-Ti** and **[2]3d-Zr**) and anion lies 40.3 kcal/mol and 48.5 kcal/mol above the contact ion-pair for the titanium and zirconium, respectively. This confirms again that the co-ordinatively unsaturated cation is most likely non-existent in solution.

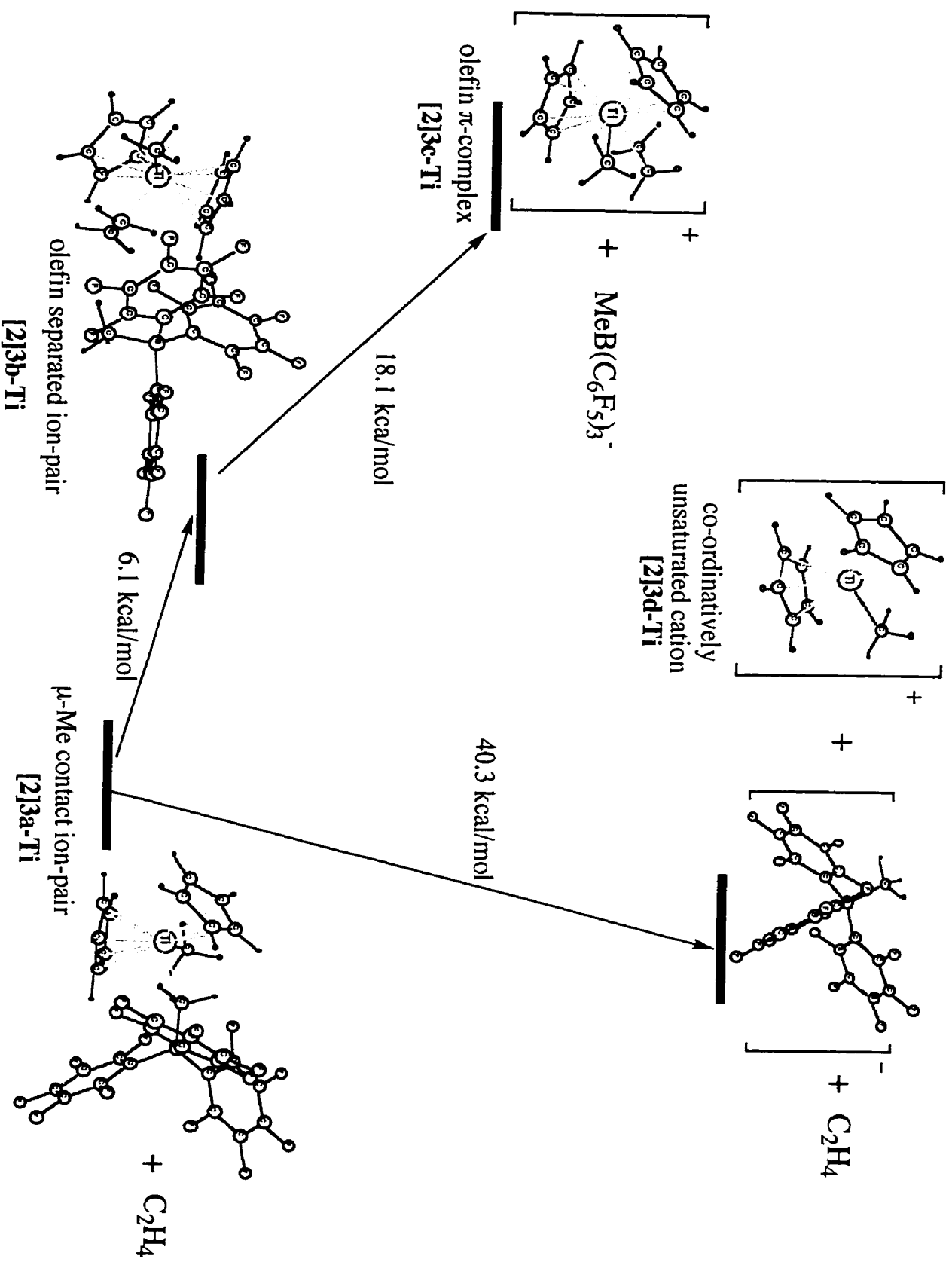


Figure 2.6 Olefin Complexed Ions and Ion-Pairs from the Cp_2TiMe_2 Precursor

2.2.3 Influence of the Solvent on Ion-Pair Formation

The influence of the solvent on ion-pair formation was modelled by explicitly including one molecule of toluene to be treated quantum mechanically along with the solute. The potential energy surface for the formation of complexes and ion-pairs associated with the solvent for the monocyclopentadienyl titanium system appears in Figure 2.7. One molecule of toluene was added to the outside of the contact ion-pair (**[2]1a-Ti**) to determine the short range solvent-solute interactions. This “solvation” does not cause notable changes in the relative stability compared to the contact ion-pair alone. The optimized structure of the solvated contact ion-pair (**[2]1f-Ti**) shows that the midpoint of the toluene aromatic ring is located 4.910 Å from the titanium on the opposite side of the anion and in a plane perpendicular to the Cp ring. There is also no significant change in the geometry of the contact ion-pair moiety, suggesting little explicit interaction between the toluene and **[2]1a-Ti**. Further solvation of the contact ion-pair results in the formation of a solvent separated ion-pair (**[2]1g-Ti**) where the toluene molecule is located between the cation and the anion. As can be seen from the structure shown in Figure 2.7, the toluene adopted an η^6 -coordination to induce a geometry similar to the bis-cyclopentadienyl structure for the cationic moiety. The anion has also turned in such a way that one of the aryl groups is pointing towards toluene. This ion-pair is 7.2 kcal/mol higher in energy than the contact ion-pair (**[2]1a-Ti**) and a free molecule of toluene in the gas phase, however, correcting for solvent effects brings it down in energy to be just slightly more stable than **[2]1a-Ti** at -0.5 kcal/mol. Dissociation of the solvent separated ion-pair lead to the formation of the solvent complexed cation (**[2]1h-Ti**) and the anion $\text{MeB}(\text{C}_6\text{F}_5)_3^-$ which are 20.8 kcal/mol less stable than the contact ion-pair (**[2]1a-Ti**), indicating that the anion still provides significant stabilization to the toluene complexed cationic metal fragment. The relative energies of these toluene associated species are in agreement with experimental results performed on the pentamethyl-cyclopentadienyl system.⁶⁷ Addition of equimolar amounts of $(\text{C}_5\text{Me}_5)\text{TiMe}_3$ and $\text{B}(\text{C}_6\text{F}_5)_3$ in a solution of hexane/toluene (10:1) resulted

in the formation of a μ -Me ion-pair that can be detected by ^1H NMR spectroscopy. Addition of small amounts of toluene to a CD_2Cl_2 solution of this ion-pair resulted in partial (~30%) conversion to the $[(\text{C}_5\text{Me}_5)\text{TiMe}_2(\eta^6\text{-MeC}_6\text{H}_5)][\text{MeB}(\text{C}_6\text{F}_5)_3]$ complex.

The potential energy surface of the CpZrMe_3 system (Figure 2.8) is similar to the titanium system with the exception that the toluene separated ion-pair (**[2]1g-Zr**) is now more stable than the contact ion-pair (**[2]1a-Zr**) by 8.0 kcal/mol. This increase in stability over the titanium system has also been observed experimentally with the pentamethylcyclopentadienyl system. Addition of equimolar amounts of $(\text{Me}_5\text{C}_5)\text{ZrMe}_3$ and $\text{B}(\text{C}_6\text{F}_5)_3$ in a solution of hexane/toluene (10:1) resulted in almost quantitative formation of a $[(\text{Me}_5\text{C}_5)\text{ZrMe}_2(\eta^6\text{-MeC}_6\text{H}_5)][\text{MeB}(\text{C}_6\text{F}_5)_3]$ complex that was isolated as a solid as opposed to the formation of the contact ion-pair in the titanium system.⁶⁶ Further dissociation of this solvent separated ion-pair (**[2]1g-Zr**) into the solvent complexed cation (**[2]1h-Zr**) and the anion is endothermic by 20.4 kcal/mol in solution.

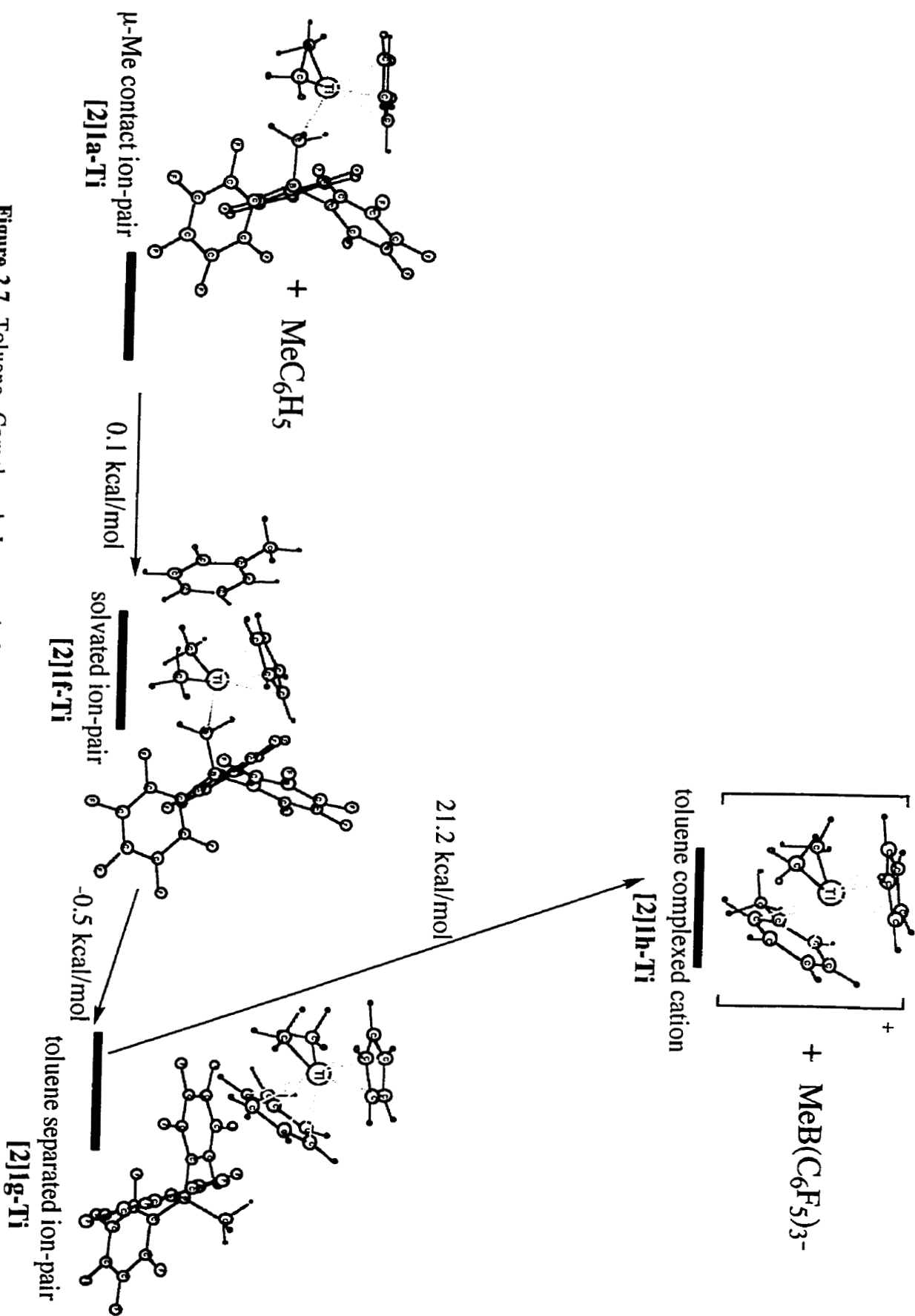


Figure 2.7 Toluene Complexed Ions and Ion-Pairs from the CpTiMe₃ Precursor

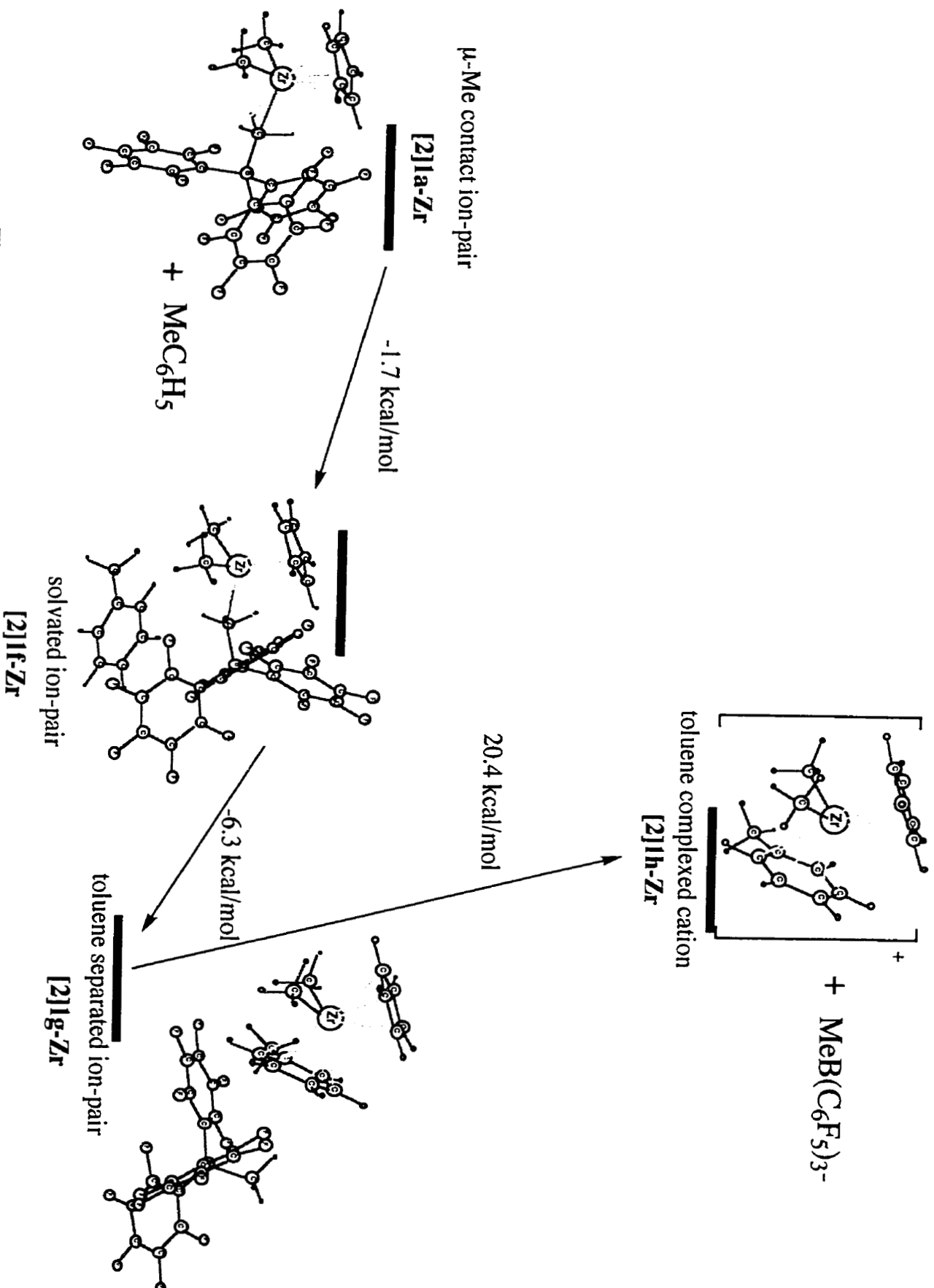


Figure 2.8 Toluene Complexed Ions and Ion-Pairs from the CpZrMe_3 Precursor

The potential energy surface for the formation of complexes and ion-pairs in the presence of toluene is shown in Figure 2.9 and 2.10 for the constrained geometry systems $\text{H}_2\text{SiCp}(\text{NH})\text{TiMe}_2$ and $\text{H}_2\text{SiCp}(\text{NH})\text{ZrMe}_2$, respectively. The solvated ion-pairs (**[2]2f-Ti** and **[2]2f-Zr**) with one molecule of toluene treated quantum mechanically is much more stabilized than the monocyclopentadienyl system at -4.2 kcal/mol for the titanium and -5.2 kcal/mol for the zirconium. In these systems, the aromatic ring of the toluene is parallel to the Cp ring and is located below the cationic moiety of the contact ion-pair. The relatively large "solvation" energy obtained for the constraint geometry systems may be a result of substituting the *tert*-butyl group in the amido ligand with a hydrogen atom in the calculations. The absence of this bulky functional allows for a closer approach of the toluene molecule to the positive metal center, and thus increasing the solvent-solute interaction. The insertion of the toluene molecule into the contact ion-pairs (**[2]2a-Ti** and **[2]2a-Zr**) to form the solvent separated ion-pairs (**[2]2g-Ti** and **[2]2g-Zr**) is endothermic by 8.8 kcal/mol for the titanium while it is thermally neutral for the zirconium system. This is consistent with the much stronger toluene binding energy observed for the zirconium in the monocyclopentadienyl system. The dissociation into the toluene complexed cation (**[2]2h-Ti** and **[2]2h-Zr**) and anion requires 16.5 kcal/mol and 16.7 kcal/mol for the titanium and zirconium respectively.

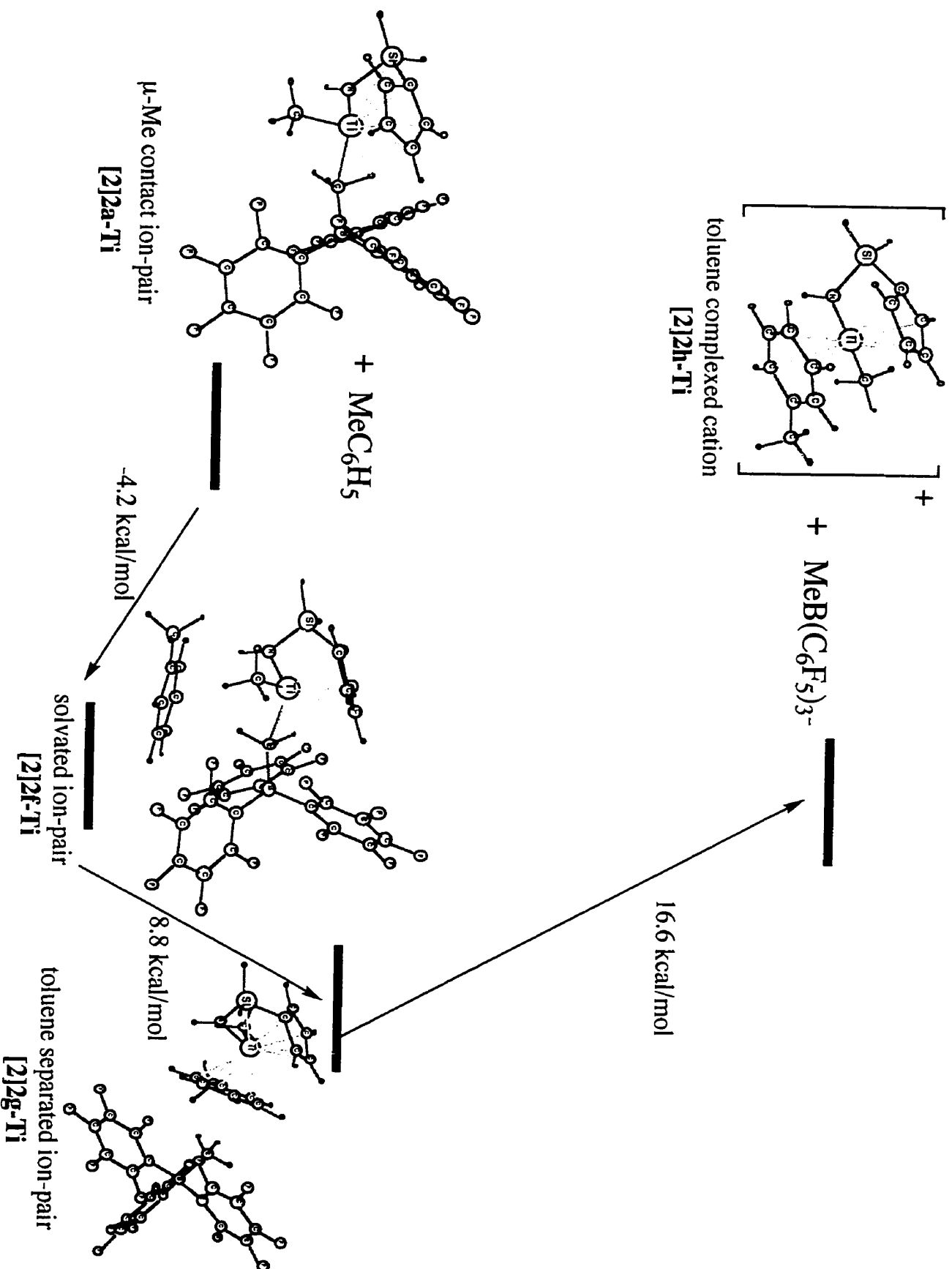


Figure 2.9 Toluene Complexed Ions and Ion-Pairs from the $\text{H}_2\text{SiCp}(\text{NH})\text{TiMe}_2$ Precursor

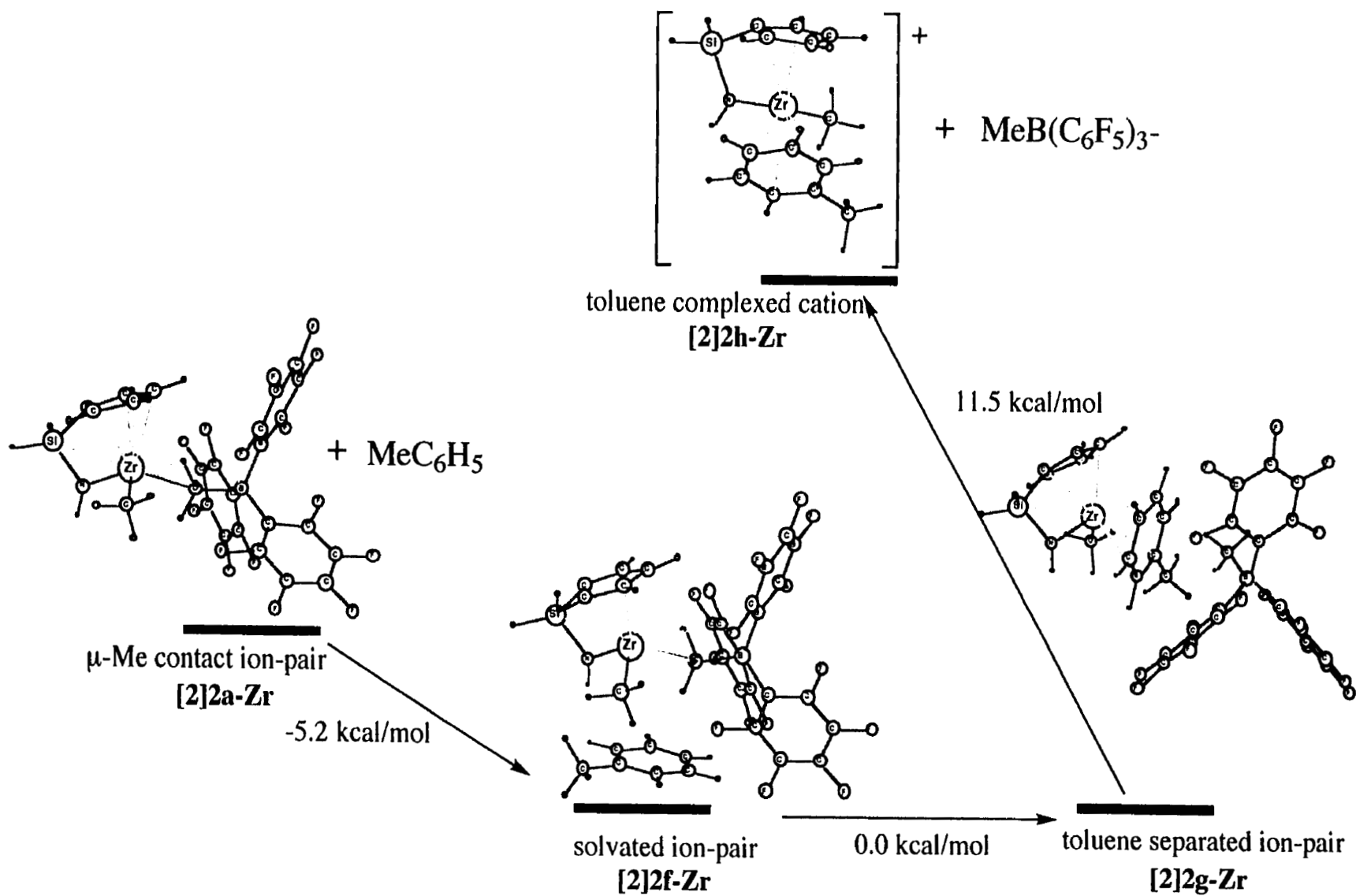


Figure 2.10 Toluene Complexed Ions and Ion-Pairs from the $\text{H}_2\text{SiCp(NH)ZrMe}_2$ Precursor

The potential energy surface for the formation of toluene complexed ion-pairs is shown in Figure 2.11 and for the titanium bis-cyclopentadienyl system. The potential energy surface for the zirconium analog shows similar features and is therefore not shown. The solvated ion-pairs ([2]3f-Ti and [2]3f-Zr) with one molecule of toluene attached is now in the order of 2.5 to 3.0 kcal/mol more stable than the contact ion-pairs ([2]3a-Ti and [2]3b-Zr) suggesting that the explicit interaction between the contact ion-pair with the solvent toluene is larger than the mono-cyclopentadienyl catalysts, but slightly smaller than the constrained geometry catalysts. The most marked contrast between these systems and the two discussed previously is the difference in stability of toluene separated ion-pairs ([2]3g-Ti and [2]3g-Zr), which now lies 20.3 and 17.1 kcal/mol above the solvated ion-pairs ([2]3f-Ti and [2]3f-Zr). The main reason for the relative instability of these species with regard to their mono-cyclopentadienyl and constrained geometry analogs can be attributed to steric factors. The second cyclopentadienyl ligand takes up more room around the metal center than a methyl ligand or an amido ligand. The steric bulk of the second Cp ring prevents the approach of the toluene, resulting in an η^2 rather than an η^6 co-ordination mode. The combination of excess steric repulsion and the decreased electronic stabilization provided by the toluene makes the solvent separated ion-pairs ([2]3g-Ti and [2]3g-Zr) an unfavorable intermediate. Further dissociation into the completely separated toluene complexed cation ([2]3h-Ti and [2]3h-Zr) and anion causes a gain of only 10.2 kcal/mol for the titanium and 11.0 kcal/mol for the zirconium, suggesting that the anion plays a less stabilizing role than in the mono-cyclopentadienyl system

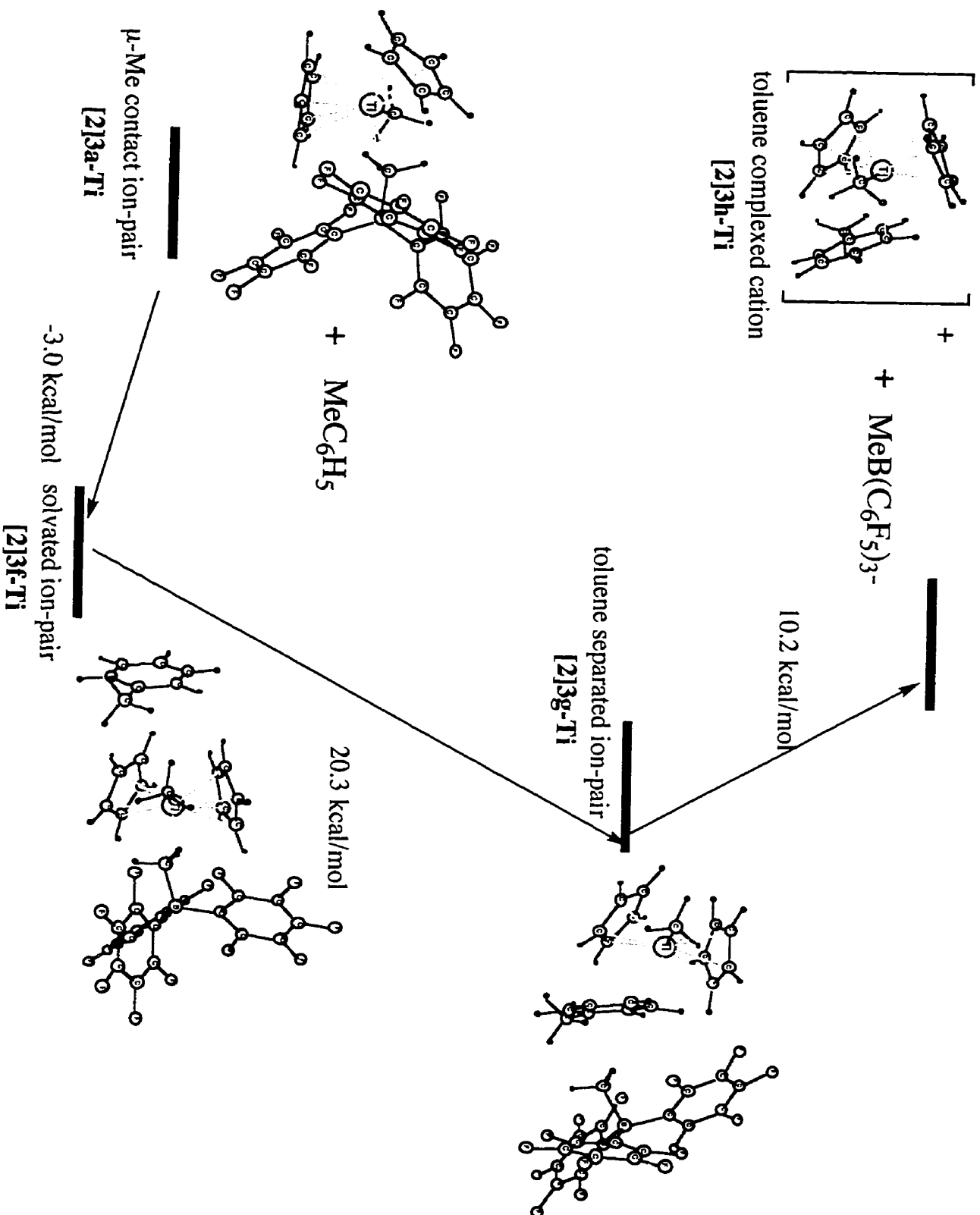


Figure 2.11 Toluene Complexed Ions and Ion-Pairs from the Cp_2TiMe_2 Precursor

2.2.4 Implications for the initial stages of ethylene polymerization

The above data suggest that changes in the ancillary ligands of the catalyst precursor can have a strong influence on the possible mechanism for ethylene complexation. Two distinctively different pathways emerge from the study of the three catalyst systems examined. The first pathway is associated with the mono-cyclopentadienyl and the constrained geometry catalyst systems. These precursors were first investigated with the hypothesis that they would achieve higher catalytic activities than their bis-cyclopentadienyl counterparts. The reasoning behind this was that the activated catalysts would be more electrophilic and less sterically hindered, allowing for more facile complexation of the olefin.¹⁰ While this may be true for the “bare” cations like [2]1d and [2]2d, our calculations suggest that the initial complexation of the olefin to the contact ion-pairs ([2]1a and [2]2a) is endothermic. Dissociation of the contact ion-pairs ([2]1a and [2]2a) to produce the co-ordinatively unsaturated cations ([2]1d and [2]2d) was found to be highly endothermic and therefore, it is unlikely that these species will be present with an appreciable concentration in the reaction mixture. In fact, the energetics show that the species with the cation and anion at infinite separation are at least 14 kcal/mol higher in energy than their analogs with the anion still in the vicinity, stressing the importance of the counterion or co-catalyst.

A proposed mechanism for the initial stages of ethylene polymerization based on our calculations is depicted in Figure 2.12. Starting from the neutral precursors, the most likely species that will form is the contact ion-pair. In toluene, this contact ion-pair can subsequently rearrange to the solvated ion-pair (step 1 of Figure 2.12) followed by the solvent separated ion-pair where one molecule of toluene is bound to the metal cationic moiety (step 2 of Figure 2.12). Both experimental evidence (as discussed in the above section) and the small calculated energy difference between the two species support that the contact ion-pair and the toluene separated ion-pair are in equilibrium. There are significant amounts of both species present for the titanium systems while the equilibrium lies far to the right (in favor of the toluene separated ion-pair) in the zirconium systems. Nevertheless, the formation of the toluene separated ion-pair should be

reversible. Once at the toluene separated ion-pair, the possible reaction pathways are going back to the contact ion-pair or proceeding to the solvent separated ions. The pathway back to the contact ion-pair is energetically more favorable of the two processes. Therefore, there should be a non-zero (albeit small) concentration of the contact ion-pair in solution at all times to facilitate ethylene complexation (step 3 of Figure 2.12). Previous studies without the counterion have indicated that step 4 of Figure 2.12, where the complexed olefin inserts into the growing polymer chain, proceeds with little or no barrier.⁶⁸

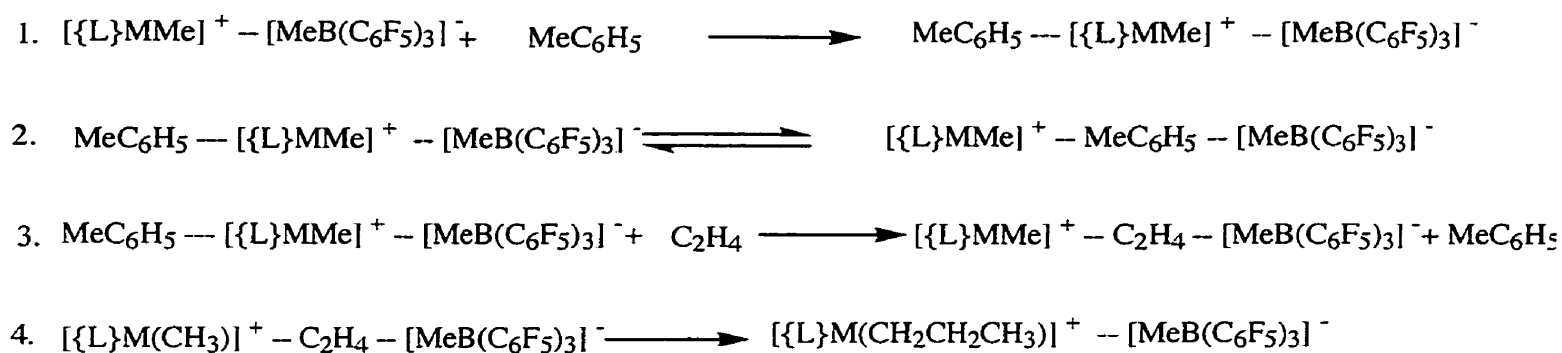


Figure 2.12 Proposed mechanism of activation for the mono-cyclopentadienyl and constrained geometry precursors.

The second mechanism is associated with the bis-cyclopentadienyl systems. The steps are related to the mechanism proposed for the mono-cyclopentadienyl and constrained geometry systems with the exception that step two is thermodynamically unfavorable, with the equilibrium lying far to the left. The steric bulk of the two cyclopentadienyl ligands prevents the co-ordination of the metal center with the toluene, making ethylene complexation a more favorable pathway. Activation of the catalyst precursor leads to the formation of the contact ion-pair and this will proceed directly to the olefin separated ion-pair as the steric hindrance provided by the two Cp ligands is less felt by the olefin because of its small size. Therefore, the bis-cyclopentadienyl systems should be the best catalyst of the three systems investigated, consistent with experimental observations.⁷ This proposed mechanism for the bis-cyclopentadienyl systems contains similar features to the titanocene/MAO and zirconocene/MAO systems studied by Fusco *et al.*^{39,40} In their

calculations, these authors found that the reaction of the metallocene with the co-catalyst to produce a 1:1 contact ion-pair is an exothermic process. Subsequent olefin complexation with this contact ion-pair is an endothermic process due to the displacement of the counter-ion from the metal center. The present calculations and the work of Fusco indicate that olefin separated ion-pairs are key intermediates for olefin polymerization and confirms the hypothesis put forth by Brintzinger of the importance of the formation of olefin separated ion-pairs in the polymerization mechanism.⁶⁹

The above proposed mechanisms are specific to polymerization that is carried out with toluene as the solvent. Different solvents have different co-ordinating abilities and therefore, will influence the relative stability of the solvent separated ion-pairs. The polarity of the solvent will also influence the relative stability of the complexed ion-pairs relative to the separated ions. The results of this study indicate that polymerization would be more facile in the presence of less co-ordinating solvents. A solvent with a higher dielectric constant would encourage charge separation, favoring the formation of solvent separated ions rather than ion-pairs. This would also help facilitate polymerization because the cationic metal center is more accessible to the incoming olefin. An earlier study by Eisch *et al.*⁷⁰ on the $\text{Cp}_2\text{TiCl}_2/\text{AlCl}_3$ and $\text{Cp}_2\text{Ti}(\text{CH}_2\text{SiMe}_3)/\text{AlCl}_3$ systems have found that the dominant type of ion-pair present is dependent on the experimental conditions such as polarity and donor character of the solvent, concentration of the catalyst and temperature. Their results from polymerization studies suggested that the non co-ordinated cation is the most reactive, followed by the contact ion-pair, and finally the arene separated ion-pair if the reaction was performed in arene solvents.

2.3 Concluding Remarks

A density functional study was conducted on the methide abstraction by $\text{B}(\text{C}_6\text{F}_5)_3$ from the mono-cyclopentadienyl, constrained geometry, and bis-cyclopentadienyl catalyst precursors to form a contact ion-pair. The calculations showed that the electron donating ability of the ligands is the most predominant factor in determining the enthalpy for the activation reaction. The higher the electron donating ability of the ligands attached to the metal center, the more negative the enthalpy

of abstraction becomes. The steric bulk of the ligands plays a small, but still significant role in determining the magnitude of the enthalpy change.

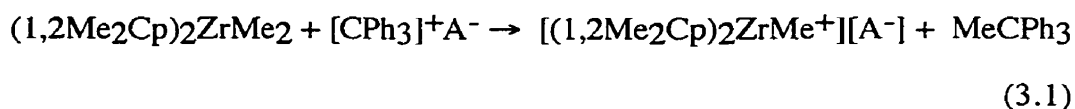
The reactions of the contact ion-pair with ethylene and with the solvent (toluene) was also investigated. The insertion of the ethylene into this contact ion-pair was found to be an endothermic process for all of the catalyst systems studied. The insertion of the toluene in between the contact ion-pair is exothermic for both of the mono-cyclopentadienyl systems and the zirconium constrained geometry catalyst, but endothermic for the titanium constrained geometry and both of the bis-cyclopentadienyl catalysts. The bis-cyclopentadienyl catalysts are predicted to have the highest activity in toluene based on the theoretical results of the present study. The steric bulk of the Cp rings prevents the approach of the toluene, making complexation with the ethylene more favorable. In general, catalysts with large ligands should be more effective in polymerizing small olefins in bulky solvents. For catalysts with less steric bulk, such as the mono-cyclopentadienyl and constrained geometry catalysts, co-ordination with the toluene is more favorable than with the ethylene. These catalysts would show better performance in less co-ordinating solvents.

Chapter 3

Activation of the Metallocene Precursor $(1,2\text{Me}_2\text{Cp})_2\text{ZrMe}_2$ by different Cocatalysts : A DFT study

3.1 Introduction

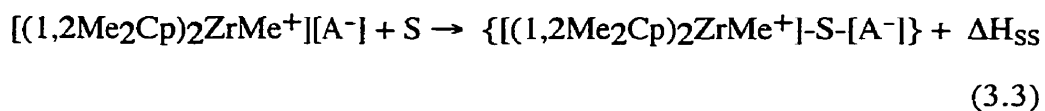
While the previous chapter dealt with the activation of different pre-catalysts by the activator $\text{B}(\text{C}_6\text{F}_5)_3$, this chapter deals with the activation of the lone metallocene precursor $(1,2\text{Me}_2\text{Cp})_2\text{ZrMe}_2$ by different cocatalysts, leading to the formation of the ion-pair. The cocatalysts include boron based compounds [$\text{B}(\text{C}_6\text{F}_5)_3$ and its derivatives, indicated as type [3]1 in this chapter], aluminium compounds [model compound for MAO and other compounds, indicated as type [3]2] and compounds of the type $[\text{CPh}_3]^+[\text{A}^-]$ [type [3]3; $\text{A}^- = \text{B}(\text{C}_6\text{F}_5)_4^-$ and other compounds]. For the type [3]3 activators, the activation, i.e. extraction of the methide group from the $(1,2\text{Me}_2\text{Cp})_2\text{ZrMe}_2$ precatalyst, is done by the trityl cation, $[\text{CPh}_3]^+$, and then the anion A^- forms the ion-pair with the cation $(1,2\text{Me}_2\text{Cp})_2\text{ZrMe}^+$, as shown in equation 3.1 below. The ion-pair thus formed does not have a methide bridge, unlike the ion-pairs formed with activators of the type [3]1 and [3]2 and the ones discussed earlier in the previous chapter.



The process of activation, leading to the formation of the ion-pair, has been discussed earlier with the enthalpy of ion-pair formation having been defined as ΔH_{ipf} . The ion-pair thus formed can then separate to form the separated cationic and anionic species, as shown before. The enthalpy for that process can be defined as the enthalpy of ion-pair separation, ΔH_{ips} :



The formation of the solvent (toluene) separated ion-pair species from such ion-pairs is also investigated, the compounds being analogous to the toluene separated compounds discussed in the previous chapter. The enthalpy of the formation of the solvent separated species is defined as ΔH_{SS} :



S = Solvent, toluene

Based on the values of ΔH_{ipf} , ΔH_{ips} , and ΔH_{SS} obtained for each of the ion-pair systems, the relative abilities of the three types of cocatalysts in activating the precatalyst $(1,2\text{Me}_2\text{Cp})_2\text{ZrMe}_2$ will be discussed and conclusions will be drawn on their effect on catalyst performance. Examples of the structures of the three different types of cocatalysts are shown in Figure 3.1.

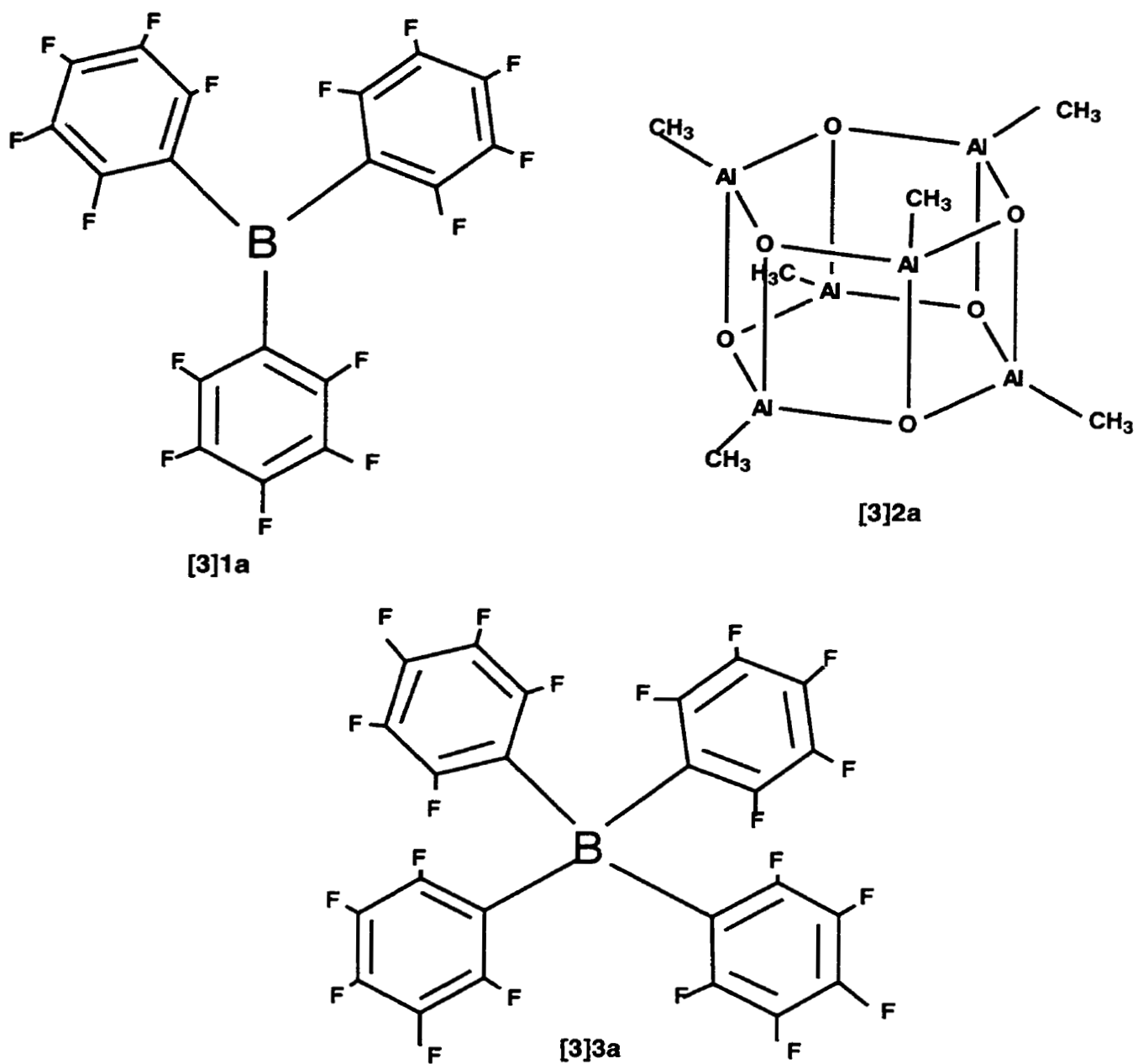


Figure 3.1 Examples of the three different types of activators studied.

3.2 Results and Discussion

3.2.1 Catalyst Activation using Boranes.

The activation of the precatalysts $(1,2\text{-Me}_2\text{Cp})_2\text{ZrMe}_2$ by $\text{B}(\text{C}_6\text{F}_5)_3$ (**[3]1a**) to give the ion-pair $[(1,2\text{-Me}_2\text{Cp})_2\text{ZrMe}]^+[\text{MeB}(\text{C}_6\text{F}_5)_3]^-$ (**[3]1a**) has been studied experimentally.⁷⁻⁸ The crystal structure of the ion-pair that was obtained from these studies revealed that the cation was attached to the anion by a (μ) Zr-Me-B bridge. The Zr-Me (bridging) bond was found to be 0.15 Å longer than the terminal Zr-Me distance. Further, the terminal B-C distances in $\text{B}(\text{C}_6\text{F}_5)_3$ were found to be only slightly longer (0.03 Å) than the bonds in the anionic $\text{B}(\text{C}_6\text{F}_5)_3\text{Me}^-$ species.

The obtained calculated structures are similar to those obtained experimentally. The optimised ion-pair is shown below in Figure 1. A comparison of selected bond angles and bond lengths with the corresponding values in the crystal structure are given below in Table 3.1. The comparison of the optimised $\text{B}(\text{C}_6\text{F}_5)_3\text{Me}^-$ anion (**[3]1a'**) and the neutral co-catalyst **[3]1a** reveals that the three C-B-C angles in the neutral co-catalyst are all roughly equal to 120 degrees while the corresponding angles in the bound anion are decreased to 113 degrees in order to accommodate the methide group. The B-C distances in the anion are also found to increase to 1.62 Å in the anion from 1.54 Å in the neutral for the same reason. The enthalpy of ion-pair formation " ΔH_{ipf} " for **[3]1a** was calculated to be -23.8 kcal/mol which compares very favourably with the experimentally⁷⁻⁸ determined value of -24.0 kcal/mol.

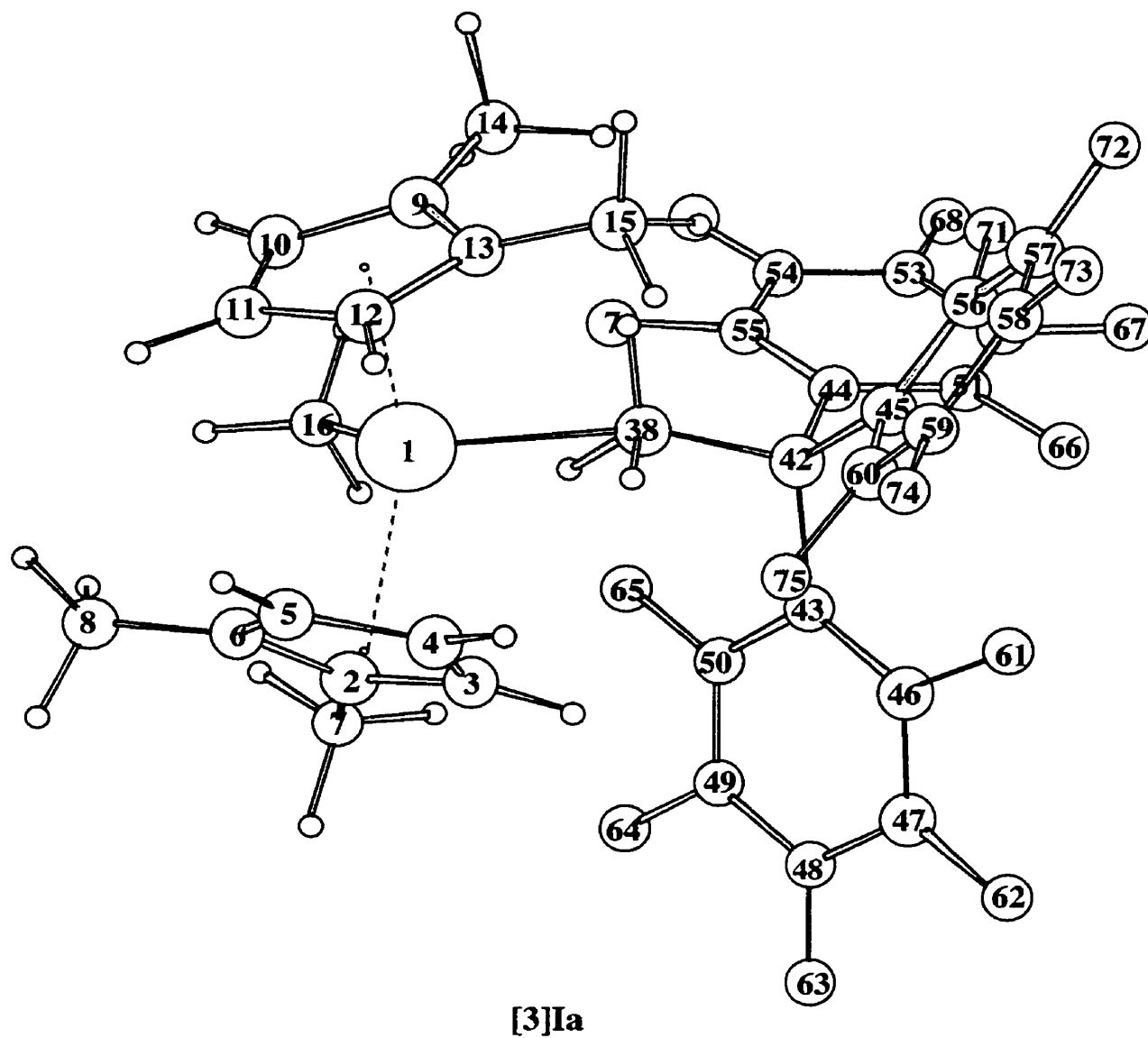


Figure 3.2 LDA optimised structures of the $[(1,2\text{Me}_2\text{Cp})_2\text{ZrMe}]^+[\text{B}(\text{C}_6\text{F}_5)_3\text{Me}]^-$ contact ion-pair

Table 3.1 Selected experimental and calculated bond distances (Å) and bond angles for contact ion-pair **[3]Ia**.

Distances ^b	Expt. ^a	Calc.	Bond Angles ^b	Expt. ^a	Calc.
Zr-C ₂	2.543	2.557	C ₄₃ -B- C ₄₅	106.5	106.8
Zr-C ₃	2.487	2.493	C ₄₃ -B-C ₄₄	112.0	114.7
Zr-C ₄	2.483	2.431	C ₄₄ -B-C ₄₅	114.3	114.1
Zr-C ₅	2.469	2.447	C ₃₈ -B-C ₄₃	112.7	108.1
Zr-C ₉	2.524	2.535	C ₃₈ -B-C ₄₄	114.3	111.1
Zr-C ₁₀	2.475	2.475	C ₃₈ -B-C ₄₅	108.7	101.8
Zr-C ₁₁	2.455	2.431	Zr-C ₃₈ -B	161.8	163.7
Zr-C ₁₂	2.498	2.431	C ₁₆ -Zr-C ₃₈	92.0	93.0
Zr-C ₁₆	2.252	2.263			
Zr-C ₃₈	2.549	2.411			
B-C ₃₈	1.663	1.635			
B-C ₄₃	1.643	1.613			
B-C ₄₅	1.665	1.615			

^a Ref. 7

^b For the numbering scheme see Figure 3.2.

Changes in the electronic density due to the formation of the ion-pair from the precursors was analysed by conducting a charge analysis on the precatalyst, **[3]Ia** and the ion-pair **[3]Ia**. The scheme for the charge analysis shown in Figure 3.2. The total charge on each of the functional groups was calculated by adding the charge present on each atom

of the functional group. The total charge on the functional groups was calculated for the precursors as well as for the ion-pair formed. The charge analysis underlines a distinct flow of electron density from the neutral catalyst precursor to the borane-anion in the ion-pair. The total charge on the cyclopentadienyl rings increased from around -0.90 to about -0.75 in the ion-pair. The positive charge on the boron atom decreased from 1.03 in the neutral precursor to 0.71 in the ion-pair. The negative charge on the C₆F₅ rings increased from -0.34 in the neutral precursor to about -0.45 in the ion-pair. It is clear that the co-catalyst activator B(C₆F₅)₃ is quite effective in withdrawing electron density from the pre-catalyst and this explains why the stability of the subsequent ion-pair formed is quite high. Our charge analysis is consistent with a formulation of the contact ion-pair [3]Ia as [(1,2-Me₂Cp)₂ZrMe]^{q+}[MeB(C₆F₅)₃]^{q-} with q=0.85.

Pre-catalyst		+	Co-catalyst		→	Ion-pair	
[3]P			[3]Ia			[3]Ia	
Zr	2.70		B	1.03		Zr	2.73
Cp ring	-0.90		C ₆ F ₅	-0.347		Cp ring	-0.77
Cp ring	-0.89		C ₆ F ₅	-0.344		Cp ring	-0.75
Methyl	-0.45		C ₆ F ₅	-0.342		Methyl	-0.35
Methyl	-0.45					Methyl	-0.20
						B	0.71
						C ₆ F ₅	-0.44
						C ₆ F ₅	-0.45
						C ₆ F ₅	-0.48

Figure 3.3 Charge analysis of ligands and functional groups in the neutral precursors and ion-pair for the [(1,2Me₂Cp)₂ZrMe]⁺[B(C₆F₅)₃Me]⁻ system.

Varying the number of fluorine atoms in the co-catalyst was found to have a significant effect in the value of ΔH_{ipf} . Deck *et al*¹¹ had experimentally determined that the polymerisation activity decreased with the decrease in the number of fluorine atoms in the co-catalyst. We optimised the structures [3]Ia-f and calculated the value for ΔH_{ipf} for each case. The results are summarized in Table 3.2. The value of ΔH_{ipf} was found to increase almost linearly with the number of fluorine atoms contained in the co-catalyst. The polymerisation activities determined by Deck *et al*¹¹ are also shown in the Table. A graph of ΔH_{ipf} against the number of fluorine atoms is shown below in Figure 3.4.

Table 3.2 Formation energies (ΔH_{ipf}) for methide bridge ion-pairs containing borates.

Co-catalyst	Ion-Pair formed	ΔH_{ipf} Calc. b,c	ΔH_{ipf} Expt. a,c	Activity a,d,e
B(C ₆ F ₅) ₃ - [3]Ia	[3]Ia	-23.8	-24.2	5.2 * 10 ⁶
B(C ₆ F ₅) ₂ (C ₆ H ₃ F ₂) - [3]Ib	[3]Ib	-21.5	-18.7	5.0 * 10 ⁶
B(C ₆ F ₅) ₂ (C ₆ H ₅) - [3]Ic	[3]Ic	-18.3	-14.8	1.3 * 10 ⁵
B(C ₆ F ₅) ₂ {C ₆ H ₃ (CH ₃) ₂ } - [3]Id	[3]Id	-18.0	-10.8	3.4 * 10 ⁵
B(C ₆ H ₅) ₃ - [3]Ie	[3]Ie	-6.7	--	
B(C ₁₀ F ₇) ₃ - [3]If	[3]If	-25.8	--	

^a Obtained from reference 11.

^b Corresponding to the process : (1,2Me₂Cp)₂ZrMe₂ + A → (1,2Me₂Cp)₂ZrMe-(μ-Me)-A + ΔH_{ipf} .

^c kcal/mol.

^d Ethylene polymerisation Activities.

^e (mol catalyst)⁻¹(atm C₂H₄)⁻¹h⁻¹

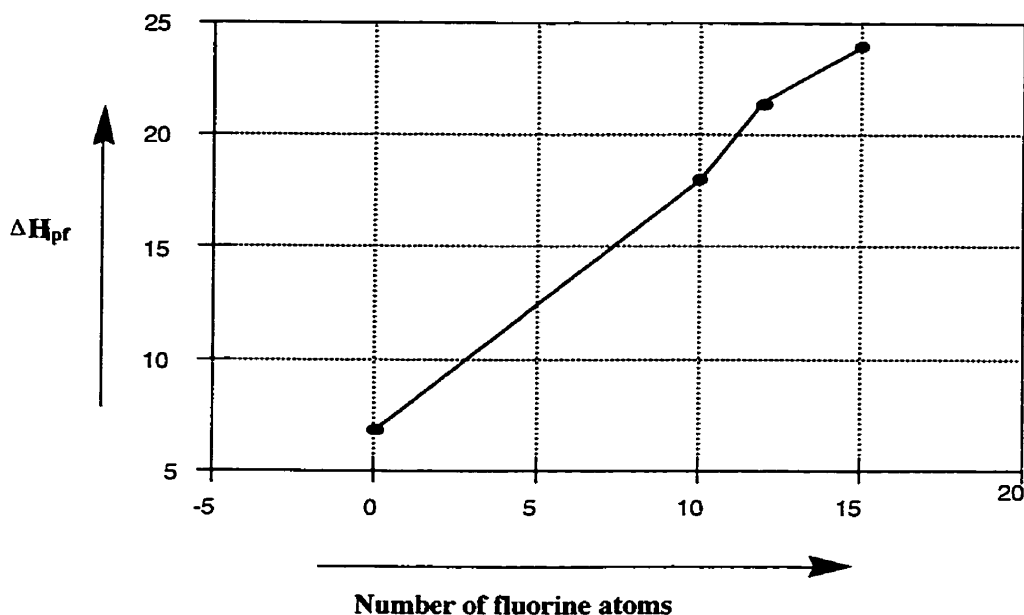


Figure 3.4 Plot of the enthalpy of ion-pair formation against the number of fluorine atoms for a series of ion-pairs with borates as the co-catalyst.

The electron-withdrawing effect of the fluorine atoms is quite clear from the graph - the increase in acidity of the boron centre with the addition of more fluorines was found to lead to greater stability of the ion-pair formed. The resultant increased charge separation between the ions in the ion-pair would also facilitate the separation of the ions in solution. This would explain the higher polymerisation activity of ion-pair systems with more fluorine atoms in the co-catalyst, as experimentally observed by Deck *et al.*¹¹ and shown in Table 3.2. A charge analysis was conducted along the same lines as in the case of [3]Ia for each co-catalyst. It was found that the flow of charge decreased with increasing replacement of the fluorine atoms by hydrogens. A "relative" charge flow index is displayed in Table 3.3 - here we see the difference in charge of a C_6F_5 group in a neutral precursor $B(C_6F_5)_2A$ (where "A" would be C_6F_5 , $C_6H_3F_2$ etc.) compared to the charge of the same C_6F_5 group in the corresponding anion. It is quite clear from the table that increasing the number of fluorine atoms has a decisive effect on increasing the charge flow.

Table 3.3 Total charge on C₆F₅-Group in neutral co-catalyst (A) and corresponding ion-pair (1,2-Me₂Cp)₂ZrMe-(μ-Me)-A

Co-catalyst A	Charge (Co-catalyst A) ^a	Charge (Ion-Pair [3]I) ^b	Charge Flow ^c
B(C ₆ F ₅) ₃	-0.34	-0.48	-0.14
B(C ₆ F ₅) ₂ C ₆ H ₃ F ₂	-0.36	-0.47	-0.11
B(C ₆ F ₅) ₂ C ₆ H ₅	-0.38	-0.46	-0.08

^a Total average charge on each C₆F₅-group in neutral co-catalyst A.

^b Total average charge on each C₆F₅-group in (1,2-Me₂Cp)₂ZrMe-(μ-Me)-A.

^c Total average flow of charge to each C₆F₅-group on ion-pair formation.

One way of improving the activity (and $-\Delta H_{\text{ipf}}$) of the co-catalyst would be to try and increase the number of fluorine atoms in the co-catalyst. This strategy has already been used by Li *et al.*¹⁰ in substituting perfluorophenyl groups by perfluoronaphthyl groups. Despite the steric problems associated with increasing the size of the co-catalyst, thereby making it more difficult to approach the pre-catalyst, this tris(β -perfluoronaphthyl)borane co-catalyst ([3]1f) was found to improve catalyst performance. Calculations were done on the [3]1f-P system. The ΔH_{ipf} was determined to be -25.8 kcal/mol (Table 3.2) which shows that this co-catalyst would indeed be more effective in extracting the methide group from the pre-catalyst.

3.2.2 Aluminum based Co-catalysts

To date the structure of MAO remains unknown. Harlan *et al.*⁵ tested experimentally a hexameric (^tBuAlO)₆ unit as a three dimensional model for MAO and found that it reacted exothermically at room temperature with Cp₂ZrMe₂ to give an activated ion-pair complex. We have, in-line with the experimental work of Harlan *et al.*⁵, employed the hexameric species (MeAlO)₆ ([3]2a) as a model for MAO in the reaction with (1,2-Me₂Cp)₂ZrMe₂ to produce the ion-pair [3]IIa of Figure 3.4. The activation

occurred with the cleavage of one Al-O bond in the model co-catalyst [3]2a, followed by coordination of the cationic zirconium centre to oxygen and migration of one methyl group from zirconium to aluminium. In the optimised ion-pair structure, Figure 3.4, the Zr-C bond distance has increased to 4.6 Å and the Al-C distance adopts the normal bond distance for a Al-C bond of 1.9 Å. The Al-O distance has increased from the normal bond length of 1.8 Å in [3]2a to 3.34 Å [3]IIa so as to facilitate the activation. The key geometrical features of the optimised ion-pair [3]IIa compares well with the corresponding parameters in the experimentally determined⁵ ion-pair structure resulting from the reaction between (tBuAlO)₆ and Cp₂ZrMe₂.

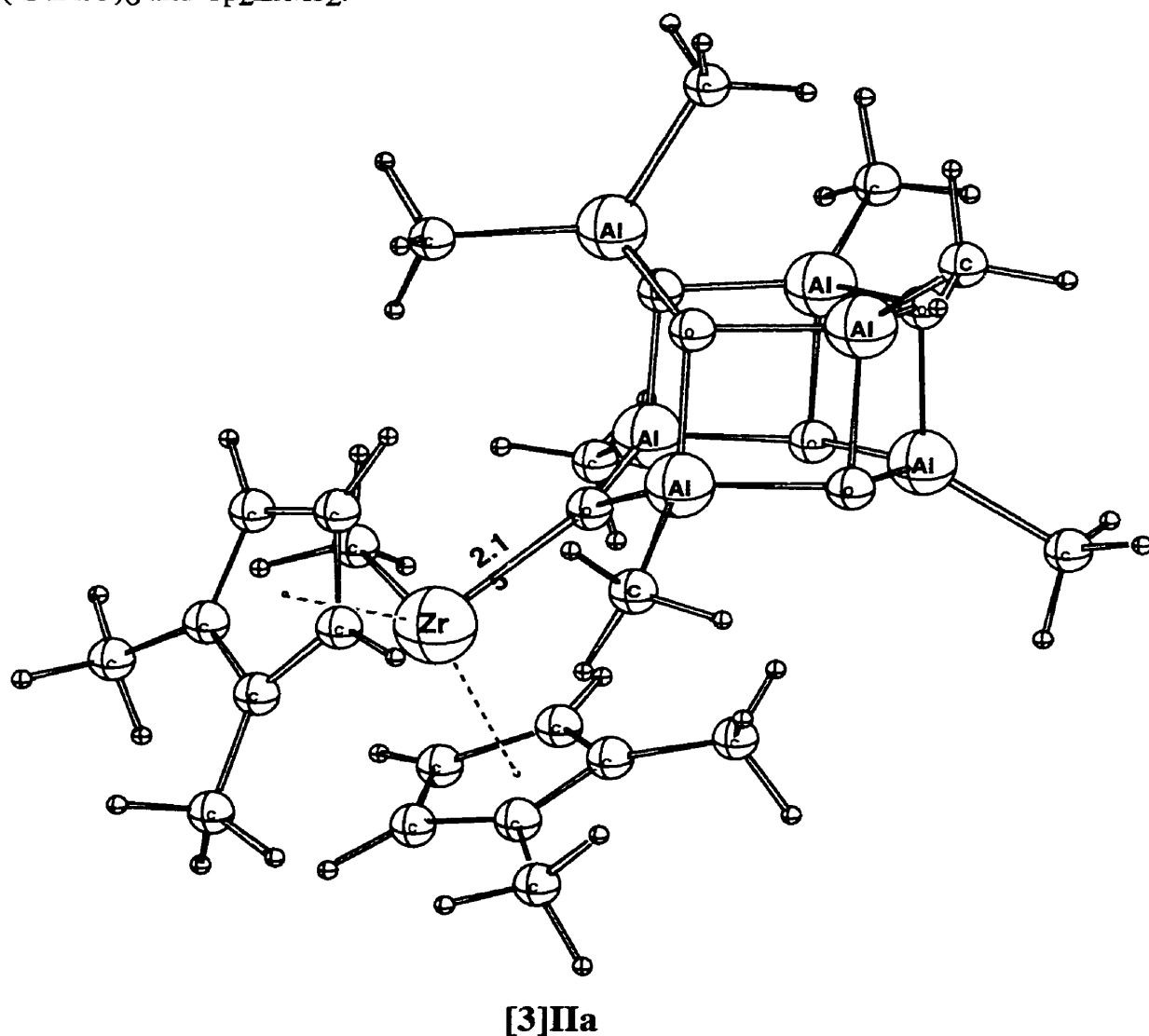


Figure 3.5 Structure of the contact ion-pair formed with MAO as the co-catalyst

The charge analysis of the ion-pair and the precursors is interesting - it shows that there is a flow of charge to the upper ring of two Al-O hexagons. From a 0.0 charge in the neutral species, the upper ring acquires a charge of -0.31 while the lower ring acquires a charge of -0.14. This charge flow in the upper ring is three times the charge flow in the corresponding B(C₆F₅)₃ case, indicating that the charge transfer for the activation using MAO is much more effective than for the boron co-catalysts studied. The scheme for the charge analysis involving the MAO system with pre-catalyst, cocatalyst [3]2a and ion-pair [3]IIa is shown below in Figure 3.6.

Pre-catalyst	+	Co-catalyst	→	Ion-pair	
[3]P		[3]2a		[3]IIa	
Zr	2.70	Upper AlOMe Ring	0.00	Zr	2.73
Cp ring	-0.90	Lower AlOMe Ring	0.00	Cp ring	-0.83
Cp ring	-0.89			Cp ring	-0.82
Methyl	-0.45			Methyl	-0.34
Methyl	-0.45			Methyl	-0.28
				Upper AlOMe Ring	-0.31
				Lower AlOMe Ring	-0.14

Figure 3.6 Charge analysis of ligands and functional groups in the neutral precursors and ion-pair for the [(1,2Me₂Cp)₂ZrMe]⁺[MAOMe]⁻ system.

The value for ΔH_{ipf} was calculated to be -15.9 kcal/mol which compares reasonably well with the experimentally obtained estimate of -10.9 kcal/mol.¹¹ The relatively low value for $-\Delta H_{\text{ipf}}$ can be attributed to the cost of cleaving completely one Al-O bond. The boron equivalent of MAO -"MBO" ([3]2b) was constructed by replacing the

aluminum atoms with borons in the 3D model used for MAO. Ion-pair formation with MBO was also done to test the ability of **[3]2b** to act as a co-catalyst. The value of $-\Delta H_{\text{ipf}}$ was calculated to be 22.3 kcal/mol which is higher than for the corresponding MAO model **[3]2a**, indicating that it might be a better co-catalyst than MAO, if it can be synthesized.

The aluminium analogue of $\text{B}(\text{C}_6\text{F}_5)_3$, $\text{Al}(\text{C}_6\text{F}_5)_3$ (**[3]2d**), was also examined as a co-catalyst. The value of ΔH_{ipf} was calculated to be -30.3 kcal/mol, which means that the ion-pair formed is about 6 kcal/mol more stable than with $\text{B}(\text{C}_6\text{F}_5)_3$. The reason for this increased stability is the stronger Zr-C (bridging) bonding in the $\text{Al}(\text{C}_6\text{F}_5)_3$ case. The Zr-C (bridging) bond was found to be shorter (2.373) in comparison to the Zr-C (bridging) bond (2.411) in the ion-pair formed with $\text{B}(\text{C}_6\text{F}_5)_3$.

We have finally looked at the possibility of AlMe_3 acting as a co-catalyst since the reaction between AlMe_3 and Cp_2ZrMe_2 as well as Cp_2ZrCl_2 has been studied by Siedle *et al.*¹² The reaction between $(1,2\text{-Me}_2\text{Cp})_2\text{ZrMe}_2$ and AlMe_3 to produce the ion-pair **[3]IIc** is only slightly exothermic with $\Delta H_{\text{ipf}} = -8.05$ kcal/mol. Thus, entropy would easily overcome the small favorable ion-pair formation energy and drive the equilibrium towards the two neutral constituents $(1,2\text{-Me}_2\text{Cp})_2\text{ZrMe}_2$ and AlMe_3 . It is quite clear that AlMe_3 would do a poor job as a catalyst activator. The small charge flow to the "anion" formed in **[3]IIc** also bears out this view. Thus according to our charge analysis **[3]IIc** should be formulated as $[(1,2\text{-Me}_2\text{Cp})_2\text{ZrMe}]^{\text{q}+}[\text{AlMe}_4]^{\text{q}-}$ with $q = 0.48$. Structural data for all the contact ion-pairs with a methide bridge are given as supplementary material.

Table 3.4 Formation energies (ΔH_{ipf}) for methide bridge ion-pairs without borates

Co-catalyst	Ion-Pair Formed	$\Delta H_{\text{ipf}}^{\text{b}}$ calc. kcal/mol	ΔH_{ipf} expt. ^a kcal/mol
MAO - [3]2a	[3]IIa	-15.9	-10.9
MBO - [3]2b	[3]IIb	-22.3	--
AlMe ₃ - [3]2c	[3]IIc	-8.1	--
Al(C ₆ F ₅) ₃ - [3]2d	[3]IIId	-30.8	--

^a Obtained from reference 11.

^b Corresponding to the process : $(1,2\text{Me}_2\text{Cp})_2\text{ZrMe}_2 + \text{A} \rightarrow (1,2\text{Me}_2\text{Cp})_2\text{ZrMe}-(\mu\text{-Me})\text{-A} + \Delta H_{\text{ipf}}$.

3.2.3 Ion-Pair Dissociation - Contact Ion-pairs with a Methide Bridge

We have calculated the energy (ΔH_{ips}) required in toluene to separate completely a number of methide bridged contact ion-pairs ([3]Ia, [3]If, [3]IIa-IIId) into $[(1,2\text{-Me}_2\text{Cp})_2\text{ZrMe}]^+$ and $[\text{AMe}]^-$ according to eq. 3.2, (Table 3.5). The required energy is substantial in all cases with $\Delta H_{\text{ips}} = 38.0$ kcal/mol ($\text{A} = \text{B}(\text{C}_6\text{F}_5)_3$) and $\Delta H_{\text{ips}} = 43.6$ kcal/mol ($\text{A} = \text{B}(\text{C}_{10}\text{F}_7)_3$) for the borane systems at the lower end and $\Delta H_{\text{ips}} = 69.2$ kcal/mol for $\text{A} = \text{AlMe}_3$ at the upper limit. In the intermediates range are $\Delta H_{\text{ips}} = 46.9$ kcal/mol ($\text{A} = \text{MBO}$), $\Delta H_{\text{ips}} = 48.3$ kcal/mol ($\text{A} = \text{Al}(\text{C}_6\text{F}_5)_3$) and $\Delta H_{\text{ips}} = 57.0$ kcal/mol ($\text{A} = \text{MAO}$). The trend correlates to some degree with the size of AMe^- and its ability to approach the cation without too much steric congestion. Thus ΔH_{ips} is largest for $\text{A} = \text{AlMe}_3$ where steric repulsion might be at a minimum in the contact ion-pair and smallest for $\text{A} = \text{B}(\text{C}_6\text{F}_5)_3$, $\text{B}(\text{C}_{10}\text{F}_7)_3$ where steric congestion is highest. The generally large values calculated for ΔH_{ips} in the case of the contact ion-pairs ([3]Ia, [3]If, [3]IIa-IIId) can in part be attributed to the strength of the zirconium-methide bond. We know from

calculations from the previous chapter that isomers to **[3]Ia** in which the borate is bound to zirconium through fluorines rather than the methide group are higher in energy.

The calculations would indicate that a complete separation of the methide bridge contact ion-pair into $(1,2\text{-Me}_2\text{Cp})_2\text{ZrMe}^+$ and the AME^- anion is unlikely. Deck *et al.*⁸ have measured an enthalpy of activation of 24.2 kcal/mol for a dissociation process in which the methide group in the contact ion-pair **[3]Ia** is completely transferred from zirconium to boron. Our calculations would indicate that this process is unlikely to be the complete ion separation of Eq. 3.2 for which we calculate a value of $\Delta H_{\text{ips}} = 38.0$ kcal/mol. We shall later show that the process observed by Deck *et al.*⁸ might be consistent with the formation of a solvent separated ion pair according to eq. 3.3.

Table 3.5 Enthalpy of ion-pair dissociation (ΔH_{ips})^a for contact ion-pairs with a methide bridge.

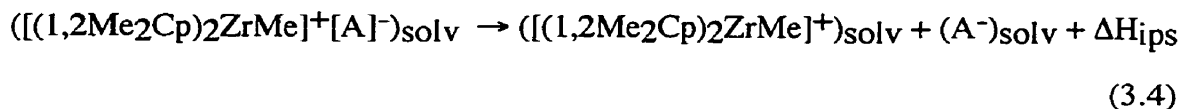
Co-catalyst	Ion-Pair Formed	ΔH_{ips} . ^b Calc
$\text{B}(\text{C}_6\text{F}_5)_3$ - [3]1a	[3]Ia	38.0
$\text{B}(\text{C}_{10}\text{F}_7)_3$ - [3]1f	[3]If	43.6
MAO - [3]2a	[3]IIa	57.0
MBO - [3]2b	[3]IIb	46.9
AlMe_3 - [3]2c	[3]IIc	69.2
$\text{Al}(\text{C}_6\text{F}_5)_3$ - [3]2d	[3]IIId	48.3

^a Corresponding to the process $(\text{Cp}_2\text{M}(\text{Me})-(\mu\text{-Me})\text{-A})_{\text{solv}} \rightarrow ([\text{Cp}_2\text{MMe}]^+)_{\text{solv}} + ([\text{MeA}]^-)_{\text{solv}} + \Delta H_{\text{ips}}$.

^b kcal/mol.

3.2.4 Ion-Pair Dissociation -Contact Ion-Pairs without a Methide Bridge

We have also considered the complete separation of the contact ion-pair $[(1,2\text{Me}_2\text{Cp})_2\text{ZrMe}]^+[\text{A}]^-$ according to the process



where $[(1,2\text{Me}_2\text{Cp})_2\text{ZrMe}]^+[\text{A}]^-$ is formed in the reaction between $(1,2\text{Me}_2\text{Cp})_2\text{ZrMe}_2$ and the activator $[\text{CPh}_3]^+\text{A}^-$. The calculated values for ΔH_{ips} of eq 3.4 are shown in Table 3.6 in the case of $\text{A}^- = \text{B}(\text{C}_6\text{F}_5)_4^-$; $\text{Al}(\text{C}_6\text{F}_5)_4^-$; $(\text{C}_2\text{B}_9\text{H}_{11})_2\text{Co}^-$; and $[\text{tBuCH}_2\text{CH}(\text{B}(\text{C}_6\text{F}_5)_2)_2\text{H}]^-$. This choice reflects key prototypes currently used in experimental studies of $[\text{CPh}_3]^+\text{A}^-$ activators.

Table 3.6 Enthalpy of ion-pair dissociation (ΔH_{ips})^{a,b,c} for C=contact ion-pairs without a methide bridge.

Counterion	Ion-Pair Formed	ΔH_{ips} Calc.
$\text{B}(\text{C}_6\text{F}_5)_4^-$ - [3]3a	[3]IIIa	22.06
$\text{Al}(\text{C}_6\text{F}_5)_4^-$ - [3]3b	[3]IIIb	26.20
$[(\text{C}_2\text{B}_9\text{H}_{11})_2\text{Co}]^-$ - [3]3c	[3]IIIc	34.86
$\{\text{tBuCH}_2\text{CH}[\text{B}(\text{C}_6\text{F}_5)_2]_2\text{H}\}^-$ - [3]3d	[3]IIIId	26.70

^a Corresponding to the process $([\text{Cp}_2\text{M}(\text{Me})]^+[\text{AME}]^-)_{\text{solv}} \rightarrow ([\text{Cp}_2\text{MMe}]^+)_{\text{solv}} + ([\text{MeA}]^-)_{\text{solv}} + \Delta H_{\text{ips}}$.

^b kcal/mol.

^c The solvent is toluene.

The $[(1,2\text{Me}_2\text{Cp})_2\text{ZrMe}]^+[\text{A}]^-$ systems are in general found to have a lower dissociation energy (ΔH_{ips}) than the methide bridged contact ion-pairs due to the larger steric bulk of A^- in comparison to AMe^- as well as the lack of a zirconium-methide interaction in $[(1,2\text{Me}_2\text{Cp})_2\text{ZrMe}]^+[\text{A}]^-$.

The ion-pairs formed from the borates $\text{B}(\text{C}_6\text{F}_5)_4^-$ (**[3]3a**) and $[\text{tBuCH}_2\text{CH}(\text{B}(\text{C}_6\text{F}_5)_2)_2\text{H}]^-$ (**[3]3d**) have the lowest ion-pair dissociation energies of $\Delta H_{\text{ips}} = 22.06$ kcal/mol (**[3]3a**) and $\Delta H_{\text{ips}} = 26.7$ kcal/mol (**[3]3d**), respectively. They are, aside from Coulombic forces, held together by two weak Zr-F interactions. The Zr-F contact distances were found to be 2.56 Å which is much longer than a regular Zr-F bond length of 2.14 Å. The low value for the ΔH_{ips} calculated would account for the high polymerisation activity²¹ observed for ion-pair systems with $\text{B}(\text{C}_6\text{F}_5)_4^-$ as counterion. The low ΔH_{ips} value of the anion **[3]3d** suggested by Li *et al.*¹⁶ is presumably because of its large size. Williams *et al.*¹⁸ have recently developed similar borate anions. Substituting boron in **[3]3a** with aluminum in **[3]3b** increased the value of ΔH_{ips} by around 4 kcal/mol, primarily because the fluorines on **[3]3b** are more negative and thus better able to coordinate to the electrophilic zirconium center. The anion $\text{Al}(\text{C}_6\text{F}_5)_4^-$ has not been synthesized. However, $\text{Al}(\text{C}_{12}\text{F}_9)_3\text{F}^-$ has been examined by Chen *et al.*¹⁷

Carborane anions have been used successfully as A^- in $[\text{CPh}_3]^+[\text{A}^-]$ and $[\text{PhNMe}_2\text{H}]^+[\text{A}]^-$ type activators by Hlatky *et al.*¹⁵ We have carried out calculations on the ion contact ion-pair (**[3]IIIc**) formed between $[(\text{C}_2\text{B}_9\text{H}_{11})_2\text{Co}]^-$ (**[3]3c**) and $(1,2\text{Me}_2\text{Cp})_2\text{ZrMe}^+$. It follows from Table 3.6 that the ion-pair dissociation energy (ΔH_{ips} of eq. 3.4) for **[3]IIIc** is the highest among the contact ion pairs without a methide bridge. We attribute this to a strong Zr-H interaction with a contact distance of 2.0 Å. It is possible that the introduction of per-halogenated carboranes^{19,20} would reduce ΔH_{ips} . Structural data for all the contact ion-pairs without a methyl bridge are given as supplementary material.

3.2.5 Influence of Solvent on Ion-Pair Separation - Implicit Effect

The bulk influence of the solvent on the energy of complete dissociation (ΔH_{ips}) has been studied for a number of contact ion-pairs, as shown in Table 3.7. The dissociation energies (ΔH_{ips}) were evaluated for three different solvents of increasing polarity - toluene ($\epsilon = 2.379$), chlorobenzene ($\epsilon = 5.71$) and 1,2-dichlorobenzene ($\epsilon = 9.93$) and compared to the ΔH_{ips} values determined for the gas phase. Solvent effects were included within the continuum approximation by employing the conductor-like screening model (COSMO) due to Klamt⁵³ as implemented in the ADF program.⁵⁴ It follows from Table 3.7 that ΔH_{ips} is reduced by 50% in going from the gas phase to the non-polar toluene solvent, and another 50% in going from toluene to the polar 1,2-dichlorobenzene solvent. The dependence of solvation energies^{53,54} on the dielectric constant epsilon suggests that adding more polar solvents than 1,2-dichlorobenzene will reduce ΔH_{ips} only marginally. Siedle *et al*¹² found that using dichloromethane ($\epsilon = 9.08$) allowed them to activate Cp_2ZrMe_2 by MAO whereas MAO had failed as a co-catalyst (activator) in toluene ($\epsilon = 2.379$).

Table 3.7 Influence of solvent on the calculated ion-pair dissociation energy (ΔH_{ips})^{a,b}.

Co-catalyst	Ionpair	ΔH_{ips}	ΔH_{ips}	ΔH_{ips}	ΔH_{ips}
		Gas-phase	Toluene	Chloro - benzene	1,2-dichloro- benzene
B(C ₆ F ₅) ₃ - [3]1a	[3]Ia	81.6	38.0	23.4	22.5
B(C ₁₀ F ₇) ₃ - [3]1f	[3]If	77.9	43.6	27.7	22.8
MAO - [3]2a	[3]IIa	101.8	57.0	34.5	30.2
MBO - [3]2b	[3]IIb	91.4	46.9	26.6	20.4
AlMe ₃ - [3]2c	[3]IIc	110.8	69.2	41.6	35.1
Al(C ₆ F ₅) ₃ - [3]2d	[3]IIId	85.7	48.3	31.2	25.9

^a Corresponding to the process (Cp₂M(Me)-(μ-Me)-A)_{solv} → ([Cp₂MMe]⁺)_{solv} + ([MeA]⁻)_{solv} + ΔH_{ips} .

^b kcal/mol.

3.2.6 Influence of Solvent on Ion-Pair Separation - Explicit Effect

Deck *et al.*⁸ employed NMR to detect a process in which the methide group in [3]Ia is completely dissociated from the zirconium metal centre. The process was determined to have a dissociation energy of 24.2 kcal/mol in toluene. Our much higher calculated ΔH_{ips} value of 38.0 kcal/mol (in toluene) would indicate that the process observed by Deck *et al.*⁸ is different from a complete ion-pair dissociation (eq. 3. 2).

An alternative process accounting for the dissociation of the zirconium-methide bond involves the formation of the solvent separated ion-pair (eq.3.3) in which a solvent molecule (S) is sandwiched between two counter-ions. There is experimental⁷⁰ and theoretical³⁶ evidence to support such an explicit role of a single solvent molecule. Thus Eisch *et al.*⁷⁰ were able to use NMR to demonstrate the formation of [Cp₂TiMe]⁺-S-[AlCl₄]⁻ when Cp₂TiMeCl-AlCl₃ was added to arene solvents. In this section we shall

study the possible explicit role of a single solvent molecule in the dissociation of (contact) ion-pairs. Our investigation will include ion-pairs with ([3]Ia, [3]f and [3]IIa-[3]IIId) and without ([3]IIIa-[3]d) a methide bridge.

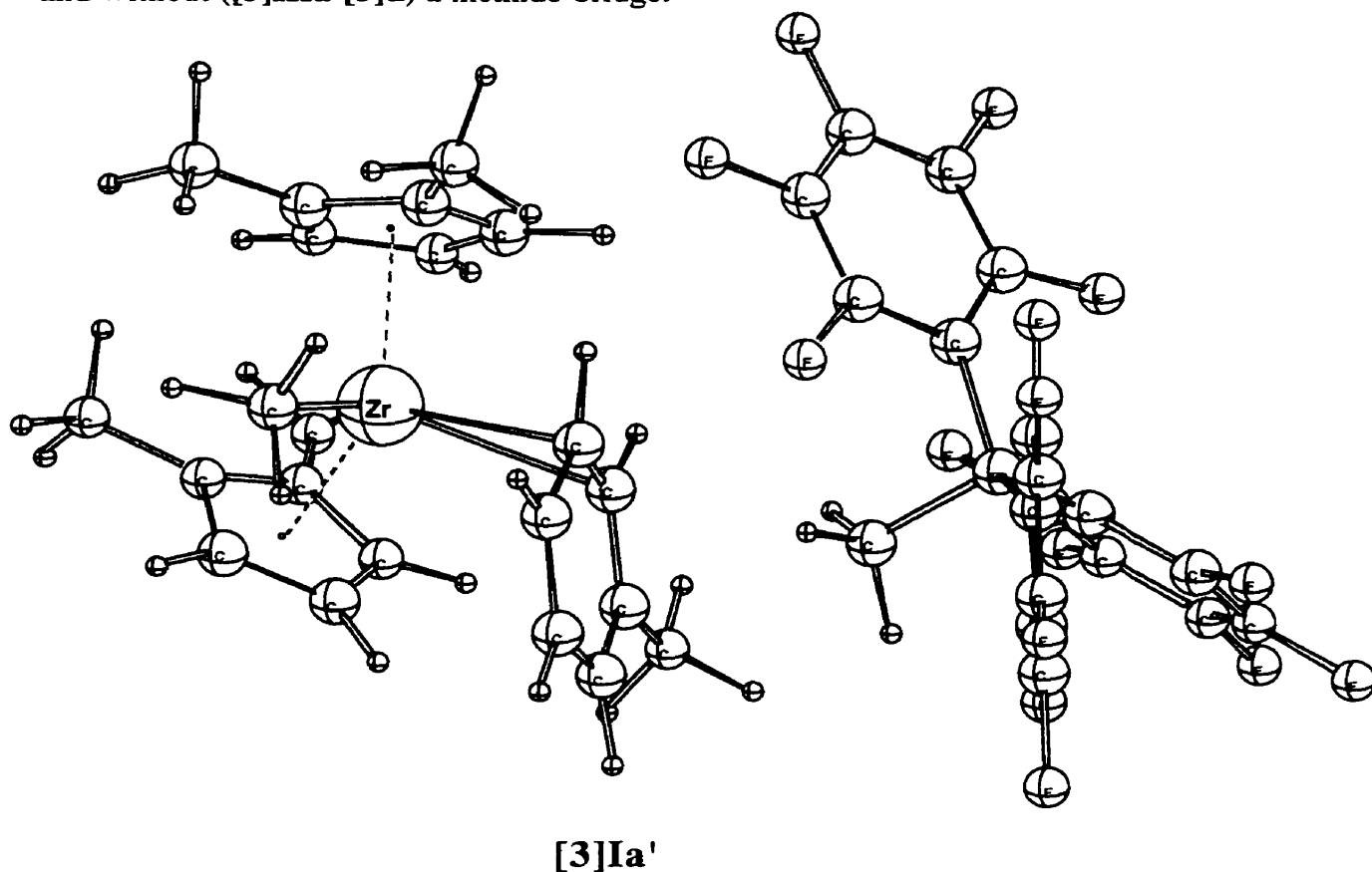


Figure 3.7 LDA optimized structure of the solvent separated ion-pair formed by the $[(1,2\text{Me}_2\text{Cp})_2\text{ZrMe}]^+[\text{B}(\text{C}_6\text{F}_5)_3\text{Me}]^-$ system in toluene.

The energies (ΔH_{SS}) required to convert the methide bridge species [3]Ia-[3]f and [3]IIa-[3]IIId into solvent separated ion-pairs are tabulated in Table 8. The optimized structure for the species [3]Ia' related to [3]Ia is displayed in Figure 3.5. We find in general that the formation of a solvent-separated ion-pair (ΔH_{SS}) for this class of species is more facile than the full ion-pair separation process (ΔH_{IPs}) by 15-20 kcal/mol. For the dissociation of the zirconium-methide bridge in [3]Ia to form [3]Ia' we find a value

(Table 3.8) of $\Delta H_{SS} = 18.7$ kcal/mol which compares reasonably well with the zirconium-methide dissociation energy of 24.2 kcal/mol observed by Deck *et al.*⁸.

Table 3.8 Enthalpy of formation of solvent separated ion-pair (ΔH_{SS})^{b,c} formed from contact ion-pairs with a methide bridge.

Co-catalyst	Solvent Sep. Ion-Pair	ΔH_{SS} Calc.	ΔH_{SS} Expt. ^a
B(C ₆ F ₅) ₃ - [3]1a	[3]Ia'	18.7	24.2
B(C ₁₀ F ₇) ₃ - [3]1f	[3]If'	18.9	--
MAO - [3]2a	[3]IIa'	32.4	--
MBO - [3]2b	[3]IIb'	25.3	--
AlMe ₃ - [3]2c	[3]IIc'	35.3	--
Al(C ₆ F ₅) ₃ - [3]2d	[3]IId'	20.58	--

^a Ref. 11

^b Corresponding to the process $((1,2\text{Me}_2\text{Cp})_2\text{ZrMe}(\mu\text{-Me-A})_{\text{solv}} + \text{S} \rightarrow ((1,2\text{Me}_2\text{Cp})_2\text{ZrMe})^+ \text{-S-}[\text{CH}_3\text{A}]^-)_{\text{solv}} + \Delta H_{\text{ips}}$.

^c kcal/mol.

The contact ion-pairs without a methide bridge ([3]IIIa-[3]IIId) are also seen to prefer separation by a single solvent molecule (ΔH_{SS}) to complete dissociation of the counter-ions (ΔH_{ips}), Table 3.9. Interestingly, for the borates [B(C₆F₅)₄]⁻ and [^tBuCH₂CH(BC₆F₅)₂H]⁻ the formation of [3]IIIa' and [3]IIId', respectively, is exothermic. Thus the borate based species [3]IIIa-[3]IIId can be expected to exhibit the highest degree of separation among all the investigated contact ion-pairs. The value of ΔH_{SS} is close to zero (0.8 Kcal/mol) for the [P'-Al(C₆F₅)₄]⁻ and 7.5 kcal/mol for carborane [(C₂B₉H₁₁)₂Co]⁻. Thus, [3]IIIb and [3]IIIc can be expected to exhibit a high degree of separation as well.

Table 3.9 Enthalpy of formation of solvent separated ion-pair (ΔH_{SS})^{a,b} formed from contact ion-pairs without a methide bridge.

Counterion	Solvent Sep Ion-pair	ΔH_{SS} Calc.
$B(C_6F_5)_4^-$ - [3]3a	IIIa'	-4.2
$Al(C_6F_5)_4^-$ - [3]3b	IIIb'	0.76
$[(C_2B_9H_{11})_2Co]^-$ - [3]3c	IIIc'	7.5
$\{^tBuCH_2CH[B(C_6F_5)_2]_2H\}^-$ - [3]3d	IIId'	-0.58

^a Corresponding to the process $([Cp_2M(Me)]^+[AMe]^-)_{solv} + S \rightarrow ([Cp_2MMe]^+-S-[MeA]^-)_{solv} + \Delta H_{ips}$.

^b kcal/mol.

3.2.7 Coordination of Solvent in Arene Separated Ion-Pairs

Deck *et al.*⁸ have measured the enthalpy of activation for the dissociation of the zirconium-methide bond in [3]Ia for three different solvents - toluene, chlorobenzene, and 1,2-dichlorobenzene. We have optimized the corresponding solvent separated ion-pair geometries for [3]Ia and calculated the related separation enthalpies ΔH_{SS} . In the case of toluene the solvent binds to the zirconium through a η^2 coordination of two carbons in the arene ring. For chlorobenzene and 1,2-dichlorobenzene there are two possibilities - the solvent can coordinate to zirconium in an η^2 fashion as in toluene or it can coordinate through the chlorine(s). Both of these possibilities were investigated for these two solvents. The results are summarised in Table 3.10. The optimised η^1 and η^2 structures for the solvent separated ion-pairs with chlorobenzene [[3]IIIa'(i) and [3]IIIa'(ii)] are shown in Figure 3.8 and Figure 3.9 respectively. For chlorobenzene it was found that the solvent preferred to coordinate through the chlorine (η^1 coordination). However, the

η^2 coordinated conformer was only slightly less stable. The energy required to form the solvent separated ion-pair for the η^1 case was 15.1 kcal/mol while the corresponding energy required to form the η^2 conformation was 15.4 kcal/mol. Thus, it is to be expected that the two conformers could exist in equilibrium with each other. For 1,2-dichlorobenzene, however, the η^2 coordinated ion-pair structure was found to be more stable than the η^1 conformation by 2.1 kcal/mol. The η^1 coordination is less favourable for 1,2-dichlorobenzene (-0.20). The Zr-Cl bond distance is also greater (2.69 Å) for 1,2-dichlorobenzene than for chlorobenzene (2.67 Å)

Table 3.10. Enthalpy of formation of solvent separated ion-pair (ΔH_{SS})^d for ion-pair [3]Ia in three different solvents

Solvent	Solvent Sep Ionpair	ΔH_{SS} Calc.	ΔH_{SS} Expt. ^a
C ₆ H ₅ CH ₃	[3]Ia'	18.7	24.2
(η^1) C ₆ D ₅ Cl ^b	[3]Ia'' (i)	15.1	11.0
(η^2) C ₆ D ₅ Cl ^c	[3]Ia''(ii)	15.4	11.0
(η^1) 1,2-C ₆ D ₄ Cl ₂ ^b	[3]Ia''' (i)	15.9	12.0
(η^2) 1,2-C ₆ D ₄ Cl ₂ ^c	[3]Ia'''(ii)	13.8	12.0

^a Obtained from reference 11.

^b Coordination through one chlorine.

^c Coordination through two carbons.

^d kcal/mol.

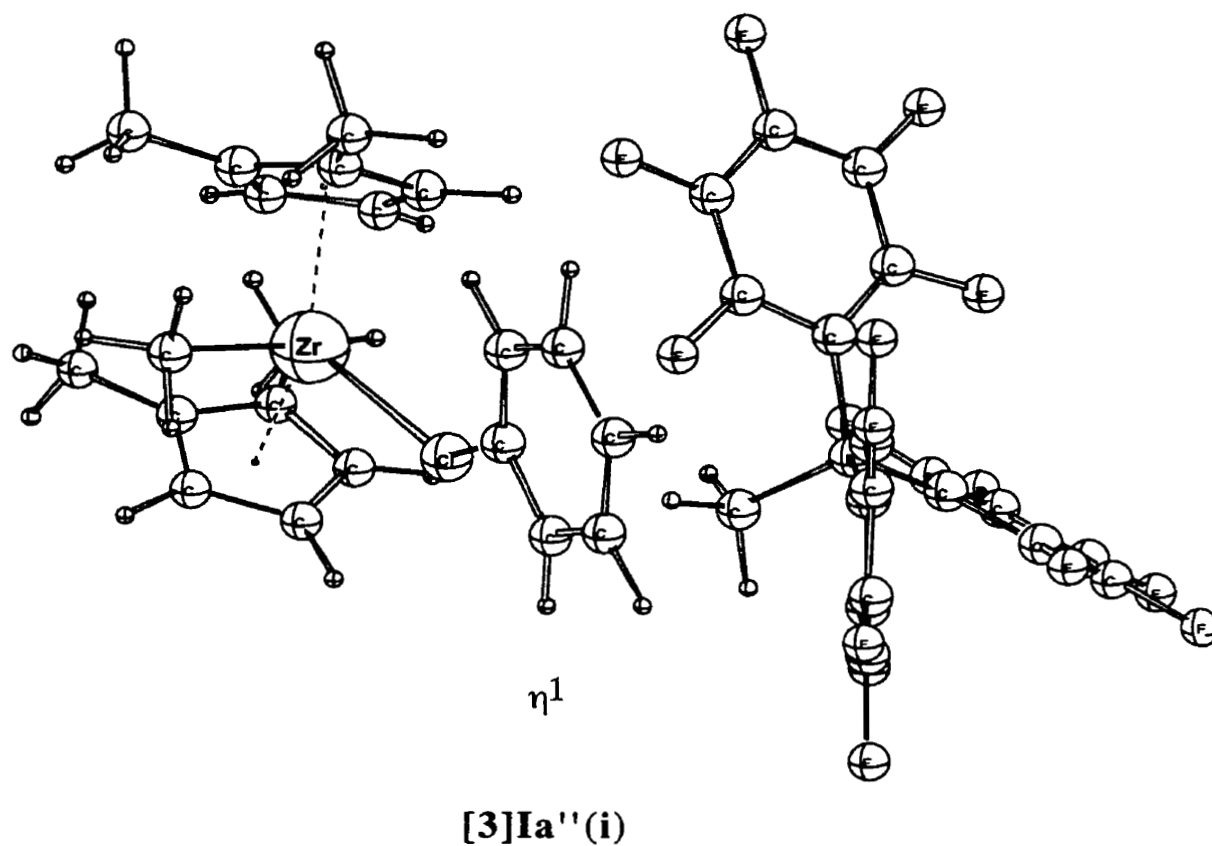


Figure 3.8 LDA optimized structure of the solvent separated ion-pair formed by the $[(1,2\text{Me}_2\text{Cp})_2\text{ZrMe}]^+[\text{B}(\text{C}_6\text{F}_5)_3\text{Me}]^-$ system in chlorobenzene, with the solvent coordinating through the chlorine.

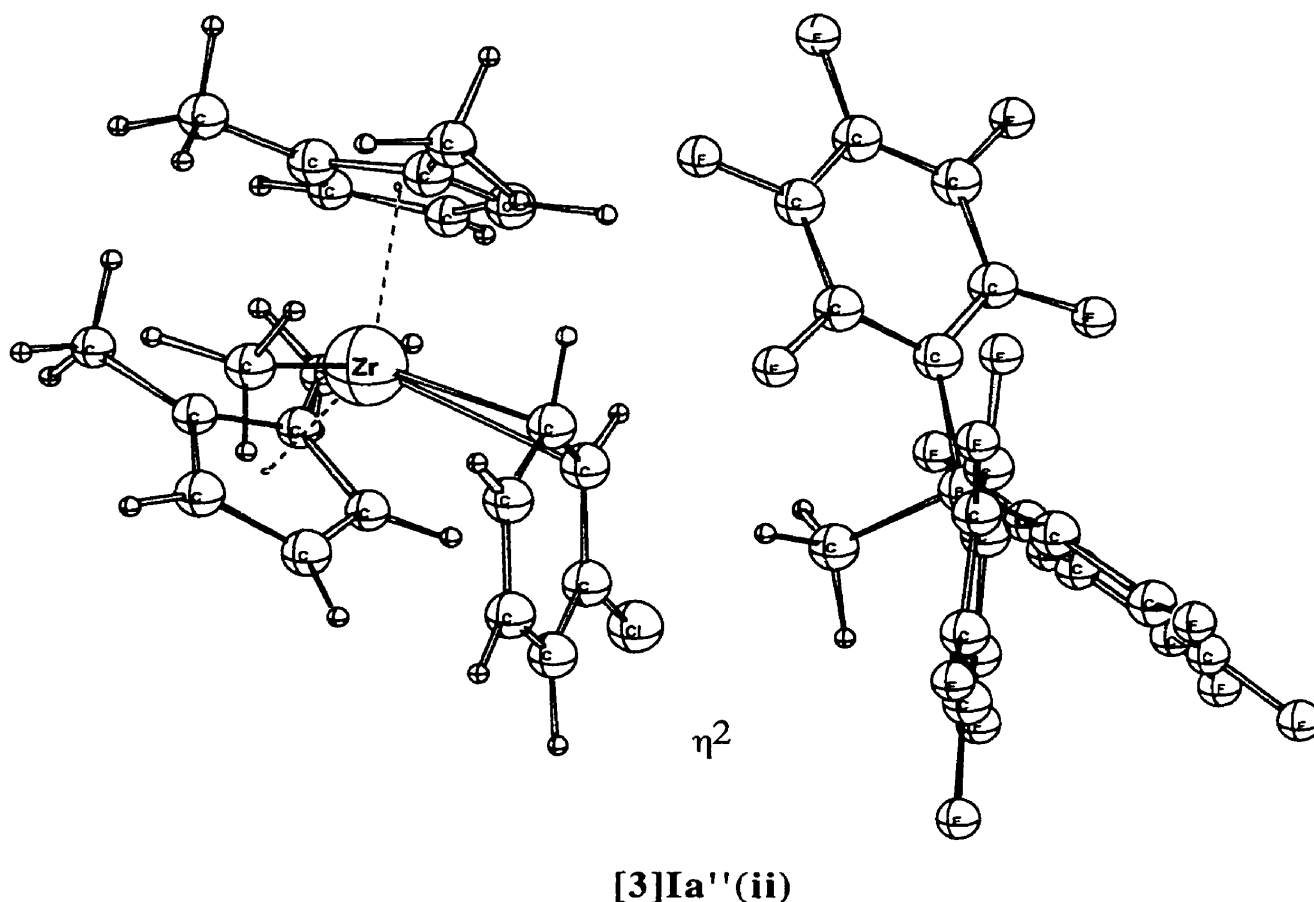


Figure 3.9 LDA optimized structure of the solvent separated ion-pair formed by the $[(1,2\text{Me}_2\text{Cp})_2\text{ZrMe}]^+[\text{B}(\text{C}_6\text{F}_5)_3\text{Me}]^-$ system in chlorobenzene, with the solvent coordinating through two carbons of the benzene ring.

3.3 Concluding remarks

A DFT based study has been carried out on the reaction between the olefin polymerisation pre-catalyst $(1,2\text{Me}_2\text{Cp})_2\text{ZrMe}_2$ and a number of Lewis Acids (**A**) to form the methide bridged (contact) ion-pair $(1,2\text{Me}_2\text{Cp})_2\text{ZrMe}-(\mu\text{-Me})\text{-A}$ (**[3]I**) (eq 3.1). The acids include the boranes $\text{B}(\text{C}_6\text{F}_5)_3$ (**[3]1a**); $\text{B}(\text{C}_6\text{F}_5)_2(\text{C}_6\text{H}_3\text{F}_2)$ (**1b**); $\text{B}(\text{C}_6\text{F}_5)_2(\text{C}_6\text{H}_5)$ (**[3]1c**); $\text{B}(\text{C}_6\text{F}_5)_2(\text{C}_6\text{H}_3(\text{CH}_3)_2)$ (**[3]1d**); $\text{B}(\text{C}_6\text{H}_5)_3$ (**[3]1e**); $\text{B}(\text{C}_{10}\text{F}_7)_3$ (**[3]1f**); as well as $(\text{MeAlO})_6$ (**[3]2a**); $(\text{MeBO})_6$ (**[3]2b**); AlMe_3 (**[3]2c**);

and $\text{Al}(\text{C}_6\text{F}_5)_3$ (**[3]2d**). The charge separation between the $(1,2\text{Me}_2\text{Cp})_2\text{ZrMe}^+$ and MeA^- fragments in **[3]I** was calculated for all **A** and it was found that the charge separation as well as $-\Delta H_{\text{ipf}}$ (negative of the formation enthalpy) increases through the series **[3]1e**, **[3]1c**, **[3]1b** and **[1a]** with the number of fluorine atoms. A good activating Lewis acid (**A**) has the equilibrium shifted strongly from the pre-catalyst and **A** towards **[3]I**, and this is the case for all **A** except **[3]1e** and **[3]2c**.

Also considered was the complete dissociation in solution (toluene) of **[3]I** into the counter-ions $[(1,2\text{Me}_2\text{Cp})_2\text{ZrMe}]^+$ and $[\text{AMe}]^-$ with the dissociation enthalpy ΔH_{ips} as well as the formation from **[3]I** of the solvent separated ion-pair ($\text{S} = \text{toluene}$) $[(1,2\text{Me}_2\text{Cp})_2\text{ZrMe}]^+ \text{-S-} [\text{AMe}]^-$ with the reaction enthalpy ΔH_{ss} . The two types of separation processes have both been postulated as the second and final step in the activation of the pre-catalyst. It is concluded that the formation of $[(1,2\text{Me}_2\text{Cp})_2\text{ZrMe}]^+ \text{-S-} [\text{AMe}]^-$ is the more likely separation process. Consideration has also been given to the influence of solvent polarity on the separation processes with $\text{S} = \text{toluene}$, chlorobenzene and 1,2-dichlorobenzene.

Finally discussed are ΔH_{ips} and ΔH_{ss} for the ion-pair $(1,2\text{Me}_2\text{Cp})_2\text{ZrMe}^+[\text{A}]^-$ (**[3]III**) with $\text{A}^- = \text{B}(\text{C}_6\text{F}_5)_4^-$, **[3]3a**; $\text{Al}(\text{C}_6\text{F}_5)_4^-$, **[3]3b**; $[\text{C}_2\text{B}_9\text{H}_{11})_2\text{Co}]^-$, **[3]3c**; and $\{\text{tBuCH}_2\text{CH}[\text{B}(\text{C}_6\text{F}_5)_2]\text{H}\}^-$; **[3]3d**; where **[3]III** is formed from the reaction of the pre-catalyst $(1,2\text{Me}_2\text{Cp})_2\text{ZrMe}_2$ with the activator $[\text{C}(\text{C}_6\text{H}_5)_3]^+[\text{A}^-]$. It is found that **[3]III** type ion-pairs are easier to dissociate than **[3]I** held together by a methide bridge.

The formation of olefin separated ion-pairs for these systems, analogous to the ones considered in Chapter 2; the competition of the same with the solvent separated ion-pair species, and other competitive processes possible in solution are considered in the next chapter.

Chapter 4

A DFT Study of the Competing Processes Taking Place in Solution during Polymerisation

4.1 Introduction

We have, in the previous chapter, looked at the relative abilities of different cocatalysts and counterions in activating the pre-catalyst $(1,2\text{Me}_2\text{Cp})_2\text{ZrMe}_2$ to produce the cationic catalyst species $(1,2\text{Me}_2\text{Cp})_2\text{ZrMe}^+$ in solution. However the cation once formed may not be readily accessible to the alkene monomer, leading to monomer insertion and hence to polymerisation. Experimental studies^{10,25-27} have revealed that insertion can be inhibited by the competition for the vacant cationic site by the other species present - the neutral catalyst precursor, the activator or the solvent, as shown in Figure 4.1. These competing species can complex to the cation and form dormant products that would have to be dissociated before insertion can proceed. The reaction leading to the formation of such dormant compounds is shown below in Eq. 4.1, with 'D' representing the species coordinating to the cation in solution :



ΔH_{dp} = Enthalpy of dormant product formation

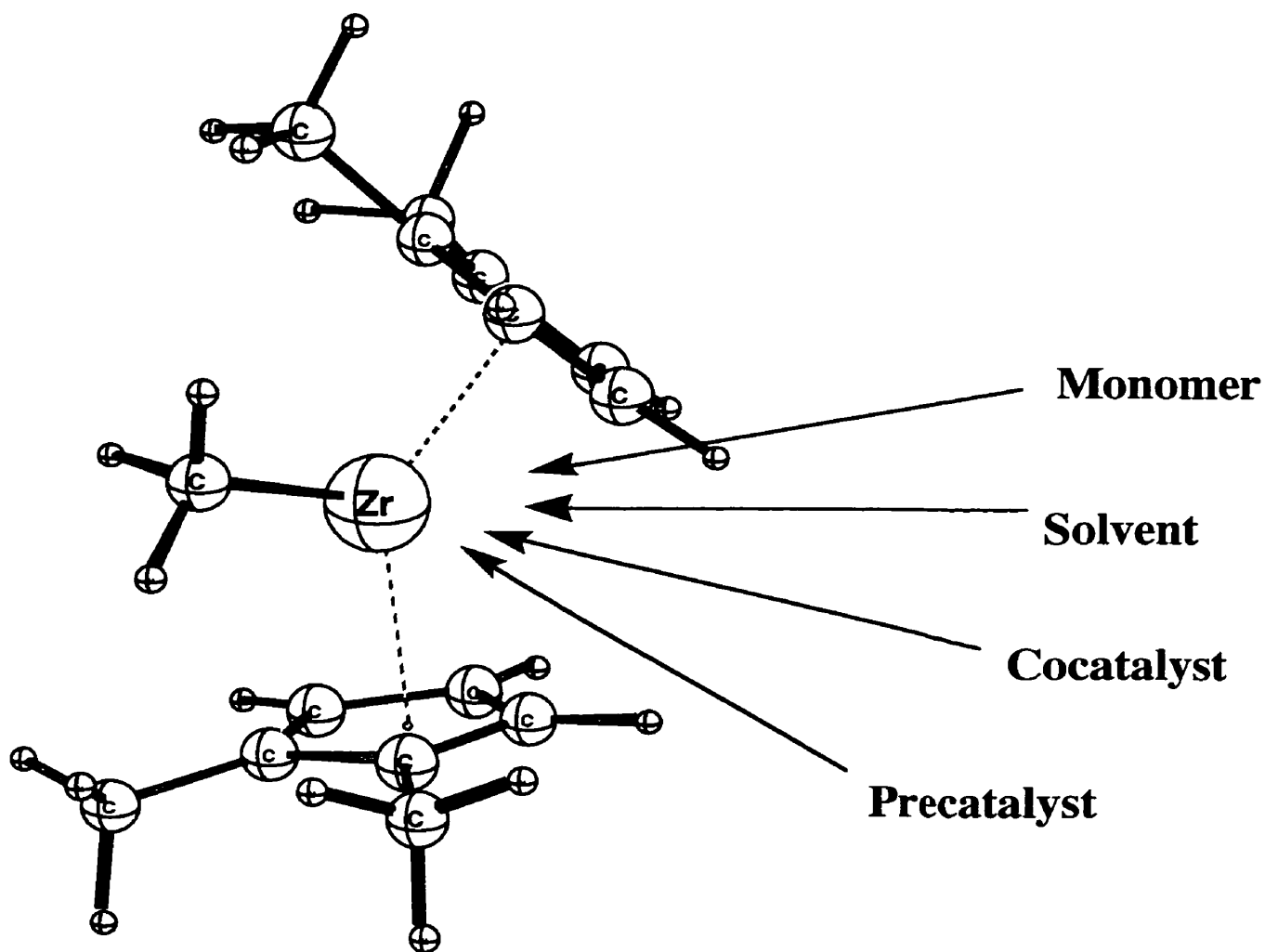
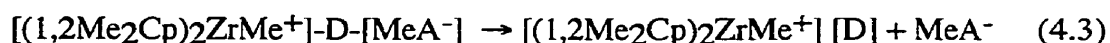
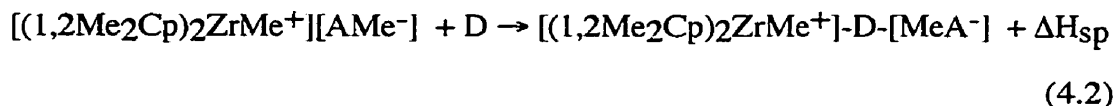


Figure 4.1 Possible competitors for the vacant coordinate site in the cationic catalyst $[(1,2\text{Me}_2\text{Cp})_2\text{ZrMe}]^+$

Moreover, from the results obtained in the previous chapter, it was clear that the total dissociation of the ion-pair formed during activation was an energetically unfavourable process. Hence a possible route to the formation of dormant complexes could be via the dormant species D inserting into the ion-pair and coordinating to the cation, thereby forming a sandwiched compound (equation 4.2). The compound thus formed can then dissociate to form the separated anion and the dormant complex $[(\text{Cp})_2\text{MMe}^+][\text{D}]$ (equation 4.3)



Formation of dormant complexes, as discussed in eqs. 4.1, 4.2 and 4.3 above can explain why the activity of the catalyst systems is low at the beginning of the polymerisation process, as has been experimentally observed.⁷¹⁻⁷³ For polymerisation to occur, the olefin present in solution has to compete successfully with the other species in solution. The olefin monomer can also form analogous olefin separated sandwich complexes prior to insertion into the metal-alkyl bond. A study of the enthalpy of forming such sandwiched ethylene complexes ($\Delta\text{H}_{\text{Es}}$) and a comparison of the same to the $\Delta\text{H}_{\text{Sp}}$ values for the corresponding ion-pair systems can provide an insight into the relative competing abilities of the different species in solution.

This chapter focusses on these competing reactions in solution and attempts to develop an understanding of the different processes that might be taking place at the start of the polymerisation.

4.2 Results and Discussion

4.2.1 Formation of Dormant Products before Monomer Insertion

The formation of dormant products between the catalyst and other species present in solution (eq. 4.1) was studied to determine the feasibility of the formation of such compounds. Marks *et al.*¹⁰ reported the formation of the dormant cationic (μ) complex ([**4**]Ia') between the cation $(1,2\text{-Me}_2\text{Cp})_2\text{ZrMe}^+$ (**P'**) and the precursor $(1,2\text{-Me}_2\text{Cp})_2\text{ZrMe}_2$ (**[4]1a**). The crystal structure of the cationic complex was used as the starting point of our geometry optimisation calculations for this dormant complex. The

optimised geometry is shown below in Figure 4.2. The structure obtained was found to be comparable to the experimental structure obtained by Marks et. al. The methyl bridging the two metal centres was found to be equidistant from the two zirconium metal centres. The Zr-C(bridging) bond length was 0.15 Å longer (2.39 Å) than the corresponding terminal Zr-C bond length.(2.25 Å). Furthermore the two Cp rings on one Zr metal centre were found to be rotated approximately 90 degrees with respect to the Zr-(μ)C-Zr bond to avoid steric interaction with the other two Cp rings. A comparison of selected bond angles and bond lengths with the corresponding values in the crystal structure are given below in Table 4.1.

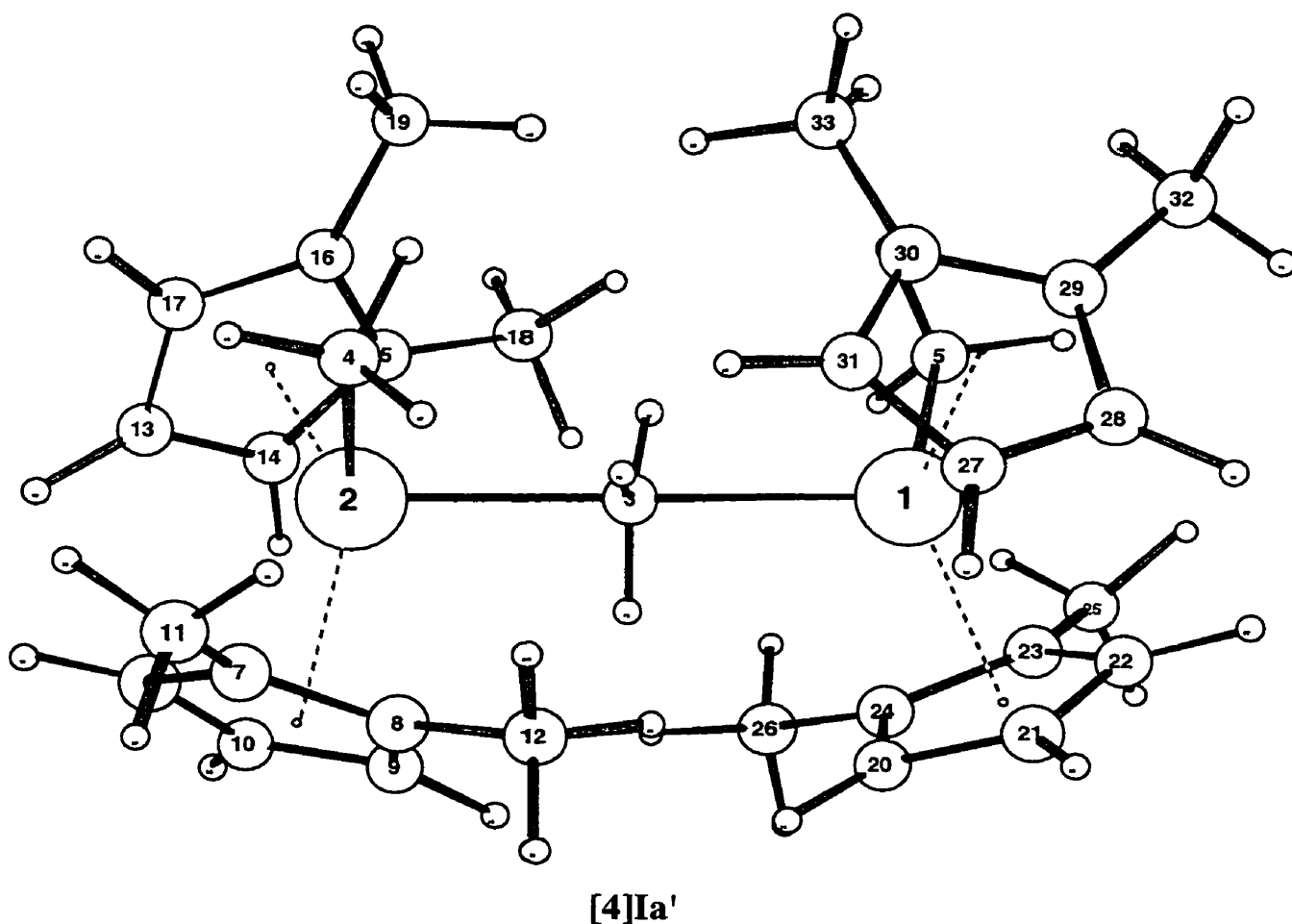


Figure 4.2 LDA optimized structure of the $[(1,2\text{Me}_2\text{Cp})_2\text{ZrMe}]^+ - [(1,2\text{Me}_2\text{Cp})_2\text{ZrMe}]_2$ dormant complex.

Table 4.1 Selected experimental and calculated bond distances (Å) and bond angles for contact ion-pair **[4]Ia**

Distances ^b	Expt. ^a	Calc.	Bond Angles ^b	Expt. ^a	Calc.
Zr1-C3	2.432	2.397	Zr1-C3-Zr2	170.9	171.1
Zr2-C3	2.405	2.377	C3-Zr2-C4	92.0	92.9
Zr1-C5	2.235	2.257	C3-Zr1-C5	93.7	93.3
Zr2-C4	2.255	2.260	C3-Zr2-C8	84.1	83.3
Zr2-C6	2.451	2.453	C3-Zr2-C9	81.8	81.7
Zr2-C7	2.574	2.534	C3-Zr2-C10	110.5	111.0
Zr2-C8	2.574	2.535	C3-Zr1-C27	102.0	104.1
Zr2-C9	2.508	2.495	C3-Zr1-C28	132.0	134.3
Zr2-C10	2.452	2.451	C3-Zr1-C29	121.5	123.2
Zr1-C27	2.476	2.442			
Zr1-C28	2.480	2.446			
Zr1-C29	2.551	2.523			
Zr1-C30	2.548	2.550			
Zr1-C31	2.512	2.502			

^a Obtained from reference 10.

^b For the numbering scheme see Figure 4.2.

The value of ΔH_{dpf} for the formation of **[4]Ia'** was calculated to be -25.2 kcal/mol. The complex formed between the cation **P'** and the co-catalyst, $\text{B}(\text{C}_6\text{F}_5)_3$ (**[4]Ib'**), solvent $\text{C}_6\text{H}_5\text{CH}_3$ (**[4]Ic'**) and TMA (**[4]Id'**) were also optimised to

determine the enthalpy of formation of these complexes with the cation. The results are shown below in Table 4.2.

Table 4.2 Enthalpy of formation of dormant products (ΔH_{dp})^{a,b} from the coordinated complex for species [4]1a to [4]1d.

Species	Complex Formed	ΔH_{dp} Calc. ^{a,b}
(1,2Me ₂ Cp) ₂ ZrMe ₂ - [4]1a	[4]1a'	-25.8
B(C ₆ F ₅) ₃ - [4]1b	[4]1b'	-9.9
C ₆ H ₅ CH ₃ - [4]1c	[4]1c'	-10.1
AlMe ₃ - [4]1d	[4]1d'	-25.5

^a Corresponding to the process $(1,2\text{Me}_2\text{Cp})_2\text{ZrMe}^+ + [\text{D}] \rightarrow [(1,2\text{Me}_2\text{Cp})_2\text{MMe}^+][\text{D}] + \Delta H_{dp}$

^b kcal/mol.

The values of ΔH_{dp} for [4]1b' and [4]1c' [-10.1 kcal/mol and -9.9 kcal/mol respectively] show that the formation of these compounds would not be very favourable processes. Therefore the co-catalyst and the solvent are not expected to be as effective in competing for the catalyst site as the counterion, pre-catalyst or TMA ($\Delta H_{dp} = -25.5$ kcal/mol). The optimized complex formed with TMA is shown below in Figure 4.3. In this case the 4 centred bridge complex was found to be the more stable structure for the complex, instead of the μ -methyl bridged complex. This is in agreement with the structures observed experimentally²³ by NMR spectroscopy. The significant value of ΔH_{dp} for the formation of this compound [4]1d' bears out the view that TMA can be an inhibiting agent in catalyst systems activated by MAO or in systems where it is used as a scavenger.

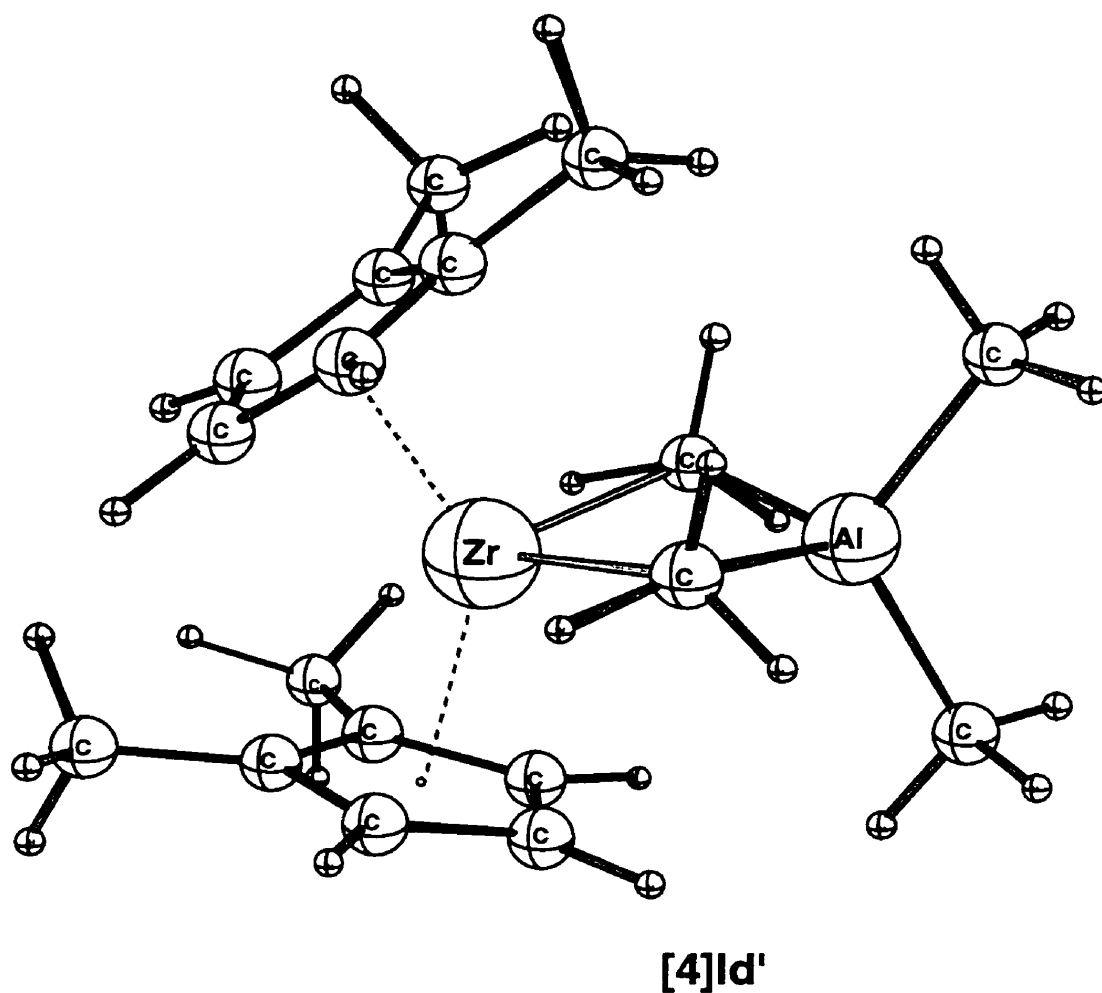


Figure 4.3 LDA optimized structure of the $[(1,2\text{Me}_2\text{Cp})_2\text{ZrMe}]^+-\text{AlMe}_3$ dormant complex

The enthalpy for the formation of the ion-pair from the cation and the counterion $\text{B}(\text{C}_6\text{F}_5)_3\text{CH}_3^-$ ([4]1a) was determined to be -38.2 kcal/mol, as discussed earlier in Chapter 3. This implies that for any of the other species discussed above to dislodge the anion [4]1a completely from the ion-pair and make the dormant species would be thermodynamically unfavourable, given the numbers obtained in Table 4.2. However the competing species, **D**, can coordinate to the cation in the presence of the anion, as shown in eq.4.2, forming sandwiched compounds. The possibility of formation of such a sandwiched compound with TMA is discussed later. However in systems with bigger

counterions [eg. $B(C_6F_5)_4^-$ (**[4]3a**) etc.] where the enthalpy of formation of the ion-pair from the cation **[4]P'** and the anion is of the range 25-30 kcal/mol, the formation of such inhibiting compounds by completely dislodging the anion from the vicinity of the ion-pair may well be a possibility.

4.2.2 Complexes formed after Ethylene Monomer Insertion

Compounds **[4]Ia'** and **[4]Id'** had been observed, as stated earlier, by X-Ray analysis, but Tritto *et al.*²³ did not observe the corresponding dormant complexes after the insertion of one, or more, monomer units into the zirconium - methyl bond. This was explained by assuming that the dormant complexes formed after insertion of the monomer were less stable. We tested this hypothesis by optimising the complexes (**[4]1a''** and **[4]1d''**) formed from the reaction between the pre-catalyst **[4]1a** and TMA with the cation, after insertion of one ethylene monomer into the zirconium-carbon bond to form the propyl chain. The other two competing species - co-catalyst and solvent - were not considered because the calculations with the **[4]Ib'** and **[4]Ic'** complexes formed with such compounds had shown that they are not strong competitors for the cationic site. For the geometry of the cationic complex **[4]Id''** three possible ways of coordination of TMA to the cation were considered. One mode of coordination was through the two methyl groups, forming the 4-centred bridge complex **[4]Id''(iii)**, similar to the structure studied earlier before monomer insertion (**[4]Id'**). The other structure considered was the (μ) methyl bridged complex **[4]Id''(ii)**, stabilised by a beta-agostic interaction, and the (μ) methyl bridged complex without a beta agostic interaction **[4]1d''(i)**. The structures considered for the three possibilities are shown below in Figure 4.4. Calculations showed that **[4]Id''(iii)** was more stable by about 3.9 kcal/mol in comparison to **[4]Id''(ii)** and by about 7.8 kcal/mol in comparison to **[4]Id''(i)**. Hence the enthalpy of formation of the structure **[4]Id''(iii)** was used to determine the values of ΔH_{dp} . For the case of the precatalyst **P**, two structures were considered, as shown in Figure 4.5 - the (μ) methyl

bridged complexes with and without a beta-agostic interaction. ([4]Ia''(ii) and [4]Ia''(i) respectively). The 4-centred bridge structure was not considered as it was clear that high steric hindrance would make that a highly unstable structure. Calculations showed that the structure [4]Ia''(i), without beta-agostic interactions, was 8.4 kcal/mol more stable than [4]Ia''(ii). Hence the formation of the complex was considered to determine the value of ΔH_{dp} . The results are shown in Table 4.3. The values indicate that the [4]Ia'' and [4]Id'' complexes are indeed less stable than the corresponding [4]Ia' and [4]Id' complexes by about 10 kcal/mol. This implies that though the formation of such complexes cannot be ruled out, it is possible that with the increase in the size of the alkyl chain, the stability, and hence the competing ability, of the dormant complexes formed in solution is decreased.

Table 4.3 Enthalpy of formation of dormant products (ΔH_{dp})^{a,b} from the coordinated complex for the species [4]1a and [4]1d, after the insertion of the ethylene monomer.

Species	Complex Formed	ΔH_{dp} Calc. a,b
(1,2Me ₂ Cp) ₂ ZrMe ₂ - [4]1a	[4]Ia''	-14.5
AlMe ₃ - [4]1d	[4]Id''	-15.0

^a Corresponding to the process $(1,2Me_2Cp)_2ZrMe^+ + [D] \rightarrow [(1,2Me_2Cp)_2ZrMe^+][D]$

+ ΔH_{dp}

^b kcal/mol.

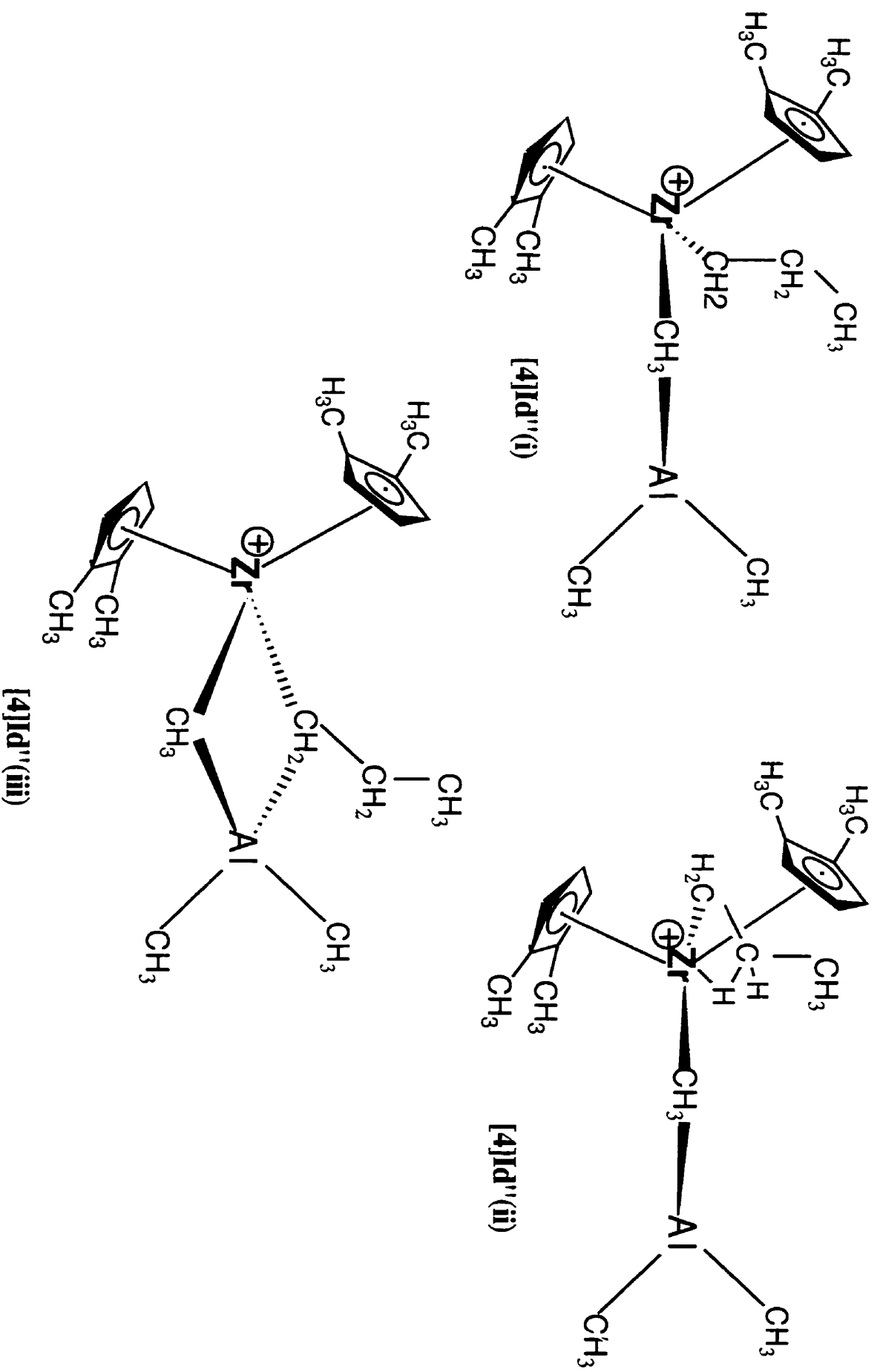


Figure 4.4 Possible modes of coordination of AlMe_3 to the cation $[(1,2\text{Me}_2\text{Cp})_2\text{ZrPr}]^+$

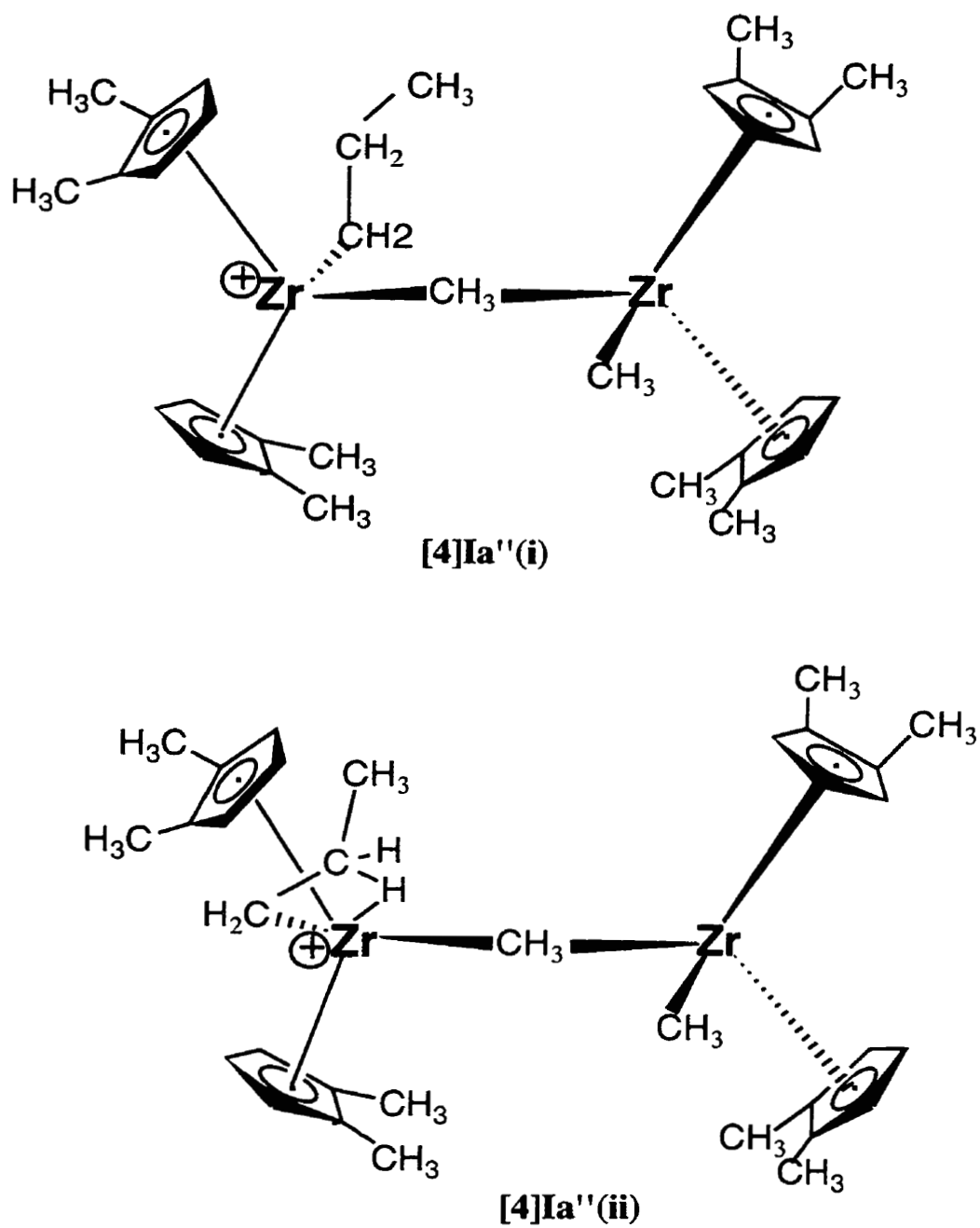


Figure 4.5 Possible modes of coordination of the precatalyst, $[(1,2\text{Me}_2\text{Cp})_2\text{ZrMe}]_2$, to the cation $[(1,2\text{Me}_2\text{Cp})_2\text{ZrPr}]^+$

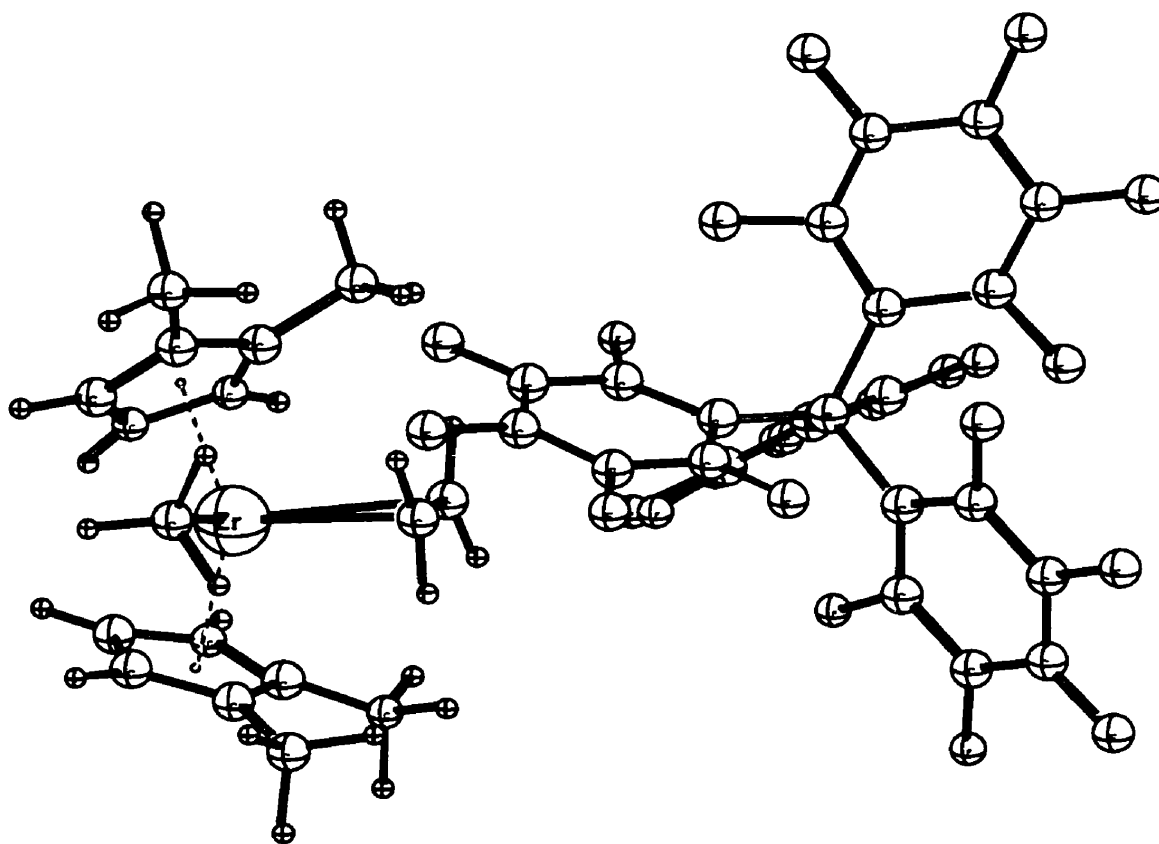
4.2.3 Formation of Sandwiched Compounds

The possibility of one of the competing species present in solution inserting between the cation and the anion to form sandwiched complexes, with the cation coordinating to the pre-catalyst, solvent or TMA (eq.4.2) might be a feasible route to forming dormant complexes. This type of sandwiched compounds were investigated in the previous chapter for certain ion-pair systems with the solvent toluene as the sandwiched species. From the values of the ΔH_{dp} obtained and shown in Table 4.2, it is clear that the formation of such a compound is more likely when the sandwiched species is TMA or the pre-catalyst. Naga *et al.*²⁶ experimentally obtained this type of complex for the ion-pair $[(1,2\text{Me}_2\text{Cp})_2\text{ZrMe}^+][\text{B}(\text{C}_6\text{F}_5)_3\text{CH}_3^-]$, when using TMA as a scavenging agent. The formation of such a complex (**[4]Id'**) was studied for the ion-pair **[4]Ia** with TMA as the sandwiched species. The enthalpy of formation of **[4]Id'** (ΔH_{sp}) was determined to be 4.4 kcal/mol which would imply that this type of compounds can readily be formed in solution. The formation of a similar complex with the precursor as the sandwiched species was not studied due to size limitations, but it is clear from the similar values of ΔH_{dp} for the formation of the products **[4]1a'** and **[4]1d'**, studied earlier, that the enthalpy of formation of such compounds would be quite similar.

The marginally endothermic value of ΔH_{sp} obtained (4.4 kcal/mol) for this process shows that the formation of such compounds is a distinct possibility for such ion-pair systems. Furthermore, the subsequent dissociation to form the anion **[4]1a** and the dormant complex of the cation with TMA (**[4]1d'**) takes an additional 14.6 kcal/mol. If one takes entropic effects into account, this may be a feasible reaction and this may indicate a likely process to form dormant complexes such as **[4]1d'** (and, by inference, **[4]1a'**) in solution.

4.2.4 Ethylene Separated Ion-Pairs

The formation of dormant complexes of the type [4]Id' in solution seems likely, judged from the value of ΔH_{SP} obtained in the previous section. In the previous chapter, we had looked at the the formation of sandwiched species involving the solvent toluene. However, if the polymerisation process has to proceed, then the monomer has to compete successfully with the solvent and the other species for the vacant coordinate site. That is, it should be able to complex with the cation prior to the insertion into the zirconium-carbon bond. In such a case, analogous to the solvent, pre-catalyst and TMA separated ion-pairs, we would get an ethylene separated ion-pair species. We looked at the possibility of such a competition by studying sandwiched compounds formed with ethylene as the monomer. Olefin separated ion-pairs have been studied and reported earlier in Chapter 2. For reasons of comparison we studied the formation of olefin separated ion-pairs for a group of four systems - two with methyl bridges and two without. The geometry of the ethylene separated ion-pair ([4]IIIA) formed with the $B(C_6F_5)_4^-$ anion is shown below in Figure 4.6. The enthalpies for the formation of the ethylene separated ion-pair systems (ΔH_{ES}) are shown in Table 4.4, along with the corresponding results for the enthalpies of the formation of the solvent -separated ion-pairs (ΔH_{SS}) for the same systems (reported earlier in Chapter 3). The results show that the values of ΔH_{ES} are smaller than the corresponding ΔH_{SS} values by about 5 kcal/mol for all the ion-pairs studied. In the case of the $B(C_6F_5)_4^-$ anion, the formation of the olefin separated ion-pair is actually exothermic, with the ΔH_{ES} being around -11 kcal/mol.



[4]IIIA

Figure 4.6 LDA optimized structure of the ethylene separated ion-pair complex
[(1,2Me₂Cp)₂ZrMe⁺]-C₂H₄-[B(C₆F₅)₄⁻]

Table 4.4 Enthalpy of formation of ethylene separated ion-pair (ΔH_{Es})^{a,b} and the solvent separated ion-pair (ΔH_{Ss})^{b,c} for anions 1a-4a with the cation P'.

Counterion	Complex Formed	ΔH_{Es} Calc. b,c	ΔH_{Ss} Calc. b,c
$\text{B}(\text{C}_6\text{F}_5)_3\text{CH}_3^-$ - [4]1a	[4]IA	14.2	18.7
$\text{B}(\text{C}_{10}\text{F}_7)_3\text{CH}_3^-$ - [4]2a	[4]IIA	11.9	18.9
$\text{B}(\text{C}_6\text{F}_5)_4^-$ - [4]3a	[4]IIIA	-10.9	-4.2
$[(\text{C}_2\text{B}_9\text{H}_{11})_2\text{Co}]^-$ - [4]4a	[4]IVA	2.3	-0.6

^a Corresponding to the process $[(1,2\text{Me}_2\text{Cp})_2\text{ZrMe}^+][\text{AMe}^-] + \text{Et} \rightarrow [(1,2\text{Me}_2\text{Cp})_2\text{ZrMe}^+]\text{-Et-}[\text{MeA}^-] + \Delta H_{\text{Es}}$ (Et = ethylene)

^b kcal/mol.

^c Corresponding to the process $[(1,2\text{Me}_2\text{Cp})_2\text{ZrMe}^+][\text{AMe}^-] + \text{S} \rightarrow [(1,2\text{Me}_2\text{Cp})_2\text{ZrMe}^+]\text{-S-}[\text{MeA}^-] + \Delta H_{\text{Ss}}$ (S = solvent, toluene)

One can conclude from this that for all the ion-pairs ([4]Ia - [4]IVa) studied, the ethylene would 'win' in the competition for the vacant site with toluene. However, in the case of TMA and the ion-pair [4]Ia, the value of ΔH_{Sp} was found to be 4.4 kcal/mol as opposed to 11 kcal/mol with ethylene for the same system. Therefore, species like TMA or the pre-catalyst may form more stable sandwiched complexes than ethylene. However, the TMA (as a scavenging agent in the ion-pair system [4]Ia) would be present in significantly less amounts than ethylene and the concentration of the pre-catalyst would decrease with time. Hence it is likely that with the passage of time, the ethylene would be the chief moiety binding to the cationic site and polymerisation will not be inhibited in systems using borates as counterions. This could be a possible explanation for the

enhancement in the activity of polymerisation that occurs with the passage of time in most polymerisation systems.⁷¹⁻⁷³

4.2.5 Comparison of Complexes of Ethylene Coordinated from Different Directions to the Counterion

The approach of the ethylene towards the ion-pair can take place from three different directions - as shown in Figure 4.7 below. The Approaches 1 and 2 in Figure 4.7 would lead to the formation of the sandwiched complexes, prior to insertion, similar to the complexes [4]IA-[4]IVA studied in the previous section. The Approach 3, on the other hand, would lead to the formation of a π complex with the ethylene coordinated to the cation on the other side of the anion. In this case the reaction would be similar to an S_N2 reaction, with the ethylene displacing the weakly bound anion from the other side and moving the cyclopentadienyl (Cp) rings in the process. The possibility of formation of such two different π complexes was considered for the ion-pair [4]IIIA : the sandwiched π complex {[4]IIIA(i)} and the π complex formed from Approach 3 {[4]IIIA(ii)}. The analogous complexes formed when the alkyl chain bound to the metal centre is ethyl instead of methyl, were also considered. This was done keeping in mind future work to be done in ethylene uptake and insertion, as it had been shown in previous studies with the naked cation^{68, 74-75} that the ethyl chain is the least length of the alkyl chain that has to be considered when analysing ethylene uptake and insertion processes. The π complexes formed in this case {[4]IIIA'(i) and [4]IIIA'(ii)} are shown below in Figure 4.8 for the two cases.

From the values obtained, it was found that the ethylene π complex formed by the coordination from the opposite side [4]IIIA(ii) is more stable by 4.5 kcal/mol than the sandwiched π complex [4]IIIA(i). This implies that the coordination from the opposite side (Approach 3) may be the preferred route to olefin complexation. The extended chain (ethyl) complexes [4]IIIA'(ii) is more stable than [4]IIIA'(i) by about 3.5 kcal/mol.

One would conclude that Approach 3 would be the preferred approach, as a displacement of the anion by the ethylene moiety, (as would be required from Approaches 1 and 2) would be difficult due to the large steric repulsion that would have to be overcome between the ethylene molecule and the aryl groups on the counterion, as has been concluded by findings of Lanza *et al.*³⁶

A study of the structures [4]III A'(i) and [4]III A'(ii) shows that the dihedral angle formed between the centroid C1 of one of the cyclopentadienyl (Cp) ligands, the zirconium atom, the alpha carbon of the chain and centroid C2 is -153.8 degrees in the complex [4]III A'(i) while it is +140.1 degrees in the complex [4]III A'(ii). This difference of 66.1 degrees in the dihedral angles for the two cases reveals the moving of the Cp ligands in the case of Approach 3 to accommodate the ethylene molecule, showing its similarity to an S_N2 type reaction.

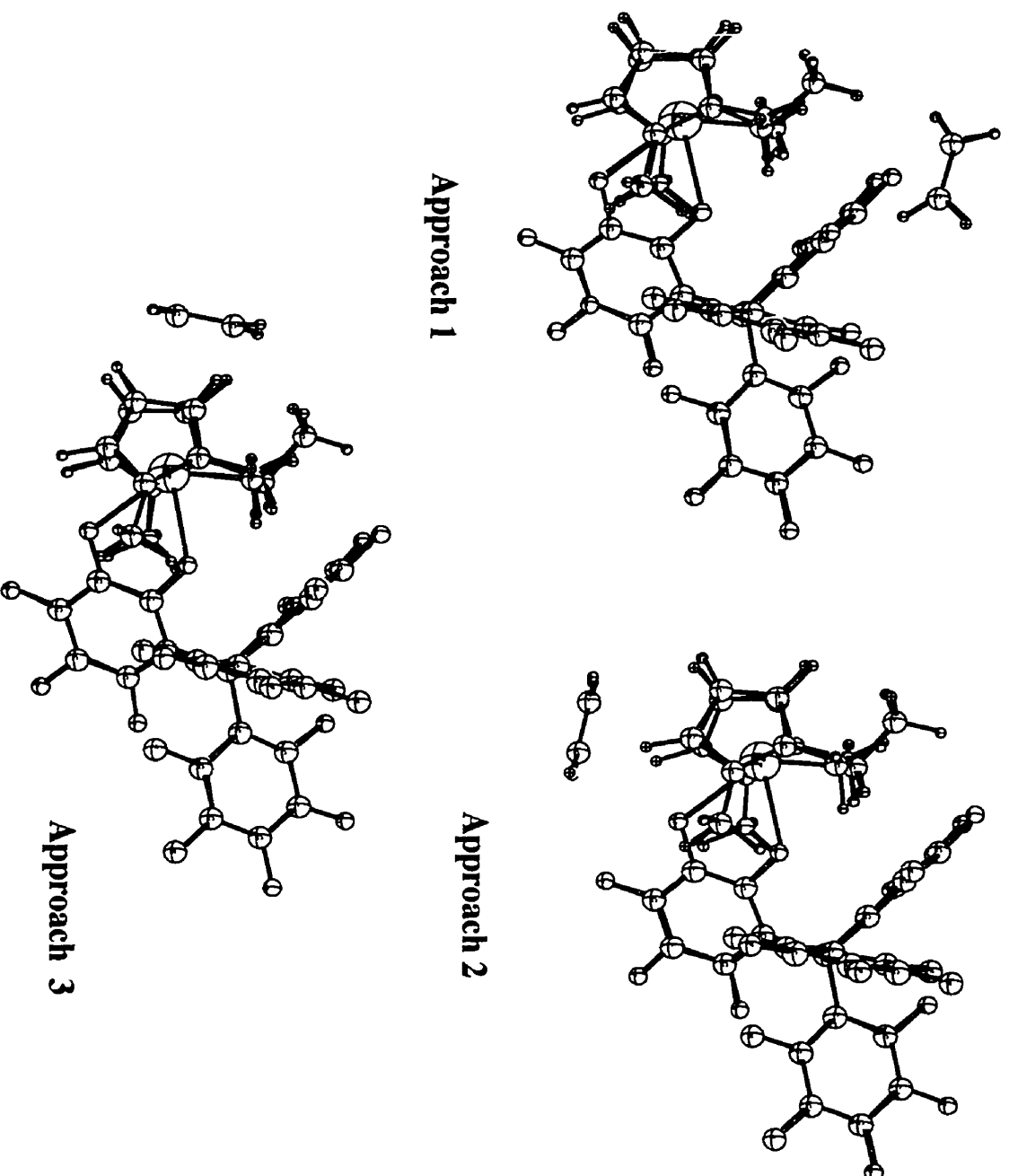


Figure 4.7 Different ways in which the monomer (ethylene) can approach the ion-pair $[(1,2\text{Me}_2\text{Cp})_2\text{ZrMe}^+\text{B}(\text{C}_6\text{F}_5)_4]^-$ system prior to uptake by the catalyst

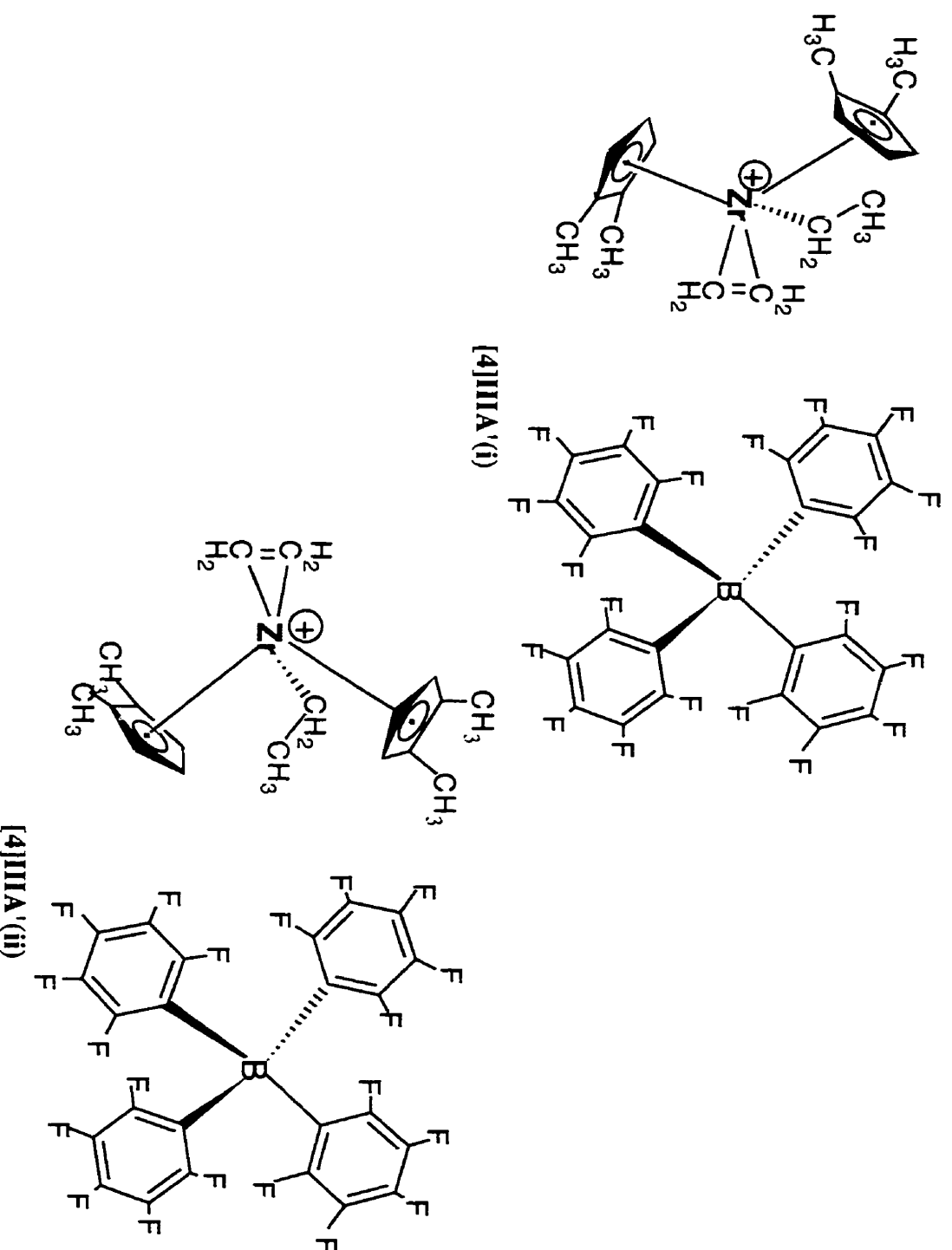


Figure 4.8 LDA optimized structures of the ethylene complexed ion-pairs formed by different approaches of the monomer (ethylene) to the $[(1,2Me_2Cp)_2ZrMe]^+[B(C_6F_5)_4]^-$ ion-pair system

4.2.6 Solvent Effects on Loss of Counterion From the Π -Complex

The total dissociation of the counterion [4]3a from the ethylene coordinated complex leading to the formation of the naked cationic complex [4]P''' and the free anion, as shown earlier in Eqn. 4.3, was calculated for both the complexes [4]IIIA'(i) and [4]IIIA'(ii). The significance of studying this reaction is that if the enthalpy of the dissociation for this reaction is not high (i.e. in the region 10-15 kcal/mol), then entropic effects would ensure that such a reaction would be feasible and then, in such a case, the loss of the counterion from the vicinity of the cationic site would be expected to occur. The enthalpy for the dissociation was considered in three different solvents : toluene ($\epsilon = 2.379$), chlorobenzene ($\epsilon = 5.71$) and 1,2-dichlorobenzene ($\epsilon = 9.93$). The results are summarised in Table 4.5. For the complex [4]IIIA'(i), the value of ΔH_{TS} in toluene (14.3 kcal/mol), is at the limit where dissociation can be predicted to occur. With the increase in the dielectric constant, the enthalpy decreases so that for chlorobenzene ($\Delta H_{TS} = 3.2$ kcal/mol) and for 1,2-dichlorobenzene ($\Delta H_{TS} = 0.3$ kcal/mol), it can be said with a fair degree of confidence that dissociation would definitely occur and the counterion would dissociate itself and no longer be present near the cation during the process of polymerisation. In the case of the complex [4]IIIA'(ii), the values of ΔH_{TS} are higher by about 3.5 kcal/mol, in the case of all the three solvents, than for the corresponding complex [4]IIIA'(i). This is due to the slightly greater stability of the π complex formed in this case in comparison to the sandwiched complex. From the results, it is clear that if solvents of lesser dielectric constants like toluene or cyclohexane are considered, the counterion is likely to remain near the cationic catalytic species [4]P''' during the insertion process. Hence a study of the insertion of ethylene into the metal-alkyl bond should take the presence of the counterion into account.

Table 4.5 Enthalpy of total separation of the ethylene complexed compounds (ΔH_{ts})^{a,b} in three different solvents for the complexes [4]III A'(i) and [4]III A'(ii).

Solvent	ΔH_{ts}^b for [4]III A'(i)	ΔH_{ts}^b for [4]III A'(ii)
C ₆ H ₅ CH ₃	14.3	16.1
C ₆ D ₅ Cl	3.2	6.7
1,2-C ₆ D ₄ Cl ₂	0.3	3.8

^a Corresponding to the process $[(1,2Me_2Cp)_2ZrMe^+Et] [AMe^-] \rightarrow [(1,2Me_2Cp)_2ZrMe^+Et]^+ [AMe^-] + \Delta H_{ts}$

^b kcal/mol.

4.3 Concluding remarks

A DFT based study was conducted on the reaction between the cation $(1,2Me_2Cp)_2ZrMe^+$ ([4]P') and the different species that can be present in solution, forming dormant products (eq. 4.1) that would have to be dissociated before catalysis can proceed with the monomer. The ion-pair system that was studied for this process was $[(1,2Me_2Cp)_2ZrMe^+]-[CH_3B(C_6F_5)_3^-]$ (Ia) and the species in solution studied that could coordinate to the cation [4]P' were the precatalyst $(1,2Me_2Cp)_2ZrMe_2$, the co-catalyst $B(C_6F_5)_3$, solvent $C_6H_5CH_3$ and $AlMe_3$ (TMA). The values of ΔH_{dp} (enthalpy of dormant product formation), obtained for the different species, showed that the precatalyst and TMA may be strong competitors for the vacant coordinate site. The value of $-\Delta H_{dp}$ for the formation of similar dormant products for these two species with the cation $(1,2Me_2Cp)_2ZrPr^+$ ([4]P'') decreased by about 10 kcal/mol showing that the possibility of forming such complexes decreases after insertion of one or more monomer units into the zirconium-alkyl bond.

Also considered was the possibility of a separation process for the ion-pair $[(1,2Me_2Cp)_2ZrMe^+]-[CH_3B(C_6F_5)_3^-]$ ([4]Ia) with the insertion of TMA between the ions leading to a dormant sandwiched complex $[(1,2Me_2Cp)_2ZrMe^+]-TMA-[CH_3B(C_6F_5)_3^-]$ ([4]Id') with the reaction enthalpy ΔH_{sp} . The low value of ΔH_{sp} (4.4

kcal/mol) obtained makes this a possible process in solution and indicates a possible pathway for the formation of the dormant product $[(1,2\text{Me}_2\text{Cp})_2\text{ZrMe}^+]\text{-TMA}$ (**[4]1d'**).

The formation of the corresponding sandwiched ethylene separated ion-pair species was considered for the ionpairs formed with the cation **[4]P'** and the counterions $\text{B}(\text{C}_6\text{F}_5)_3\text{CH}_3^-$ (**[4]1a**), $\text{B}(\text{C}_{10}\text{F}_7)_3\text{CH}_3^-$ (**[4]2a**), $\text{B}(\text{C}_6\text{F}_5)_4^-$ (**[4]3a**) and $[(\text{C}_2\text{B}_9\text{H}_{11})_2\text{Co}]^-$ (**[4]4a**) with a formation enthalpy of ΔH_{es} . A comparison between the values of ΔH_{es} and ΔH_{ss} (enthalpy of formation of the corresponding solvent-toluene-separated complex) shows that the ethylene would be preferred to the solvent in such cases. However a comparison between ΔH_{es} and ΔH_{sp} for the ion-pair **[4]1a** shows that TMA (and by inference, the pre-catalyst) may be better coordinators to the cation in such sandwiched complexes and can inhibit the catalysis process in the initial stages of the polymerisation.

Finally discussed are the possible modes of uptake of the ethylene by the cation in the presence of the counterion. The uptake leading to the sandwiched π complex **[4]IIIA'(i)** and the π complex with the ethylene coordinated to the opposite side, **[4]IIIA'(ii)** were considered and a comparison of their relative stabilities shows that the ethylene complex **[4]IIIA'(ii)** was stabler by about 11 kcal/mol in comparison to **[4]IIIA'(i)**, implying that the approach of the ethylene to the cation from a direction opposite to the counterion may be the preferred route to uptake and subsequent insertion. The energy of dissociation of the anion from the π complex was calculated in three different solvents: toluene ($\epsilon = 2.379$), chlorobenzene ($\epsilon = 5.71$) and 1,2-dichlorobenzene ($\epsilon = 9.93$). For the complexes **[4]IIIA'(i)** and **[4]IIIA'(ii)**, the value (around 15.0 kcal/mol) obtained for the dissociation of the anion $\text{B}(\text{C}_6\text{F}_5)_4^-$ (**[4]3a**) in toluene indicates that in the case of non-polar solvents like toluene and cyclohexane the counterion is likely to remain near the catalyst during the process of polymerisation. Hence the influence of the counterion has to be taken into account while studying the catalysis process. On the other hand, for more polar solvents like chlorobenzene and 1,2-dichlorobenzene, the low values

of ΔH_{TS} (less than 5 kcal/mol) indicate that the counterion is likely to dissociate and not be around the cation when polymerisation is taking place.

Chapter 5

Summary and Future Prospects

Experimental studies^{7-8, 21-24} have shown that the presence of the counterion and the solvent can significantly affect the catalyst performance during olefin polymerisation. The objective of this thesis was to present a study of the effect of these species on the catalytic activity of pre-catalysts of the type $\{L\}_2MR_2$ {where L = ligands of the type Cp etc. and R = alkyl; groups like methyl etc.}

The second chapter focussed on the activation of different such pre-catalysts by the cocatalyst $B(C_6F_5)_3$. Three different types of pre-catalysts were investigated : mono-cyclopentadienyl, constrained geometry and the bis-cyclopentadienyl systems. The calculations showed that the electron donating ability of the ligands is the most predominant factor in determining the enthalpy for the activation reaction and reinforced the experimental observation⁷ that the bis-cyclopentadienyl systems would be the best catalysts of the three systems investigated. The formation of olefin and solvent separated ion-pairs was found to be distinct possibilities for all the three systems.

The third chapter considered the activation of the lone bis-cyclopentadienyl catalyst precursor $(1,2Me_2Cp)_2ZrMe_2$ by a variety of boron (type 1) and aluminium (type 2) based cocatalysts. These co-catalysts had been experimentally found to be effective activators. A third type of activator - $[CPh_3^+][A^-]$ (type 3) {where $A^- : B(C_6F_5)_4^-$ etc.} - was also considered. The results indicated that using activators of type 3 would lead to the most effective polymerisation systems. The total dissociation of the ion-pairs leading to the formation of the cation and the separated anion was found to be thermodynamically unfavourable in comparison to the partial separation of the ion-pair and the insertion of the solvent (toluene) to form solvent separated ion-pairs, consistent with the findings from the second chapter. The ease of dissociation was found to improve in solvents of greater polarity.

The fourth chapter was a study of the competing processes, between the different species present in solution, for the vacant site in the cationic catalyst $(1,2\text{Me}_2\text{Cp})_2\text{ZrMe}^+$ during the early stages of the polymerisation. The results showed that the species TMA (trimethyl aluminium) and the pre-catalyst could potentially form dormant species in solution. The stability of such dormant species was however, found to be reduced with the increase of the length of the alkyl chain associated with the catalyst. The relative stabilities of olefin (ethylene) and solvent separated species was also considered for different ion-pair systems, and the formation of the olefin separated ion-pair systems was found to be more favourable for all the cases considered. Calculations showed that the total separation of the counterion from the ethylene complexed ion-pairs was unlikely in solvents of low polarity, like toluene.

The results obtained from the work make it clear that the counterion and the solvent play an important role during the early stages of the olefin polymerisation using metallocene and related single site catalysts. One conclusion that can be drawn from the study is that the counterion has to be as non-coordinating to the cation as possible, if it is to be easily dissociated to allow the olefin to reach the vacant coordinate site. Hence an improvement that suggests itself is the employment of larger and more weakly coordinating anions to the cation. Such anions have been experimentally investigated¹⁶⁻¹⁸ and the results that have been obtained suggest²¹ that this does indeed lead to an improvement in catalyst performance. It is also clear from the study that the polarity of the solvent can be important in influencing the processes that occur after ion-pair formation. Using solvents of greater polarity (like chlorobenzene and 1,2 dichlorobenzene) can lead to greater ease of dissociation of the counterion from the cation and thereby facilitate the polymerisation process.

Investigations in the second chapter revealed that the bis-cyclopentadienyl systems would be the best catalysts in toluene. However, there has been recent experimental activity to discover new zirconium and titanium based catalyst systems that do not contain

cyclopentadienyl rings as ligands.⁷⁶⁻⁷⁸ Theoretical investigations, similar to those done for the metallocene systems in this work, could provide interesting results about the relative abilities of these systems to act as effective catalysts.

This study was limited to the investigation of the processes occurring in solution at the start of the polymerisation process : the activation of the precatalyst and the competing processes in solution after formation of the cationic catalyst. Future theoretical studies that can be considered would be the study of olefin uptake and subsequent insertion into the metal-alkyl chain, in the presence of the counterion. One can predict a barrier to olefin monomer uptake in the presence of the counterion, due to the need of the olefin monomer to displace the counterion from the cation. This would be an improvement on previous theoretical studies involving only the naked cation^{68,74-75} where no uptake barrier has been observed. A molecular dynamics simulation of the uptake and insertion processes should also provide insightful results.

Bibliography

- (1) Bochmann, M. *J. Chem.Soc., Dalton Trans.* **1996**, 225.
- (2) Pasynkiewicz, S. *Polyhedron* **1990**, 9, 429.
- (3) Mason, M. R.; Smith, J. M.; Bott, S. G.; Barron, A. R. *J. Am. Chem. Soc.* **1993**, 115, 4971.
- (4) Atwood, J. L.; Hrcir, D. C.; Priester, R. D.; Rogers, R. D.; *Organometallics* **1983**, 2, 985.
- (5) Harlan, C. J; Bott, S. G.; Barron, A. R. *J. Am. Chem. Soc.* **1995**, 117, 6465.
- (6) Barron, A.R.; 218'th ACS national meeting, New Orleans, August 22-26, 1999.
- (7) Yang, X.; Stern, C.L.; Marks,T.J. *J. Am. Chem. Soc.* **1994**, 116, 10015.
- (8) Deck, P. A.; Marks, T. J. *J. Am.Chem. Soc.* **1995**, 117, 6128.
- (9) Jia, L.; Stern, C.L.; Marks, T. J. *Organometallics* **1997**, 16, 842.
- (10) Li, L.; Marks, T. J. *Organometallics* **1998**, 17, 3996.
- (11) Deck, P.; Beswick, C. L.; Marks, T. J. *J. Am. Chem. Soc.* **1998**, 120, 1772.
- (12) Siedle, A. R.; Newmark, R. A.; Lamanna, W. M.; Shroepfer, J. N. *Polyhedron*, **1990**, 9, 301.
- (13) Bochmann, M.; Lancaster, S. J. *Angew. Chem. Int. Ed. Engl.* **1994**, 33, 1634.
- (14) Bochmann, M.; Lancaster, S.J. *Organometallic Chem.* **1995**, 497, 55.
- (15) Hlatky, G. Gregory; Eckman, R. R.; Turner, H. W. *Organometallics* **1992**, 11, 1413.
- (16) Jia, L.; Yang, X.; Stern, C. L.; Marks T. J. *Organometallics* **1994**, 13, 3755.
- (17) Chen, Y-X.; Stern, C. L.; Marks, T. J. *J. Am. Chem .Soc.* **1997**, 119, 2582.
- (18) Williams, V. C.; Piers, W. E.; Clegg, W.; Collins, S.; Marder, T. B. *J. Am. Chem. Soc.* **1999**, 121, 3244.

- (19) Jelinek, T.; Baldwin, P.; Scheidt, W. R.; Reed, C. A. *Inorg. Chem.* **1993**, *32*, 1982
- (20) Strauss, S. H. 218th ACS national meeting, New Orleans, August 22-26, 1999.
- (21) Chien, J. C. W.; Tsai, W. M.; Rausch, M. D. *J. Am. Chem. Soc.*, **1991**, *113*, 8570.
- (22) Giardello, M.A.; Disen, M.S.; Stern, C.L.; Marks, T. J. *J. Am. Chem. Soc.* **1995**, *117*, 12114.
- (23) Tritto, I.; Donetti, R.; Sacchi, M.C.; Locatelli, P.; Zannoni, G. *Macromolecules* **1999**, *32*, 264.
- (24) Tritto, I.; Donetti, R.; Sacchi, M.C.; Locatelli, P.; Zannoni, G. *Macromolecules* **1997**, *30*, 1247.
- (25) Karl, J.; Erker, G.; Frohlich, R.; *J. Am. Chem. Soc.*, **1997**, *119*, 11165.
- (26) Naga, N.; Shiono, T.; Ikeda, T. *J. Mol. Cat. A*, **1999**, *150*, 155.
- (27) Bochmann, M.; Lancaster, J. L. *Angew. Chem. Int. Ed. Engl.* **1994**, *33*, 1634.
- (28) Woo, T.K.; Margl, P.M.; Ziegler, T.; Blöchl, P.E. *Organometallics* **1997**, *16*, 3454.
- (29) Woo, T.K.; Margl, P.M.; Lohrenz, J.C.W.; Blöchl, P.E.; Ziegler, T. *J. Am. Chem. Soc.* **1996**, *118*, 13021.
- (30) Margl, P.M.; Lohrenz, J.C.W.; Ziegler, T.; Blöchl, P.E. *J. Am. Chem. Soc.* **1996**, *118*, 4434.
- (31) Fan, L.; Harrison, D.; Woo, T.K.; Ziegler, T. *Organometallics* **1995**, *14*, 2018.
- (32) Meier, R.J.; Doremaele, G.H.J.V.; Tarlori, S.; Buda, F. *J. Am. Chem. Soc.* **1994**, *116*, 7274.
- (33) Yoshida, T.; Koga, N.; Morokuma, K. *Organometallics* **1995**, *14*, 746.
- (34) Weiss, H.; Ehrig, M.; Ahlrichs, R. *J. Am. Chem. Soc.* **1994**, *116*, 4919.

- (35) Bierwagen, E.P.; Bercaw, J.E.; Goddard, W.A. III. *J. Am. Chem. Soc.* **1994**, *116*, 1481.
- (36) Lanza, G.; Fragala, I. L.; Marks, T. J. *J. Am. Chem. Soc.* **1998**, *120*, 8257.
- (37) Lanza, G.; Fragala, I. L. *Topics in Catalysis* **1999**, *7*, 45.
- (38) Klesing, A.; Bettonville, S. *Phys. Chem. Chem. Phys.*, **1999**, *1*, 2373.
- (39) Fusco, R.; Longo, L.; Masi, F.; Garbassi, F. *Macromol. Rapid Commun.* **1998**, *19*, 257.
- (40) Fusco, R.; Longo, L.; Masi, F.; Garbassi, F. *Macromolecules* **1997**, *30*, 7673.
- (41) Bernardi, F.; Bottoni, A.; Miscione, G. P. *Organometallics* **1998**, *17*, 16.
- (42) Baerends, E. J.; Ellis, D. E.; Ros, P. *Chem. Phys.* **1973**, *2*, 41.
- (43) Baerends, E.J.; Ros, P. *Chem. Phys.* **1973**, *2*, 52.
- (44) te Velde, G.; Baerends, E.J. *J. Comp.Phys.* **1992**, *92*, 84.
- (45) Fonseca, C. G.; Visser, O.; Snijders, J. G.; te Velde G.; Baerends, E. J. In *Methods and Techniques in Computational Chemistry, METECC-95*; Clementi, E., Corongiu, G., Eds.; STEF; Cagliari, 1995; p 305.
- (46) Ravenek, W. in Algorithms and Applications on Vector and Parallel Computers; te Riele, H. J. J.; Dekker, T. J.; vand de Horst, H. A. Eds. Elsevier: Amsterdam, The Netherlands, 1987.
- (47) te Velde, G.; Baerends, E. J. *J. Comput.Chem.* **1992**, *99*, 84.
- (48) Boerrigter, P. M.; te Velde, G.; Baerends, E. J. *Int. J. Quantum Chem.* **1998**, *33*, 87.
- (49) Verslius, L.; Ziegler, T. *J. Chem. Phys.* **1988**, *88*, 322.
- (50) Vosko, S. H.; Wilk, L.; Nusair, M. *Can. J. Phys.* **1980**, *58*, 1200.
- (51) Krijn, J ; Baerends, E.J. *Fit Functions in the HFS-Method* ; Free University of Amsterdam, 1984.
- (52) Perdew, J.P. *Phys. Rev. B* **1992**, *46*, 6671
- (53) Klamt, A.; Schuurmann, G. *J. Chem. Soc. Perkin Trans.* **1993**, *2*, 799.

- (54) Pye, C. C.; Ziegler, T. *Theor. Chem. Acc.* **1999** V 101, 396-408.
- (55) Hirshfeld, F.L. *Theoret. Chim. Act.* **1977**, 44, 129.
- (56) Wiberg, K.B.; Rablen, P.R. *J. Comp. Chem.* **1993**, 1412, 1504.
- (57) Mulliken, R. *J. Chem. Phys.* **1955**, 23, 1833.
- (58) Mulliken, R. *J. Chem. Phys.* **1955**, 23, 2343.
- (59) Jia, L.; Yang, X.; Ishihara, A.; Marks, T.J. *Organometallics* **1995**, 14, 3135.
- (60) Wang, Q.; Quyoum, R.; Gillis, D.J.; Jeremic, D.; Tudoret, M.J.; Baird, M.C. *J. Organomet. Chem.* **1997**, 527, 7.
- (61) Chen, Y.-X.; Marks, T.J. *Organometallics* **1997**, 16, 3649.
- (62) Gassman, P.G.; Macomber, D.W.; Hershberger, J.W. *Organometallics* **1983**, 2, 1470.
- (63) Calabro, D.C.; Hubbard, J. L.; Blevins, C.H. II.; Campbell, A.C.; Lichtenberger, D.L. *J. Am. Chem. Soc.* **1981**, 103, 6839.
- (64) Miller, E.J.; Landon, S.J.; Brill, T.B. *Organometallics* **1985**, 4, 533.
- (65) Yang, X.; Stern, C.L.; Marks, T.J. *Angew. Chem. Int. Ed. Engl.* **1992**, 31, 1375.
- (66) Herzog, A.; Liu, F. Q.; Roesky, H.W.; Demsar, A.; Keller, K.; Noltemeyer, M.; Pauer, F. *Organometallics* **1994**, 13, 1251.
- (67) Gillis, D.J.; Tudoret, M.J.; Baird, M.C. *J. Am. Chem. Soc.* **1993**, 115, 2543.
- (68) Woo, T.K.; Fan, L.; Ziegler, T. *Organometallics* **1994**, 13, 2252.
- (69) Brintzinger, H.H.; Fischer, D.; Mülhaupt, R.; Rieger, B.; Waymouth, R.M. *Angew. Chem. Int. Ed. Engl.* **1995**, 34, 1143.
- (70) Eisch, J.J.; Pombrik, S.I.; Zheng, G.X. *Organometallics*, **1993**, 12, 3856.

- (71) Bochmann, M.; Jaggar, J. A.; Nicholls, C. *Angew. Chem. Int. Ed. Engl.* **1990**, *29*, 780.
- (72) Gauthier, J. W.; Corrigan, F. J.; Nicholas, J. T.; Collins, S. *Macromolecules*, **1995**, *28*, 3771.
- (73) Henrici-Olive, G.; Olive, S. *Angew. Chem. Int. Ed. Engl.* **1967**, 790.
- (74) Lohrenz, J. C. W.; Woo, T. K.; Fan, L.; Ziegler, T. *J. Organomet. Chem.* **1995**, *497*, 91.
- (75) Woo, T. K.; Fan, L.; Ziegler, T. *Organometallics* **1994**, *13*, 423.
- (76) Stephan, D. W.; Guerin, F.; Spence, H. R. v. H.; Koch, L.; Gap, X.; Brown, S. J.; Swabey, J. W.; Wang, Q.; Xu, W.; Zoricak, P.; Harrison, D. G. *Organometallics* **1999**, *18*, 2046.
- (77) Stephan, D. W.; Stewart, C. J.; Guerin, F.; Spence, H. R. v. H.; Xu, W.; Harrison, D. G.; *Organometallics* **1999**, *18*, 1116.
- (78) Zhang, S.; Piers, W. E.; Gao, X.; Parvez, M.; *J. Am. Chem. Soc.* **2000**, *122*, 5499.